The Development of Locally Bioavailable COX-2 Inhibitors

A

Dissertation

Presented to the Faculty of

The University of Houston

College of Pharmacy

Department of Pharmacological and Pharmaceutical Sciences

In Partial Fulfillment of

The Requirement for the Degree of

DOCTOR OF PHILOSOPHY

By

Yong Ma

May, 2015

The Development of Locally Bioavailable COX-2 Inhibitors

Yong Ma

Approved By:

Ming Hu, Ph.D. (Advisor)

Diana S-L Chow, Ph.D.

Romi Ghose, Ph.D.

Greg Cuny, Ph.D.

Shuxing Zhang, Ph.D.

F. Lamar Pritchard, Ph.D.
Dean, College of Pharmacy
University of Houston

May, 2015

ABSTRACT

Objective: The effectiveness of the selective COX-2 inhibitors in colorectal cancer chemoprevention has been demonstrated in previous studies. However, these drugs are not safe agents to patients due to their toxicity in the cardiovascular system. The long-term goal in this project is to develop new selective COX-2 inhibitors which can be used as effective and safe agents for colorectal cancer chemoprevention in human. The objective in the current studies is to develop a series of new compounds which are able to inhibit colonic COX-2 activity but not systemically bioavailable.

Methods: The new compounds were designed by using celecoxib as the template. Their inhibitory effects on COX-2 activity were studied in cell-based assays or by employing recombinant human COX-2 enzyme. The metabolic properties of the new compounds were characterized by *in vitro* tools and models before pharmacokinetics studies were conducted in rats. Among all the new compounds, the inhibitory effect of the lead compound **6a1** on colonic COX-2 activity was then confirmed in inflamed rat colon by *in situ* perfusion. During the perfusion, blood and bile samples from rats were also collected for studying the absorption, metabolism and excretion of **6a1** in rats. The relevant studies were also conducted with celecoxib to show the differences between celecoxib and the locally bioavailable COX-2 inhibitors.

Results: 8 new compounds with phenolic groups in their structures were successfully designed, synthesized and purified. In the cell-based assays and by employing human recombinant COX-2 enzymes, the new inhibitors were confirmed as COX-2 inhibitors, although they were less potent than celecoxib. In the *in vitro* characterization, some of the

new compounds were very efficiently conjugated by phase II enzymes with the conjugation rates largely depended on the phenolic group species. A pharmacokinetics study in rats demonstrated the low oral bioavailability of **6a1**, which was selected as the lead compound among the new compounds based their inhibitory effects on COX-2 activity and *in vitro* conjugation rates. When the inflamed rat colon was perfused with 70 μM **6a1**, an inhibitory effect on colonic COX-2 activity was observed to be similar with that in the perfusion with 1 μM celecoxib. The blood concentration of **6a1** was lower than its IC_{50} on COX-2 activities during the perfusion, due to the extensive first-pass metabolism and excretion of **6a1** in liver. In contrast, the blood concentration of celecoxib in the systemic circulation was > 10-fold higher than its IC_{50}.

Conclusion: We successfully developed several new COX-2 inhibitors which were effective to inhibit COX-2 activity in inflamed rat colon but rapidly metabolized and excreted in liver. For these new compounds, the extensive first-pass metabolism in liver resulted in a poor oral bioavailability and extremely low blood concentrations in the systemic circulation, reducing or avoiding the exposure of the cardiovascular systems. Compared with celecoxib, the locally bioavailable COX-2 inhibitors are more promising to be developed as safe agents in colorectal cancer prevention.

ACKNOWLEDGEMENT

Firstly I want to express my gratitude and appreciation to my advisor Dr. Ming Hu. He offered me the opportunity to transfer from biology to pharmaceutical sciences. In last six years, he has dedicated a lot of time, energy and patience in tutoring me to be a junior researcher in pharmaceutical sciences. His personality has also influenced me. In my future career, I would try to be a hard-working, strong-minded, open-minded, and good-tempered person like him.

I want to thank Dr. Diana Chow, Dr. Romi Ghose, Dr. Greg Cuny and Dr. Shuxing Zhang for being my committee members. They were competent teachers who imparted their knowledge in pharmaceutical sciences to me. I appreciate their time and attention specifically devoted to my research project.

My appreciation also goes to every member in Dr. Ming Hu's lab, especially Dr. Song Gao, Terry Yin, Tao Niu, Shufan Ge and Yu He. They made my time in Dr. Ming Hu's lab memorable. I will always be in touch with you and our friendships will last forever. I also want to say thank you to all the faculty, staff and students in the Department of Pharmacological and Pharmaceutical Sciences.

Last but not least, my deepest appreciation to my family members including my parents in China and my wife Haoqing. For so long time, with their love and support, I am always be encouraged to pursuit what I want.

TABLE OF CONTENTS

LIST OF TABLES

LIST OF SCHEMES

LIST OF FIGURES

LIST OF ABBREVIATIONS

CYP	cytochrome P450
FMO	flavin-containing monooxygenase
UGT	uridine 5'-diphospho-glucuronosyltransferase
SULT	sulfotransferase
GST	glutathione *S*-transferase
M.W.	molecular weight
UDPGA	uridine diphosphate glucuronic acid
PAPS	3'-phosphoadenosine-5'-phosphosulfate
ER	endoplasmic reticulum
DHEA	dehydroepiandrosterone
PhIP	2-amino-1-methyl-6-phenylimidazo[4,5-b]pyridine
ABC transporters	ATP-binding cassette transporter
TMD	transmembrane domain
NBD	nucleotide-binding domain
ATP	adenosine triphosphate
P-gp	P-glycoprotein
MDR1	multidrug resistance protein 1
BCRP	breast cancer resistance protein

271	MRP	multidrug-resistant protein
272	BBB	brain-blood barrier
273	PG	prostaglandin
274	AA	arachidonic acid
275	PLA_2	phospholipase A_2
276	PLC	phospholipase C
277	PLD	phospholipase D
278	COX	cyclooxygenase
279	EGF	epidermal growth factor
280	TXA_2	thromboxane A_2
281	TXB_2	thromboxane B_2
282	PTGS	prostaglandin-endoperoxide synthase
283	CRC	colorectal cancer
284	NSAID	non-steroidal anti-inflammatory drug
285	OA	osteoarthritis
286	PreSAP trial	Prevention of Colorectal Sporadic Adenomatous Polyps trial
287	APPROVe trial	Adenomatous Polyp Prevention on Vioxx trial
288	AD	Alzheimer's disease
289	APC trial	Adenoma Prevention with Celecoxib trial
290	FDA	Food and Drug Administration

291	RA	rheumatoid arthritis
292	FAP	familial adenomatous polyposis
293	WBA	whole blood assay
294	WHMA	William Harvey modified whole blood assay
295	SAR	structure-activity relationship
296	BCS	biopharmaceutic classification system
297	3,7-DHF	3,7-dihydroxyflavone
298	THF	tetrahydrofuran
299	EDTA	ethylenediaminetetraacetic
300	GSH	L-glutathione reduced
301	LPS	lipopolysaccharides
302	DMSO	methyl sulfoxide
303	EtOAc	ethyl acetate
304	ATCC	American Type Culture Collection
305	PBS	phosphate-buffered saline
306	DMEM	Dulbecco's modified eagle medium
307	FBS	fetal bovine serum
308	UPLC	ultra-performance liquid chromatography
309	MS	mass spectrometer
310	TLC	thin-layer chromatography

311	FC	flash chromatography
312	DAD	diode array detector
313	MRM	multiple reaction monitor
314	IC_{50}	half maximal inhibitory concentration
315	NO	nitric oxide
316	PK	pharmacokinetics
317	SD rats	Sprague Dawley rats
318	DTT	dithiothreitol
319	HBSS	Hanks' balanced salt solution
320	TEER	trans-epithelial electrical resistance
321	IACUC	Institutional Animal Use and Care Committee
322	TNBS	2,4,6-trinitrobenzenesulfonic acid
323	β-CD	β-cyclodextrin
324	IBD	inflammatory bowel disease
325	SPE	solid phase extraction
326		
327		
328		

Chapter 1 Review of the Literature

1.1 Introduction to drug metabolism

Drug metabolism is a general term for the biomedical transformation process of drugs or xenobiotics by the various enzymatic systems in living organisms. The drug metabolism usually results in the alterations of the molecular structure, physicochemical properties, and pharmacological effects of the drug substances, and also leads to their terminal elimination from the organisms. Depending on the reactions occurring to the substrates, the drug metabolism can usually be categorized as phase I metabolism or phase II metabolism [1]. The phase I metabolism is the functionalization phase which generates functional groups such as carboxyl (-COOH), hydroxyl (-OH), amino ($-NH_2$), or sulfhydryl (-SH) in the molecules (Figure 1). The phase II metabolism is the conjugative phase which conjugates a methyl group, glutathione, glucuronic acid, sulfonic acid or other structures to the substrates. The phase I and II metabolism may occur subsequently in the biotransformation of one drug, but they are not necessarily linked to each other.

1.1.1 Phase I metabolism

The reactions in phase I metabolism of the drugs or xenobiotics include oxidation, reduction, hydrolysis, hydration, cyclization, decyclization, isomerization and other modifications [2]. The phase I metabolism of the drug substances usually involves the enzymes from the cytochrome P450 (CYP) family, as well as esterases, alcohol or aldehyde dehydrogenases, hydrolases, monoamine oxidases, flavin-containing monooxygenases (FMOs), peroxidases and the other enzymes. The phase I drug metabolism plays an important role in the metabolism of most drugs and is usually considered as the basic pathways for the biotransformation of drugs *in vivo*. With similar structures to the parent drugs, the phase I metabolites may possess a lower or higher potency and may lead to new therapeutic effects or side effects [3]. The metabolites in phase I

metabolism which are sufficiently polar can be readily excreted from the body. However, many products in phase I metabolism are still not rapidly eliminated and require either further phase I metabolism or subsequent phase II metabolism to be hydrophilic.

1.1.1.1 **CYPs**

The CYPs are hemeproteins. So far more than 11,000 distinct CYPs have been named in animals, plants, fungi, protists, and bacteria [4]. The CYPs are the most important enzymes for the phase I drug metabolism in mammalians, and they are responsible for ≥ 75% of the total metabolism of market drugs in humans [5, 6]. Also, many drugs or prodrugs are bioactivated by the CYPs to form the active metabolites [7, 8]. The CYPs also play important roles in the metabolism of many endogenous substances including steroid hormones, cholesterols, vitamin D, bilirubin, etc [9-11].

The members in the CYP superfamily are involved in various reactions and they differ from each other in structure and catalytic properties [12]. However, they all contain a heme cofactor. In humans, the CYPs are primarily membrane-embedded proteins in the mitochondria or the endoplasmic reticulum inside cells. The CYPs can be detected in most tissues of human and participate in various physiochemical processes. The CYPs expressed in the intestinal tract or liver can be involved in the metabolism of xenobiotics. So far more than 50 CYPs has been identified in humans and they belong to 18 families [13]. The most relevant CYPs involved in drug metabolism in humans are the CYP3A4, 2D6, 2C8, 2C9, 2C19, 1A1, 1A2, 2E1, 2A6, 2B6 and 1B1 [14]. Among these CYPs, the CYP3A4, 1A2, 2D6 and the ones in the 2C subfamily are the most important CYP isoforms which account for more than 75% of total interactions between the drugs and CYPs [15]. Slobodan Rendic provided a comprehensive summary on the reactions in the drug metabolism catalyzed by human CYPs [16].

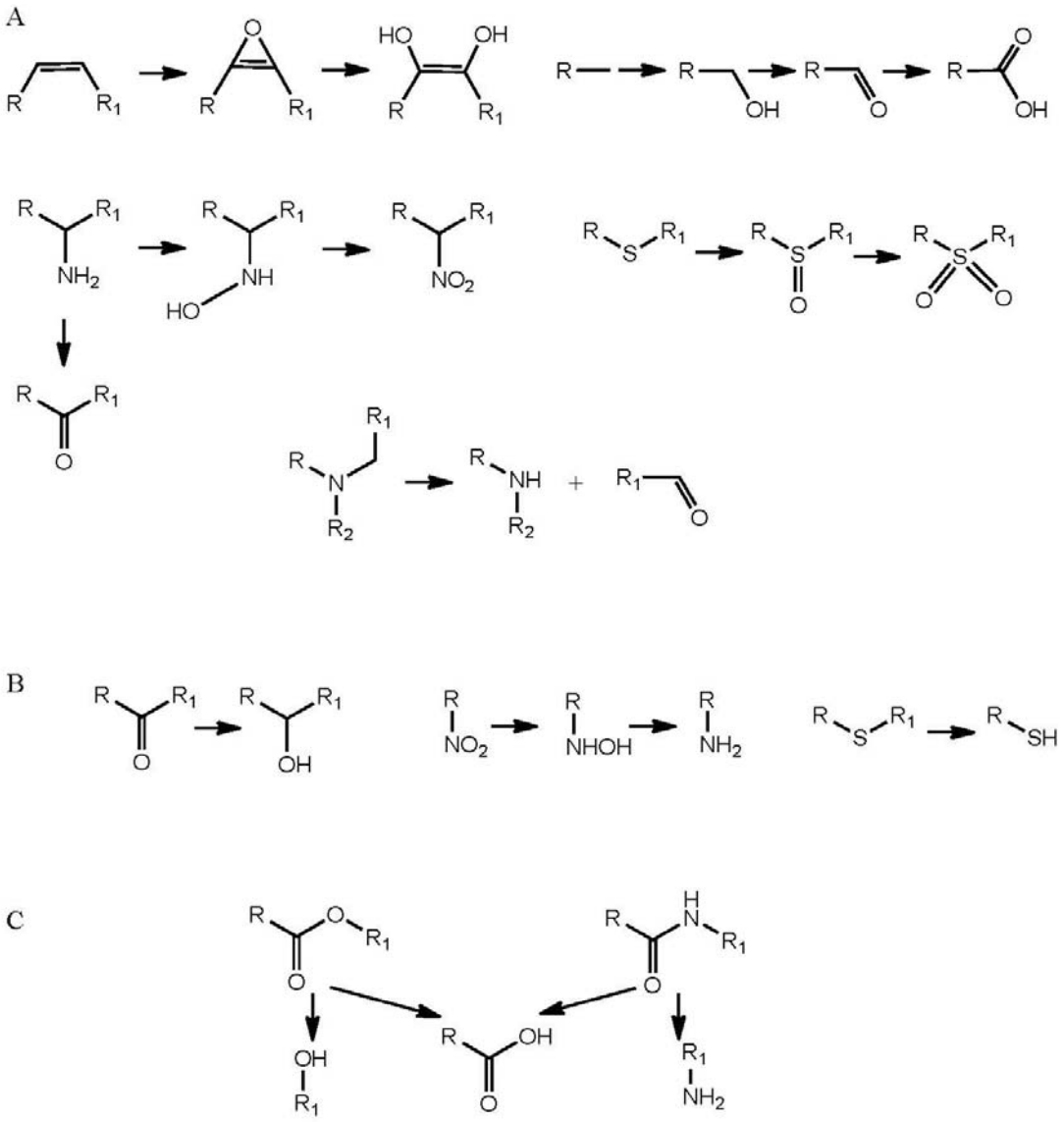

Figure 1. Typical reactions in phase I drug metabolism.

(A) Oxidation. (B) Reduction. (C) Hydrolysis.

1.1.2 Phase II metabolism

The phase II metabolism of drugs is usually a conjugative phase which incorporates an endogenous substance into the structure of substrate through certain functional groups. The reaction types include mainly glucuronidation, sulfation, acetylation, methylation, glutathione conjugation and glycine conjugation. The production of phase II conjugates usually requires the catalysis by a member from the transferase families with broad substrate specificity in the presence of the corresponding cofactor. The enzymes involved in the phase II metabolism are uridine 5'-diphospho-glucuronosyltransferases (UGTs), cytosolic sulfotransferases (SULTs), glutathione *S*-transferases (GSTs), methyltransferases and so on. Among these enzymes, the UGTs and SULTs are the two most important enzyme families in the phase II metabolism of drugs.

Compared with the phase I metabolism, the molecular weights (M.W.s) of the drug substances are usually more remarkably increased in the phase II metabolism. In general, the phase II metabolites tend to be less pharmacologically effective than the parent drugs, due to the possible interruption in their binding to the therapeutic targets [17]. However, it should be noted that such a judgment is not always right. For example, the 6-glucuronide of morphine is an agent with pain-relieving effects which is more potent than morphine, whereas morphine 3-glucuronide has been demonstrated to be ineffective [18]. The phase II metabolites are usually much more hydrophilic than the parent drugs and phase I metabolites. Thus it is usually difficult for them to penetrate the membrane passively [19].

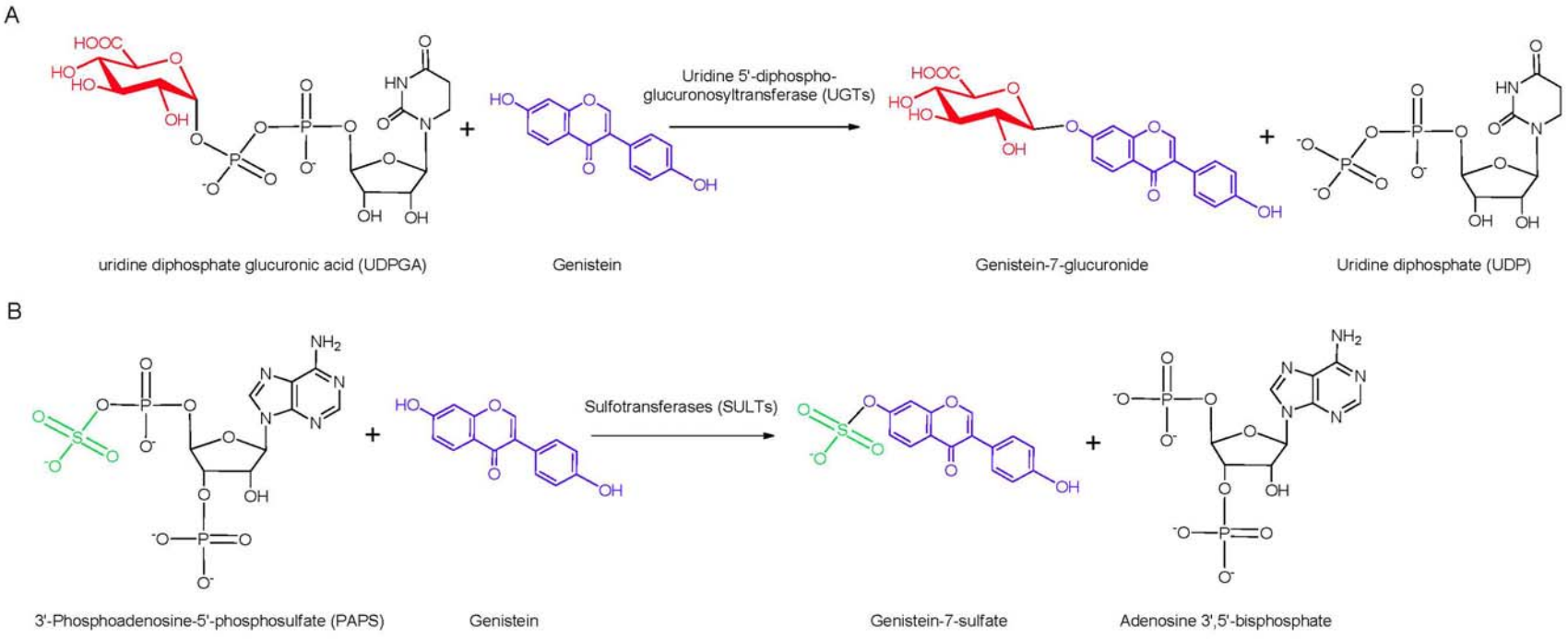

403

404 **Figure 2. Major Phase II Metabolism: Glucuronidation and Sulfation.**

405 (A) Catalyzed by uridine 5'-diphosphoglucurosyltransferase (UGTs), a glucuronic acid group is transferred from the cofactor uridine 5'-
406 diphospho-glucuronic acid (UDPGA) to genistein. (B) Genistein is also substrate for sulfotransferases (SULTs) and can be conjugated with a
407 sulfate group. The cofactor for SULTs is 3'-Phosphoadenosine-5'-phosphosulfate (PAPS).

408

1.1.2.1 **UGTs**

In the glucuronidation reactions, the glucuronosyl group were usually transferred from the cofactor uridine 5'-diphospho-glucuronic acid (UDPGA) to the substrates with –OH, -NH_2, -SH or –COOH in their structures (Figure 2, A). The resulting glucuronides are usually much more hydrophilic than their parent drugs and can be actively excreted by transporters in the intestine, liver or kidney.

As one of the most important phase II metabolism pathways, the glucuronidation of many xenobiotics and also endogenous substances is catalyzed by the UGTs in mammalians. The UGTs are membrane-bound enzymes located in the endoplasmic reticulum (ER) inside the cell. So far, the mammalian UGT superfamily gene includes 117 members, which can be divided into four families: UGT1, UGT2, UGT3 and UGT8. The human UGT genes belong to two families (UGT1 and UGT2) and three subfamilies (UGT1A, UGT2A and UGT2B) [20].

In human, UGTs are broadly distributed in many tissues and organs [21]. The expressions of UGTs in the gastrointestinal tract and liver are usually considered to be the most relevant in drug metabolism, while the UGTs in the kidney also contribute significantly to the metabolism of certain drugs [22]. The liver has the most abundant expression of UGTs in the human body, and the UGTs in the gastrointestinal tract can also conjugate drugs or natural products efficiently before they enter the systemic circulation. The UGT isoforms expressed in the liver are UGT1A1, 1A3, 1A4, 1A6, 1A9, 2B4, 2B7, 2B10, 2B11, 2B15, 2B17 and 2B28. The UGTs isoforms expressed in the gastrointestinal tract are mainly UGT1A1, 1A3, 1A4, 1A6, 2B4, 2B15 and also the non-hepatic isoforms UGT1A7, 1A8, and 1A10. The UGT isoforms in the same subfamily usually shares more than 60% homology in their amino acid residue sequences, and thus they usually have overlaps with each other in the substrate specificities but differences in binding affinities and reaction rates [23]. The *in vitro* glucuronidation by human liver or intestinal microsomes usually reveals a comprehensive efficiency of multiple UGT isoforms in the

conjugation of drugs or natural products. When the recombinant human UGT isoforms are employed, the glucuronidation rate of certain substrate by one specific UGT isoform can be determined and compared with that of the other isoforms.

1.1.2.2 **SULTs**

The sulfation is another important phase II metabolism pathway other than glucuronidation in the human body. In the sulfation reaction, the substrate will be conjugated with a sulfo group transferred from the cofactor 3'-phosphoadenosine-5'-phosphosulfate (PAPS) with the help of various sulfotransferases (Figure 2, B). The SULTs are responsible for the sulfation occurring in the metabolism of drugs and other xenobiotics. Also, the SULTs can catalyze the sulfation of many endogenous hormones and neurotransmitters [24].

To date, more than 47 mammalian SULT isoforms have been cloned and can be categorized into five distinct gene families of SULTs: SULT1, SULT2, SULT3, SULT4, and SULT5 [25]. In humans, 13 distinct SULT isoforms have been identified as SULT1A1, 1A2, 1A3, 1A4, 1B1, 1C2, 1C4, 1E1, 2A1, 2B1_v1, 2B1_v2, 4A1_v1 and 4A1_v2. Among the human SULTs, SULT1A1, 1A3, 1B1, 1E1 and 2A1 are the most important isoforms and also the most extensively studied. In the liver, SULT1A1 is the predominant isoform and it is also widely distributed in other tissues and organs such as the intestine, lung, brain and kidney [26]. The endogenous substrates for SULT1A1 activity are hormones including iodothyronines and estrogens [27, 28]. The xenobiotic substrates of SULT1A1 are usually simple phenolic compounds or amides like acetaminophen and minoxidil. In addition to SULT1A1, SULT2A1, 1B1 and 1E1 are also substantially expressed in the human liver [26]. SULT1A3 and SULT1B1 are the most abundant isoforms in the human intestine, followed by SULT1A1, 1E1 and then 2A1 [26]. SULT1A3 is expressed in the developing human fetal liver, but not expressed in adult human liver. Besides simple phenolic compounds, the substrates of SULT1A3 include endogenous catecholamines such as the neurotransmitters dopamine and norepinephrine [29]. Like SULT1A1, SULT1B1 catalyzes the

sulfation of iodothyronines [29]. Estrogens are also substrates of SULT1E1 as well as SULT1A1. SULT2A1 is responsible for the sulfation of steroids including dehydroepiandrosterone (DHEA) [30]. The SULTs can also participate in the detoxifying process of carcinogens such as 2-acetamidofluorene and 2-amino-1-methyl-6-phenylimidazo[4,5-b]pyridine (PhIP) [31].

1.1.3 Transporter-mediated excretion of drug metabolites

The transporters are integral transmembrane proteins which mediate the uptake or efflux of certain substances across the cellular membrane. After metabolism inside the enterocytes or hepatocytes, some phase I metabolites and most phase II metabolites of the drugs and xenobiotic are too hydrophilic to penetrate the cellular membrane by passive diffusion. The excretion of these metabolites is mainly dependent on active transportation by the efflux transporters. The most pharmacologically relevant efflux transporters in humans are members in the ATP-binding cassette (ABC) transporters family [32]. The members of the ABC transporters superfamily are widely distribute in nature and can be found in different species from prokaryotes to humans. An ABC transporter usually consist two protein domains: the transmembrane domain (TMD) and the nucleotide-binding domain (NBD)[32]. The membrane-spanning TMD binds to the substrates and transport them across the membrane by conformational changes. The NBD is responsible for the binding and hydrolysis of adenosine triphosphate (ATP), which provides energy for the transportation of substrates across the membrane [33]. In humans, a total of 49 ABC transporters are known and can be classified into 7 families [32]. The most important efflux transporters involved in the excretion of the drugs and metabolites are P-glycoprotein (P-gp, or multidrug resistance protein 1, MDR1), breast cancer resistance protein (BCRP), and multidrug-resistant proteins (MRPs).

1.1.3.1 **P-gp**

P-gp is a glycoprotein which belongs to the ABCB family. The role of P-gp in regulating the distribution and bioavailability of drugs is the most extensively studied among all the efflux transporters in human [34]. P-gp is abundantly expressed in the small intestine, colon, liver, kidney and also the brain-blood barrier (BBB) [35]. The substrates of P-gp are excreted into the intestinal lumen, bile and urine, or prevented from entering the brain extracellular fluid. P-gp shows broad substrate specificity and plays an important role in the transportation of a lot of drugs including glucocorticoids, chemotherapeutic agents, protease inhibitors, immunosuppressive agents, cardiac glycosides and so on [36]. Also, the endogenous substances such as lipids, steroids, peptides and bilirubin can also be transported by P-gp. Some cancer cells expressing high levels of P-gp are resistant to multiple therapeutic agents due to the function of P-gp as an efflux transporter [37, 38]. Meanwhile, it should be noticed that the function of P-gp can be inhibited by many drugs including cyclosporine and verapamil, leading to potential drug-drug interactions in humans [39].

1.1.3.2 **BCRP**

BCRP belongs to the ABCG family. In humans, it is expressed in the apical sides of the intestinal epithelium, the canalicular side of hepatocytes, and the proximal tubule brush border membrane kidney [40]. BCRP enhances the excretion of the drugs and other xenobiotics into the intestinal lumen, bile and urine [41]. It is also expressed in BBB and help to prevent xenobiotics from entering the brain extracellular fluid [42]. Besides those, BCRP is significantly expressed in the placenta to help protect the fetus from xenobiotics in the maternal circulation [43]. In the lactating mammary gland, the function of BCRP is to excrete vitamins into milk [44]. The substrates of BCRP include the drugs (mitoxantrone, SN-38, flavopiridol, cimetidine and so on), the drug metabolites (the glucuronides and sulfates), the xenobiotics (i.e., PhIP), and the endogenous substrates (estrone 3-sulfate, folic acid and so on) [45].

1.1.3.3 **MRPs**

The MRPs are the members in the ABCC family. This family contains 9 transporters which are often referred as MRPs, including MRP1-8 and ABCC12 [46]. Like P-gp and BCRP, the MRPs are also widely distributed in human tissues, especially the intestine, liver, kidney and BBB [46]. In the human intestinal epithelium, MRP2 and MRP4 are expressed on the apical side, while MRP1, MRP3, and MRP5 are expressed on the basolateral side [47]. In the hepatocytes, MRP1, MRP3, MRP4 and MRP6 are expressed on the sinusoidal side and MRP2 is expressed on the canalicular side [48]. The main function of MRPs is to transport organic anions, especially the glucuronides, sulfates or glutathione conjugates of the xenobiotics and endogenous substances across the cellular membrane [49]. They can also transport bile salts, bilirubin glucuronide, cysteinyl leukotrienes and prostaglandins [50]. Among all the MRPs, MRP1 and MRP2 are the most fully characterized for the functions, while the continuing studies are revealing more and more information about the other MRPs.

1.1.4 The first-pass effect in oral drug administration

After oral administrations, the drugs absorbed in the gastrointestinal tract may be extensively metabolized in the intestinal epithelium and/or liver before they reach the systemic circulation and reach the target tissue in the human body. This is the "first-pass" effect in oral administration which may limit the oral bioavailability of many drugs and natural products [51]. Because the first pass effect usually leads to reduced drug concentrations in the systemic circulation and target tissues, drug candidates with substantial first-pass metabolism are conventionally not favored in drug development [17]. The representative drugs with a significant first-pass effect include morphine, midazolam, raloxifene, propranolol, cimetidine, lidocaine and many more [52, 53].

1.1.4.1 **Enteric circulation**

In the gastrointestinal tract, the absorption of hydrophobic drugs largely depends on passive diffusion of the drug molecules from the lumen into the epithelium [54]. In the presence of

metabolic enzymes abundantly expressed in the enterocytes, the drug substances can be rapidly biotransformed to the metabolites after the absorption [55]. With the help of transporters embedded on the apical or basolateral sides of the gastrointestinal epithelium, the metabolites which are much more hydrophilic than their parents can be excreted [53]. The metabolites excreted to the intestinal lumen, especially the phase II metabolites such as glucuronides and sulfates, can be hydrolyzed by bacterial enzymes from the microflora in the gastrointestinal tract (Figure 3). The reproduced drug parents are available for absorption again. Although the enteric circulation decreases the absorption efficacy of drugs, the retention time of drugs in the intestinal lumen is prolonged, which may promote the efficacy of therapeutic agents in the treatment of diseases in the gastrointestinal tract [56].

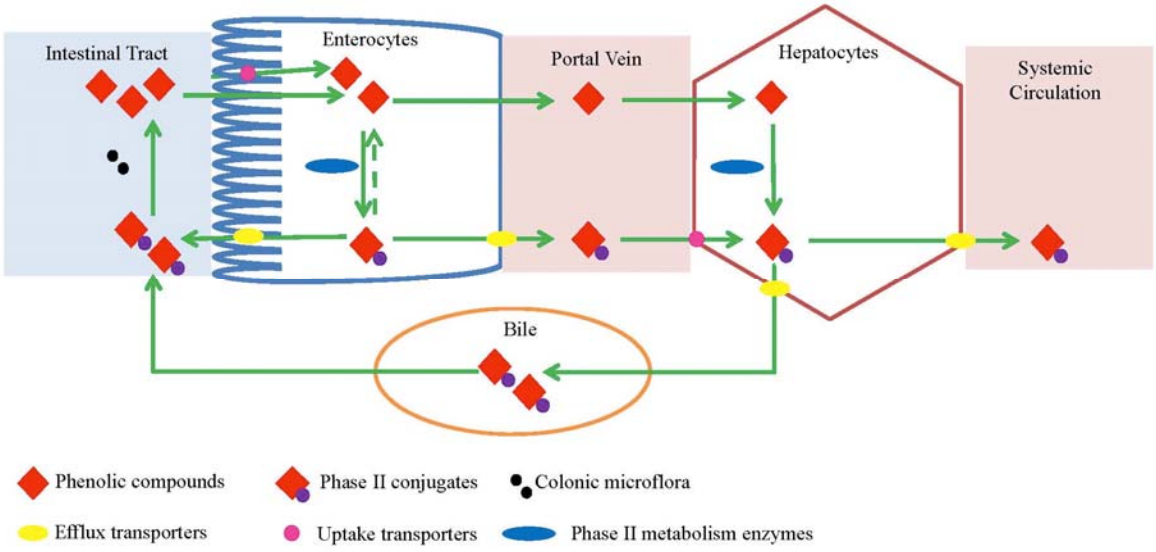

Figure 3. Enteric and enterohepatic circulation of the phenolic compounds and their phase II metabolites *in vivo*.

The intestine and liver are the major sites for phase II metabolism of the phenolic compounds in humans. The phenolic compounds can be conjugated by phase II metabolism enzymes such as UGTs and SULTs. In the enterocytes, the conjugates can be excreted to the intestinal lumen by efflux transporters. In the hepatocytes, the conjugates can also be excreted back to the intestine through the bile duct. The conjugates are hydrolyzed by the colonic microflora to generate unconjugated phenolic compounds which are available for reabsorption. The two processes are termed as enteric and enterohepatic circulation, respectively.

1.1.4.2 **Enterohepatic circulation**

The enterohepatic circulation refers to the circulation of certain xenobiotics and endogenous substances (e.g., bile salts and bilirubin) between the intestinal tract and liver (Figure 3) [57]. After the absorption in the intestinal tract, the drugs delivered to the liver by portal vein can be efficiently extracted by the hepatocytes. With or without metabolism, the drugs and/or their metabolites excreted to bile from the canalicular side of hepatocytes will reach the intestinal tract eventually [58]. The absorption, extraction, excretion and reabsorption procedures create a cycle which limits the oral bioavailability of drugs. For the drugs and natural products which can be extensively conjugated as glucuronides and sulfates in the intestine or liver, the hydrolysis of the phase II metabolites by bacterial hydrolases in the intestinal tract is a prerequisite for the reabsorption [59].

1.1.4.3 **Low oral bioavailability of the natural phenolic compounds**

The natural phenolic compounds include phenolic acids, flavonoids, stilbenoids, coumarins, lignans, curcuminoids, etc [60]. The anti-aging, anti-oxidation, anti-inflammation, and anti-proliferation effects of the natural phenolic compounds have been successfully demonstrated in many studies which were conducted *in vitro* or animal models [61, 62]. However, their beneficial effects on human health are still questionable due to the low oral bioavailability in humans which results in the low plasma concentration and/or local concentrations in the target tissues or organs. The major reason for the low oral bioavailability of the natural phenolic compounds is usually the extensive first-pass metabolism in the intestinal tract and/or liver [60]. The phenolic can be excellent substrates of the phase II metabolic enzymes, mainly UGTs and SULTs [63]. The conjugates of phenolic compounds are excreted from the apical side of enterocytes to the intestinal lumen, or from the cannalicular side of hepatocytes to the intestinal tract via the bile duct. Following hydrolysis of conjugates by bacterial enzymes and reabsorption, the enteric and

579 enterohepatic circulations are completed. The first-pass elimination substantially decreases the
580 portion of phenolic compounds entering the systemic circulation in humans.

581 1.2 Introduction to the cyclooxygenase-2 inhibitors

582 1.2.1 Cyclooxygenases

583 The prostaglandins (PGs) are a family of long chain lipid compounds with diverse physiological
584 and pathological effects in animals and humans [64]. The PGs are very important endogenous
585 hormone-like substances which can be produced in almost all the tissues in the human body. They
586 can be detected in almost all the tissues and work in an autocrine or paracrine manner [65]. The
587 main physiological functions of PGs include inducing constriction or dilation in vascular smooth
588 muscle cells, decreasing intraocular pressure, inducing aggregation or disaggregation of platelets,
589 controlling cell growth, regulating calcium movement, regulating hormones, protection of the
590 intestinal epithelium from irritations, regulating the glomerular filtration rate in kidney, etc [66].
591 They also play very important roles in pathological conditions such as pain, fever, inflammation,
592 and tumorigenesis [67].

593 The PGs are derived enzymatically from fatty acids via several steps with the help of different
594 enzymes in each step. Arachidonic acid (AA), a typical starting substance in the biosynthesis
595 pathways of PGs, is freed from the inner side of the cellular membrane after the cleavage of
596 phospholipids by phospholipase A_2 (PLA_2), phospholipase C (PLC), or phospholipase D (PLD)
597 [68]. The first two steps (*bis*-dioxygenation and subsequent reduction) in the biotransformation of
598 AA are catalyzed the cyclooxygenases (COXs), a family of enzymes which are responsible for
599 the production of PGH_2 [69]. The COXs are membrane-bound glycoproteins containing a heme as
600 the cofactor. They usually function as homo-dimmers embedded in the subcellular endoplasmic
601 reticulum. Each subunit in the dimers comprises an epidermal growth factor (EGF) domain, a
602 membrane binding domain, and a catalytic domain which contains the active sites [70]. The

603 cyclooxygenase and peroxidase functions of the COXs depend on respective active sites, and the
604 two active sites are separated but linked. The nascent COXs are not active until endogenous
605 oxidants like a hydroperoxide bind to the peroxidase site and oxidize the heme to a ferryl-oxo-
606 porphyrin radical [71]. The radical then abstracts an electron from tyrosine 385, resulting in the
607 primed cyclooxygenase active site with a tyrosyl radical. After that, in the cyclooxygenase active
608 site, the pro-*S* hydrogen is abstracted from carbon-13 of the substrate AA by the tyrosyl radical,
609 which initiates the catalyzing circulation in the cyclooxygenase active site. The circulation
610 involves two molecules of oxygen and quenching/regeneration of the tyrosyl radical, producing
611 one molecule PGG_2 in each turnover as the first intermediate in the biosynthesis of PGs (Figure
612 4). PGG_2 then binds to the peroxidase active site and is reduced to the final product PGH_2 [71].

613 The half-life of PGH_2 is only a few minutes and it serves as the substrate of different enzymes
614 which are the downstream elements of COXs in the biosynthesis of PGs [72]. For example, PGH_2
615 is biotransformed to PGE_2 by PGE_2 synthase, to PGD_2 by PGD_2 synthase, to prostacyclin (PGI_2)
616 by PGI_2 synthase, or to thromboxane A_2 (TXA_2) by TXA_2 synthase. PGI_2 and TXA_2 are both
617 unstable and rapidly degrade to 6-keto-$PGF_{1\alpha}$ and thromboxane B_2 (TXB_2), respectively (Figure 5)
618 [73]. These synthases are usually tissue-specifically expressed in humans. Without the presence
619 of the downstream synthases, PGH_2 produced by the COXs undergoes rapid non-enzymatic
620 breakdown to PGE_2, PGD_2, and $PGF_{2\alpha}$ [74].

621 So far, two COX isoforms have been discovered in humans and the other mammalians [75].
622 Sharing 65% homology in the amino acid sequence and the similar catalytic pockets, human
623 COX-1 and COX-2 have the same function in the biotransformation of AA to PGH_2 but differ
624 from each other in many aspects including the expression, the substrate-binding affinity, the
625 enzymatic kinetics, the distribution in tissues, the regulation of expression, the post-translational
626 modification, the modulation of activity, etc (Figure 6) [76, 77].

627

628

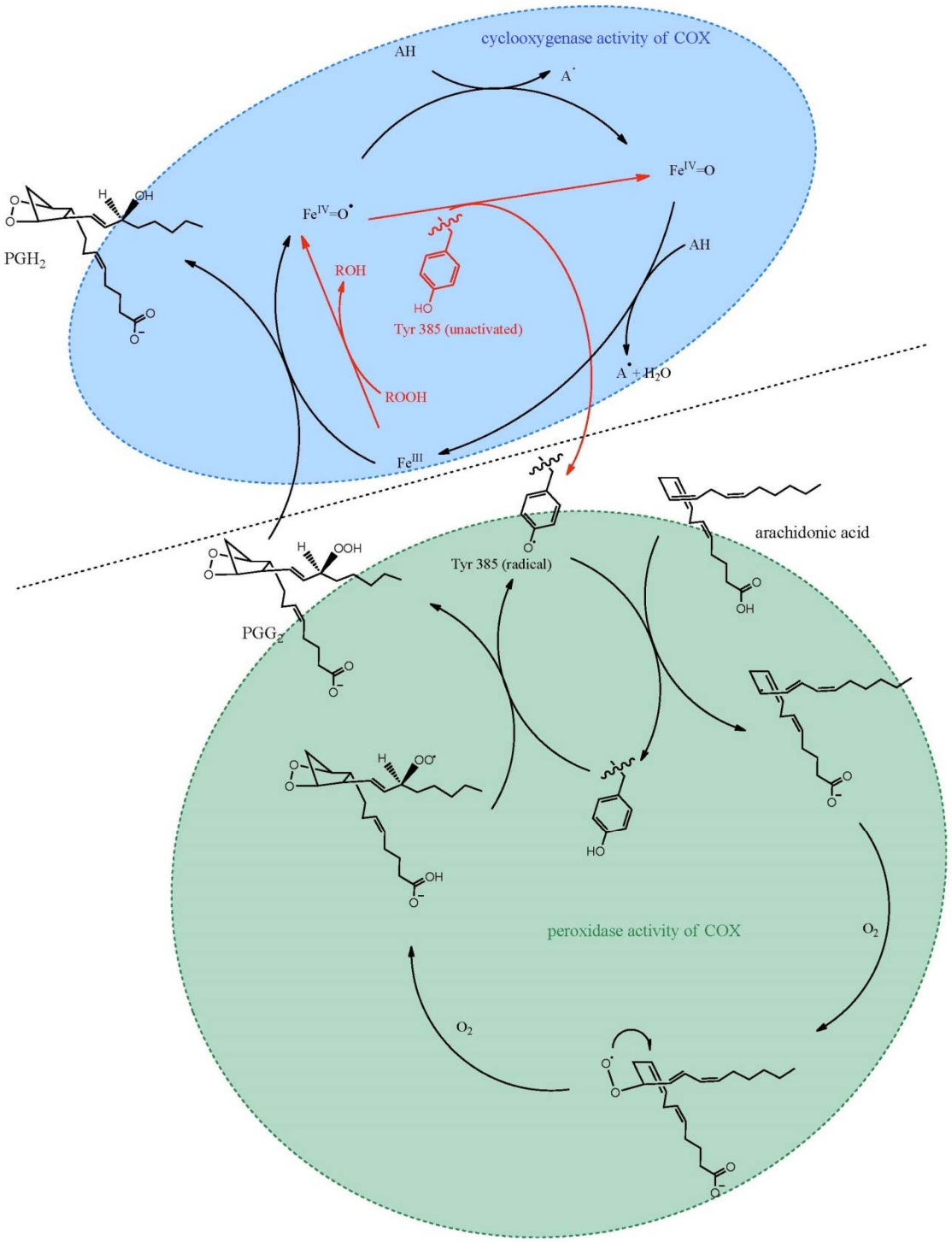
cyclooxygenase activity of COX
AH
A·
Fe^IV=O
Fe^IV=O·
AH
PGH2
ROH
HO
Tyr 385 (unactivated)
A· + H2O
ROOH
Fe^III
Tyr 385 (radical)
arachidonic acid
PGG2
peroxidase activity of COX
O2
O2

629

630

Figure 4. The catalytic mechanisms of COXs.

The COXs have both cyclooxygenase (green) and peroxidase (blue) activities. The nascent COXs are not active until the heme in the peroxidase active site is oxidize to a ferryl-oxo-porphyrin radical which will lead to the activation of tyrosine 385 in the cyclooxygenase active site (red). After the tyrosyl radical is formed, the catalyzing circulation in the primed cyclooxygenase active site will start to transform the substrate AA to PGG_2. The circulation involves two molecules of oxygen and quenching/regeneration of the tyrosyl radical, producing one molecule PGG_2 in each turnover. The PGG_2 released from the cyclooxygenase active site will then be the substrate in peroxidase active site. It is reduced to the final product PGH_2 (derived from Rouzer et al [71].).

642

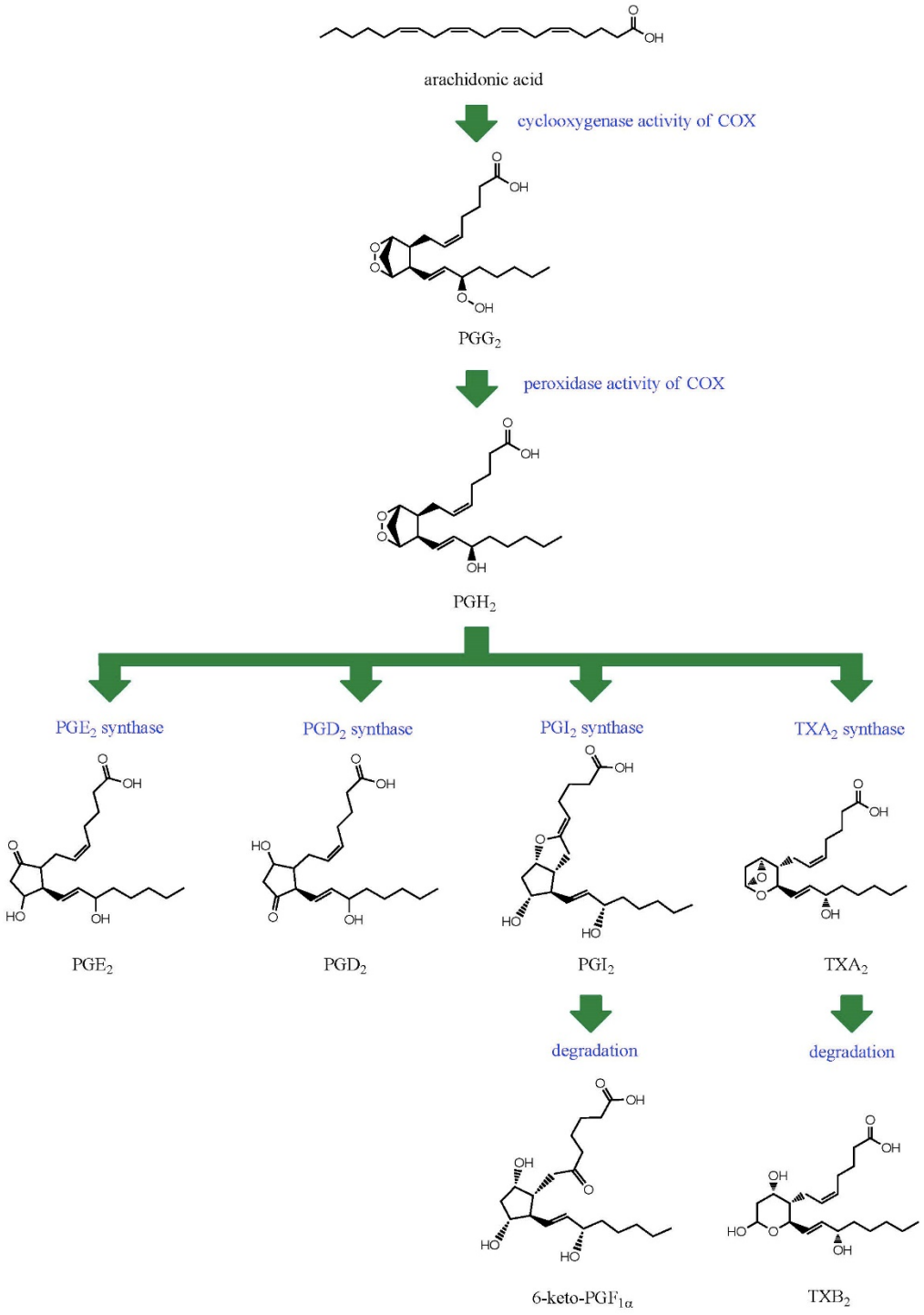
arachidonic acid
cyclooxygenase activity of COX
PGG2
peroxidase activity of COX
PGH2
PGE2 synthase
PGD2 synthase
PGI2 synthase
TXA2 synthase
PGE2
PGD2
PGI2
TXA2
degradation
degradation
6-keto-PGF1α
TXB2

643

644

Figure 5. The prostaglandins derived from COX pathways.

The half-life of PGH_2 is only a few minutes and it serves as the substrate of the enzymes other than COXs. PGH_2 is transformed to PGE_2 by PGE_2 synthase, to PGD_2 by PGD_2 synthase, to prostacyclin (PGI_2) by PGI_2 synthase, or to thromboxane A_2 by TXA_2 synthase. PGI_2 and TXA_2 are both instable and rapidly degrade to 6-keto-$PGF_{1\alpha}$ and TXB_2, respectively. These synthases are usually tissue-specifically expressed in humans. In the whole pathway, the rate-limiting step is catalyzed by the COXs.

653

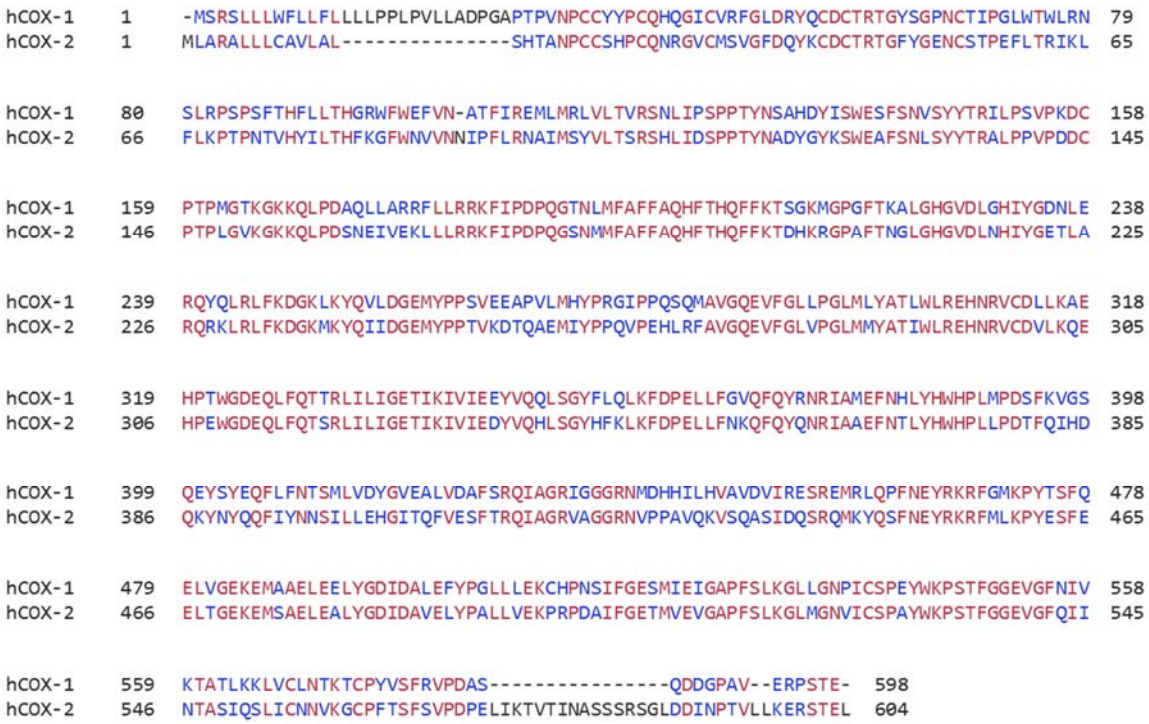

654

655 **Figure 6. The amino acid sequences of human COX-1 and COX-2.**

656

657

1.2.1.1 **Human COX-1**

COX-1 was discovered in animals and humans more than 40 year ago and first purified in 1970s [78]. Before the discovery of COX-2, COX-1 was the unique COX isoform for almost 20 years although the evidence of multiple COXs attracted the attention of researchers from the early 1970s.

Human COX-1, or prostaglandin-endoperoxide synthase 1 (PTGS1), is a 70kDa protein comprising 599 amino acid residues. It is encoded by the "housekeeping" *PTGS1* gene with the chromosomal locus as 9q32-q33.3 [79]. This gene is transcribed to a 2.8kb mRNA, which is more stable than that for COX-2 [80]. The expression of COX-1 protein in human body is constitutive and ubiquitous. The PGs generated by the COX-1-initiated pathway have various physiological functions and are required for keeping the homeostasis in human body. For example, COX-1-derived PGs contribute to the maintenance of mucosal integrity in the gastrointestinal tract, the normal platelet function, and the regulation of renal blood flow [81]. Thus in most cases, when the functions of COX-1 are altered, the homeostasis will be unfavorably disrupted. The inhibition of COX-1 activity in the gastrointestinal tract impairs the functions of mucosa and leads to ulcer and bleeding [82]. In certain circumstances, the inhibition of COX-1 activity can be beneficial. For example, the decreasing of COX-1-derived TXA_2 in platelets may contribute to the reducing of cardiovascular events [83].

1.2.1.2 **Human COX-2**

Human COX-2, or PTGS2, was firstly identified in 1991 [84]. It is a 72kDa protein comprising 604 amino acid residues. It is encoded by the *PTGS2* gene with the chromosomal locus as 1q25.2-q25.3 [79]. The mRNA in the transcription of *PTGS2* is with a length of 4.0kb, which is longer and less stable than the mRNA of COX-1 [70]. Since the discovery of COX-2 protein, it is conventionally acknowledged as an inducible COX isoform associated with pathological

682 conditions, especially inflammation and tumorigenesis [85]. During inflammation, the expression
683 levels of COX-2 in many tissue and cells are rapidly and dramatically increased upon the
684 stimulation of inducers and pro-inflammatory cytokines. For example, in the inflammatory
685 arthritis, COX-2 overexpression was observed in the synoviocytes, chondrocytes, osteoblasts,
686 monocytes/macrophages, and endothelial cells in the blood vessel of joint [86, 87]. *PTGS2* is also
687 an oncogene which promotes neoplasia, tumorigenesis, tumor angiogenesis and metastasis. The
688 overexpression of COX-2 protein has been reported in many human malignancies including lung
689 cancer [88], breast cancer [89], colorectal cancer (CRC) [90], prostate cancer [91], oral cancer
690 [92], etc. In colon cancer tissues from subjects diagnosed with CRC, the expression of COX-2 is
691 largely enhanced in cancer cells, inflammatory cells, vascular endothelial cells, and fibroblasts of
692 the lesional tissues [93]. The expression of COX-2 promotes the invasiveness and metastatic
693 potential of colon cancer cells as well as the angiogenesis in the tumor [94-96].

694 Since long ago, the researches focusing on the induction of COX-2 expression in the
695 inflammation and tumorigenesis are so impressive that COX-2 protein is principally considered
696 as an “inducible” isoform which is mainly involved in pathogenesis. However, more and more
697 evidence from plenty of studies indicate the physiological roles or homeostatic functions of COX-
698 2. For example, O'Neill et al. quantitated the mRNA levels of COX-1 and COX-2 in multiple
699 human tissues including lung, brain, pancreas, kidney, liver, mammary gland, stomach, small
700 intestine, etc., and found that all tissues contained the mRNA of both COX-1 and COX-2 [80].
701 The mRNA level of COX-2 was equal to that of COX-1 in prostate, and in lung where the COX-2
702 mRNA was the most abundant among tissues, the COX-1 mRNA level was two folds lower. The
703 genetic depletion of COX-2 in mice leads to a reduced survival rate and progressive renal
704 diseases, while the female knockout mice have lower fertility due to the failure of ovulation,
705 fertilization, and embryo implantation [97]. Most prominently, accumulating clinical experience
706 about the risk of cardiovascular events associated with specific COX-2 inhibition (see below) has

also revealed that the function of vascular endothelium can be modulated by COX-2-derived PGs [98].

1.2.2 Traditional NSAIDs

Although the COX enzymes were identified and characterized in only the past 40 years, the agents with analgesic and antipyretic effects have been employed in the treatment of infections and inflammatory diseases by humans from a very long time ago to nowadays. The oldest and most famous analgesic, aspirin, was a bioactive ingredient in herbal medicine (i.e., the crude extract of willow bark) used by the ancient Egyptians more than 3000 years ago [99]. Today, to be distinguished from the anti-inflammatory steroids, these pain-killing and fever-reducing drugs are given the name of non-steroidal anti-inflammatory drugs (NSAIDs), including aspirin (Figure 7, **1**), ibuprofen (**2**), naproxen (**3**), indomethacin (**4**), sulindac (**5**), diclofenac (**6**), piroxicam (**7**), mefenamic acid (**8**) and so on. In the treatment of inflammation by the NSAIDs, the main underlying pharmacological mechanism has been clarified as the inhibition of the COX activity in the inflamed tissues.

Before the inventions of the selective COX-2 inhibitors, most of the NSAIDs equivalently inhibit the two COX isoforms or exhibit a slight selectivity to inhibit COX-1 [100]. The most prominent side effect of these NSAID is that they increase the risk of gastrointestinal events such as nausea, vomiting, dyspepsia, ulcer, diarrhea, and bleeding in patients, especially with high doses [101]. The low oral tolerability is caused by the direct and indirect irritations in the gastrointestinal tract. Many NSAIDs are acidic compounds with carboxyl groups in their molecular structures, which can irritate the gastrointestinal epithelium directly [102]. More decisively, the inhibition of COX-1 activity in the gastrointestinal epithelium decreases the production of PGs which contribute to maintain the mucosal integrity [101]. The NSAIDs without significant preference in inhibiting the two COX isoforms are referred as the traditional NSAIDs.

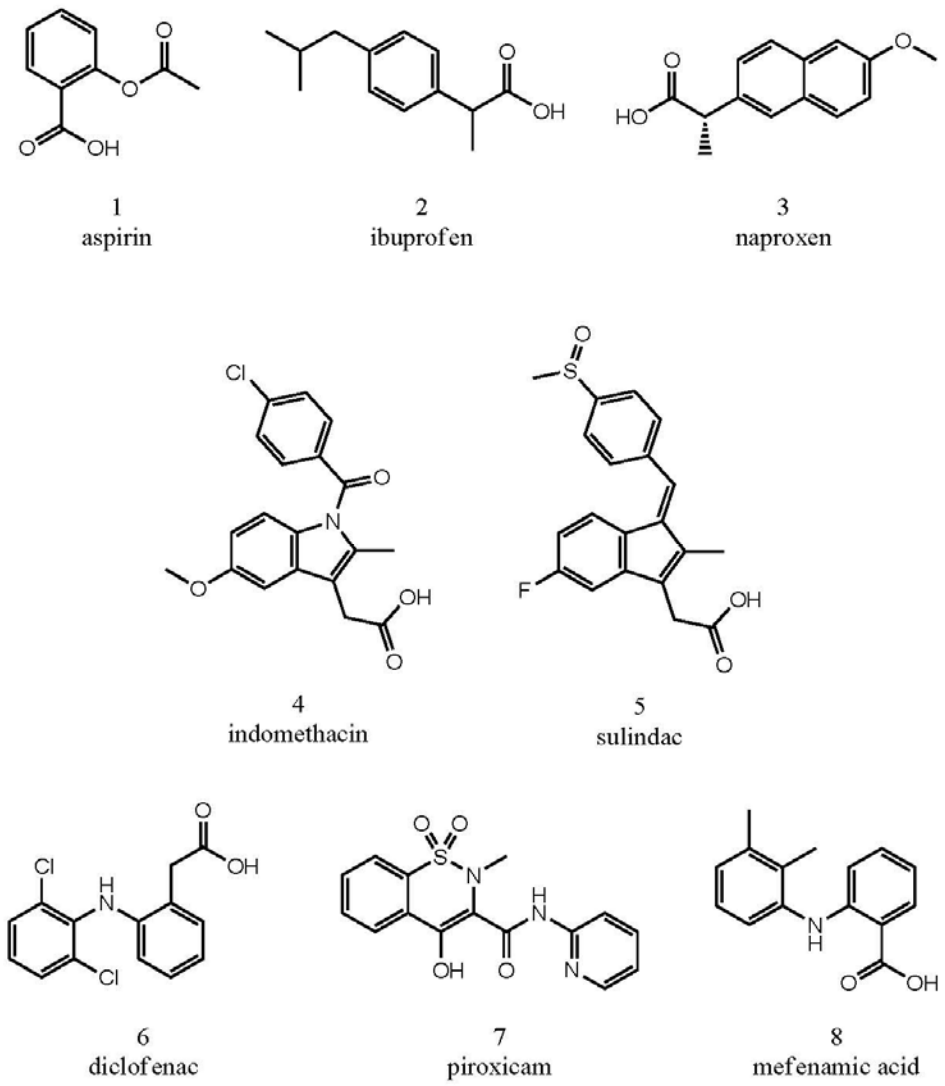

731

732 **Figure 7. Traditional NSAIDs.**

733

734

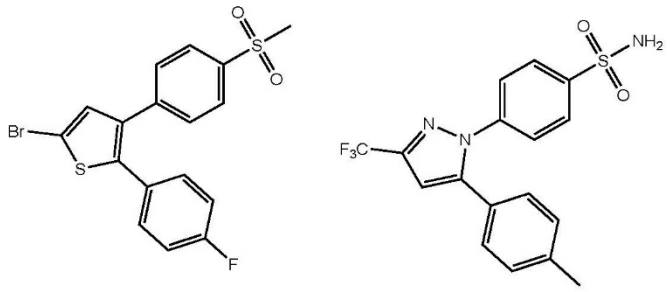

1
DuP-697

2
celecoxib

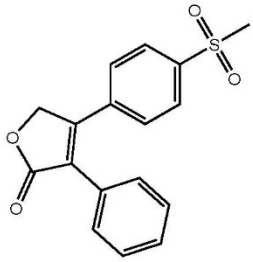

3
rofecoxib

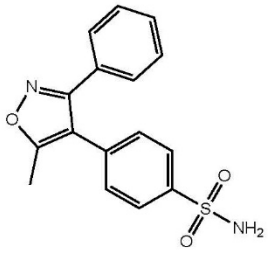

4
valdecoxib

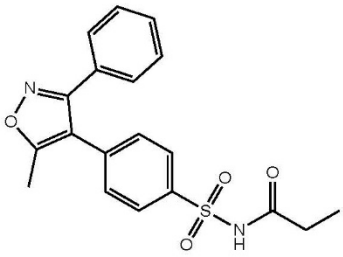

5
parecoxib

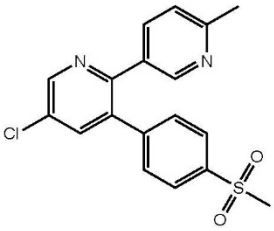

6
etoricoxib

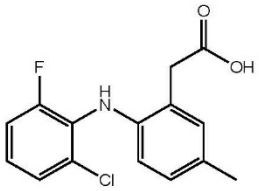

7
lumiracoxib

735

736 **Figure 8. Selective COX-2 inhibitors.**

737

738

1.2.3 The development of selective COX-2 inhibitors

Before the existence of COX-2 in animals and human was confirmed, a compound, DuP-697 (Figure 8, **1**) was already reported to possess potent anti-inflammatory effect but not induce the gastrointestinal events like the traditional NSAIDs [103]. After the discovery of the second COX isoform in animals and humans, a new class of NSAIDs was proposed as the selective inhibitors of human COX-2 activity. Driven by the hypothesis that COX-1 is constitutive and COX-2 is inflammatory, the selective COX-2 inhibitors were developed as promising agents to treat inflammations without the gastrointestinal side effects of the traditional NSAIDs [104]. Since verified as the first selective COX-2 inhibitor, DuP-697 served as the building-block in the development of the consequent selective COX-2 inhibitors.

1.2.3.1 **The structural basis for the selective COX-2 inhibition**

The successful development of the selective COX-2 inhibitors depended on the differences of the active sites between COX-1 and COX-2. The substitutions of Ile523, His513, and Ile434 in COX-1 by Val523, Arg513, and Val434 in COX-2 in the amino acid sequence account for the conformational changes in the active sites from COX-1 to COX-2 (Figure 9) [105, 106]. The substitution of Ile523 in COX-1 by Val523 in COX-2 is usually considered as the most critical [107]. The side chain of valine is less bulky than that of isoleucine, resulting in a side channel in the active site of COX-2 which is not present in that of COX-1 [105, 106]. Meanwhile, the substitution of Ile434 in COX-2 by Val434 also contributes to making a larger volume in the active site in COX-2. The Arg513 in COX-2 are an important residue in the interaction between COX-2 and the selective COX-2 inhibitors through their 4-sulfamoylphenyl or 4-(methylsulfonyl)phenyl group. The selective COX-2 inhibitors with a diaryl heterocyclic ring structure are endowed with high binding affinities in the active pocket of COX-2, but they are not able to enter the active pocket of COX-1 which is smaller than that of COX-2 [106]. In contrast,

763 the traditional NSAIDs like aspirin, ibuprofen, and naproxen are able to inhibit COX-1 and COX-
764 2 equivalently due to their relatively simple structures [108].

765

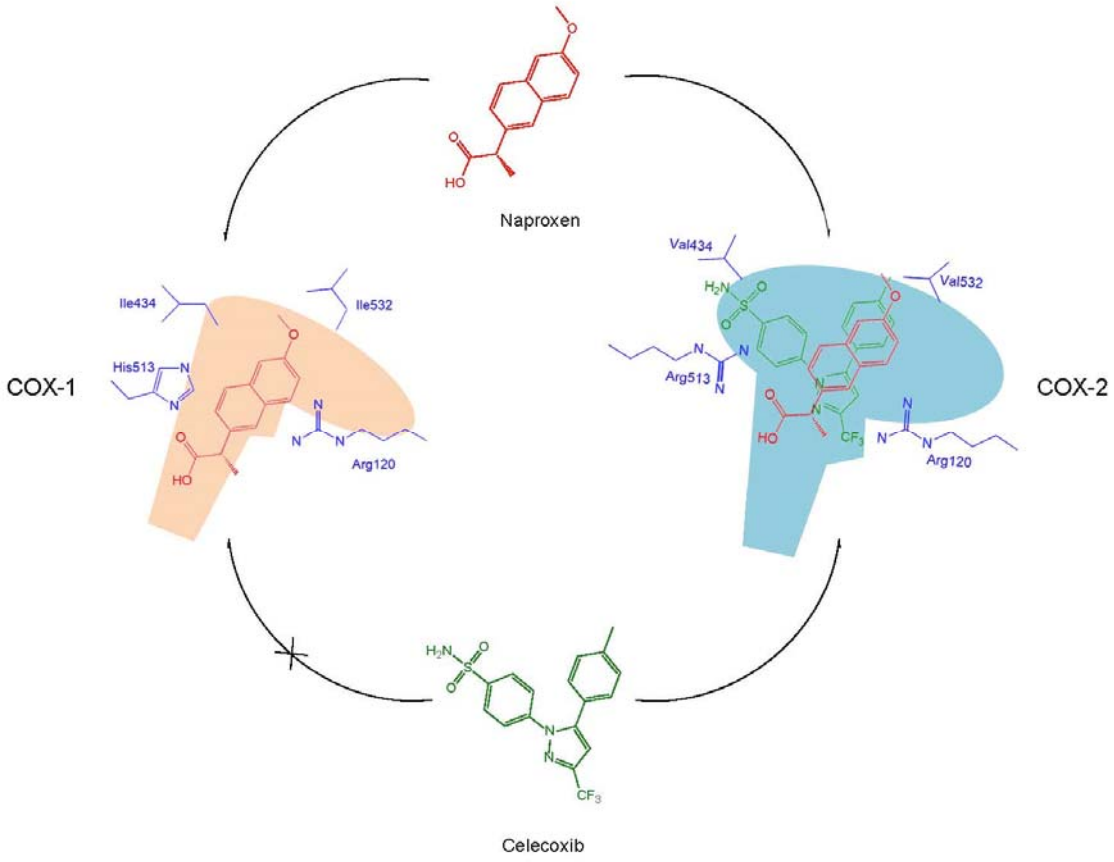

766

767 **Figure 9. The selectivity of inhibitors between human COX-1 and COX-**
768 **2.**

769 The substitutions of Ile523, His513, and Ile434 in COX-1 by Val523, Arg513, and Val434 in
770 COX-2 in the amino acid sequence result in the conformational changes in the active sites from
771 COX-1 to COX-2. The substitution of Ile523 in COX-1 by Val523 in COX-2 creates a side
772 channel in the active site of COX-2 which is not present in that of COX-1. The selective COX-2
773 inhibitors with a diaryl heterocyclic ring structure are endowed with high binding affinities in the
774 active pocket of COX-2, but they are not able to enter the active pocket of COX-1. In contrast,
775 the traditional NSAIDs like aspirin, ibuprofen, and naproxen are able to inhibit COX-1 and COX-
776 2 equivalently due to their relatively simple structures (derived from Grosser et al. [108]).

777

1.2.3.2 **The various efficacy of the selective COX-2 inhibitors**

The main advantage of the selective COX-2 inhibitors over the traditional NSAIDs is that they bring significantly lower adverse side effects in the gastrointestinal tract to patients with inflammations. For example, Langman et al. reported that compared with treatment with ibuprofen and diclofenac, treatment with rofecoxib in patients with osteoarthritis (OA) was associated with a significantly lower incidence of upper gastrointestinal tract perforations, ulcers, and bleedings [109]. Hunt et al. reported that treatment with etoricoxib reduced the incidence of endoscopically detected ulcers by approximately 50% compared with treatment with the traditional NSAIDs [110]. A similar conclusion was also made for celecoxib in a randomized controlled trial studying the celecoxib long-term arthritis safety [111]. The high gastrointestinal safety of the selective COX-2 inhibitors led to their successful launch in the market and also the popularity in patients with inflammatory diseases.

Also, because COX-2 is substantially involved in tumorigensis, the selective COX-2 inhibitors have been actively investigated as promising agents in the treatment and chemoprevention of human malignancies, primarily CRC [112]. In the Prevention of Colorectal Sporadic Adenomatous Polyps (PreSAP) trial, daily use of 400 mg celecoxib reduced the occurrence of colorectal adenomas in patients within three years after polypectomy [113]. In the Adenomatous Polyp Prevention on Vioxx (APPROVe) trial, a daily dose of 25 mg rofecoxib significantly reduced the recurrence of colorectal adenomas in patients [114]. In addition, the efficacy of the selective COX-2 inhibitors in the treatment of neuroinflammation in Alzheimer's disease (AD) has also been investigated in several clinical trials, but the results from different studies were controversial and no definite conclusion can be made before further studies [115-117].

1.2.3.3 **The cardiovascular toxicity of the selective COX-2 inhibitors**

Although the selective COX-2 inhibitors were successfully developed with a lower incidence of gastrointestinal events in patients, their adverse side effects converged in the cardiovascular systems and finally resulted in the withdrawn of several drugs from the market.

When the efficacy of celecoxib and rofecoxib in the chemoprevention of CRC was demonstrated in clinical trials, severe adverse side effects in the cardiovascular system were also observed in the patients taking daily doses of celecoxib or rofecoxib. In the Adenoma Prevention with Celecoxib (APC) trial, the risk of cardiovascular events including stroke, myocardial infarction and heart attacks was increased to 2.3 and 3.4 folds of that in placebo group by 200 mg or 400 mg celecoxib twice daily, respectively [118]. In the APPROVe, the risk was increased to 1.9 folds of that in placebo group by a daily dose of 25 mg rofecoxib [119]. Based on the results in relevant clinical trials, the concern about the cardiovascular toxicity of the selective COX-2 inhibitors resulted in the voluntary withdrawn of rofecoxib from the market by Merck, and the use of all the other selective COX-2 inhibitors is suggested to be limited in patients without appropriate alternatives, as well as only in the lowest dose and for the shortest duration necessary [120].

The reason for the cardiovascular toxicity of the selective COX-2 inhibitors is still not very clear. In recent years, the physiological roles of COX-2-derived PGs attract more and more attentions from researchers and the concept that COX-2 is mainly pathological has been largely challenged. Many experimental results support a hypothesis that selective inhibition of COX-2 in the blood vessels may lead to disruption of the hemostatic balance between different PGs [108]. This hypothesis proposes that when the production of COX-2-derived PGI_2 by the vascular endothelium was decreased, COX-1-derived platelet thromboxanes promote thrombogenesis, hypertension, and atherogenesis, which lead to the toxicity in the cardiovascular system (Figure 10). According to this hypothesis, in previous studies on the traditional NSAIDs, the cardiac protection provided by low-dose aspirin in patients can be attributed to the preferential inhibition of COX-1 in the platelets [108, 121].

826

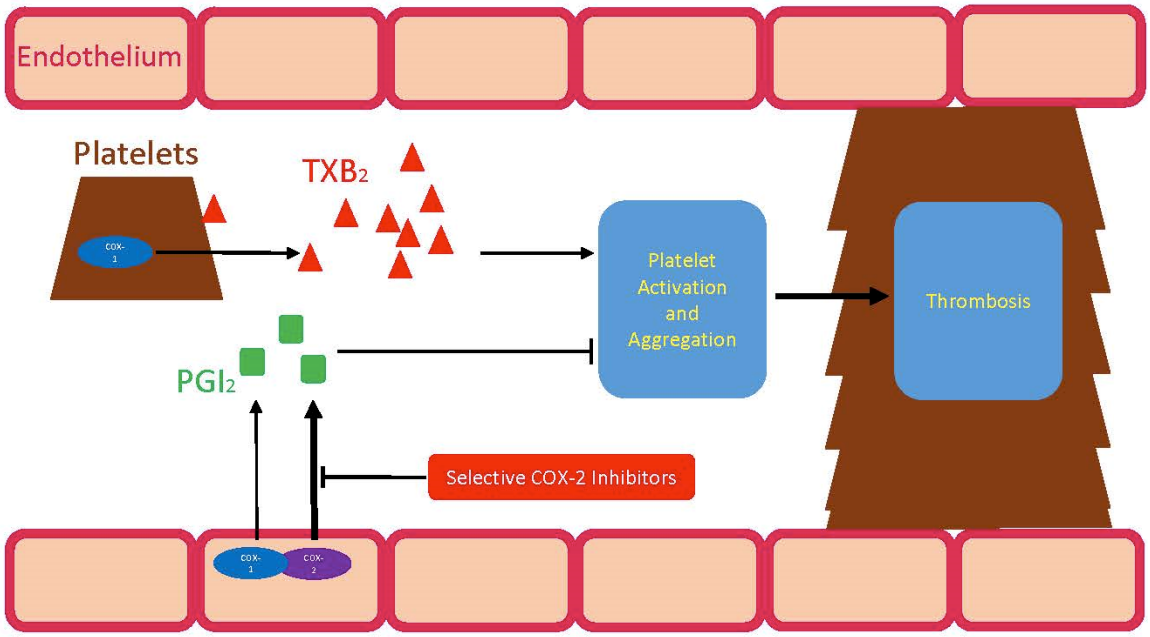

827

828 **Figure 10. The hypothesis that the selective inhibition of COX-2**
829 **disturbs vascular PG homeostasis and lead to cardiovascular events.**

830 In the vascular endothelium, the predominant PG derived from COX-1 and COX-2 is PGI_2, which
831 inhibits platelet activation and aggregation. However, in the platelet, only COX-1 is expressed
832 and the predominant products is TXB_2 which promotes thrombosis. When the COX-2 activity is
833 selectively inhibited in patients, the homeostasis between PGI_2 and TXB_2 will be unfortunately
834 disrupted. Thrombosis occurring in the cardiovascular system may lead to fatal events including
835 strokes and heart attacks (derived from Grosser et al. [108]).

836

1.2.4 Celecoxib

Celecoxib (Figure 8, **2**) is the most famous selective COX-2 inhibitors and now it is still on market. With the brand name Celebrex, celecoxib was approved to be used in the treatment of acute pain, osteoarthritis (OA), rheumatoid arthritis (RA), ankylosing spondylitis by Food and Drug Administration (FDA) in 1998. In 1999, it was approved for the treatment of colorectal polyps in patients with familial adenomatous polyposis (FAP) [122].

1.2.4.1 **The chemical synthesis of celecoxib**

The chemical synthesis routes of celecoxib and its analogues were described by Penning et al. (Scheme 1) [123]. In the presence of sodium methoxide (NaOMe) in refluxing methanol/methyl *tert*-butyl ether (MTBE), Claisen condensation of 4-mehtylacetophenone (**1**) with ethyl trifluoroacetate (**2**) yielded the dione (**3**). Celecoxib was subsequently prepared from the condensation of the dione and (4-sulfamoylphenyl)hydrazine hydrochloride (**4**) in refluxing ethanol. The yield was 43% in this 2-step preparation method. In 2011, Gaulier et al. reported a novel three linear step synthesis of celecoxib via a key regioselective direct C–H arylation reaction between a 1,3-disubstituted pyrazole and an aryl bromide, and the overall yield was 33% [124].

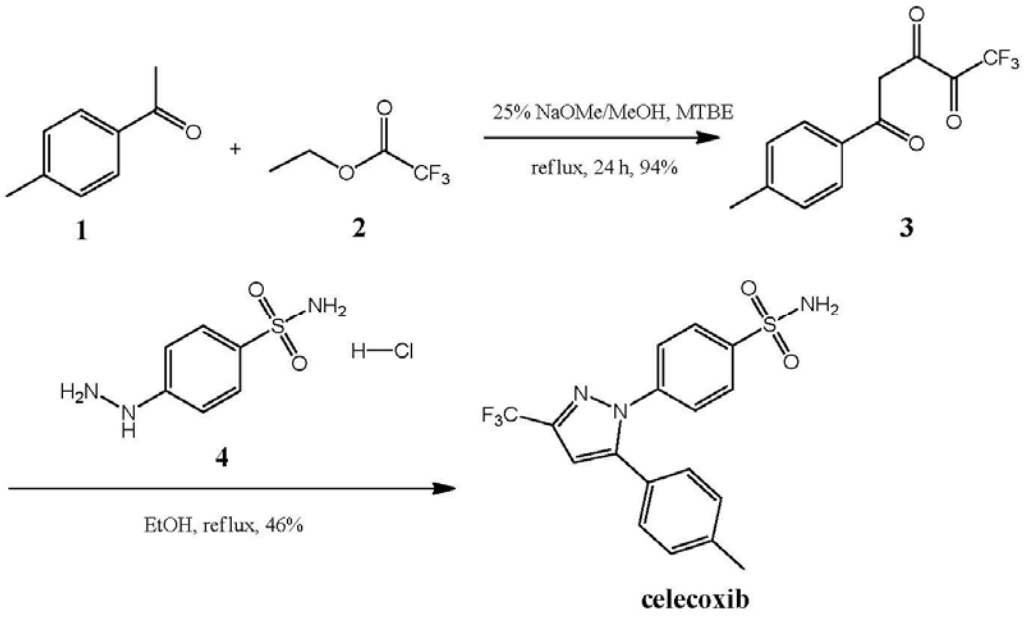

Scheme 1. Chemical synthesis of celecoxib.

1.2.4.2 **The physicochemical properties of celecoxib**

Celecoxib is poorly soluble in pure water (0.007 mg/mL, 25°C) [125]. In certain biorelevant and compendial media like fed state simulated gastric or intestinal fluids, the aqueous solubility of solubility can be enhanced to be as high as 0.1 mg/mL [126]. Celecoxib is soluble in organic solvents like methanol (114 mg/mL), ethanol (63 mg/mL) and octanol (7.8 mg/mL) [127]. The octanol/water partition coefficient of celecoxib is greater than 10^3, indicating that it is highly lipophilic. Since the pK_a of celecoxib is 11.1, it is essentially neutral in the pH range of human GI tract [126].

1.2.4.3 **The potency and selectivity of celecoxib in the inhibition of COX-2 activity**

As a potent inhibitor of COX-2, in most previous studies celecoxib was found to inhibit more than 50% of COX-2 activity at a concentration lower than 1 μM. Celecoxib has also been identified as a selective COX-2 inhibitor because its inhibitory effects on COX-1 activity is much weaker. However, the potency and selectivity of celecoxib were various when they were determined in different experimental systems. In Table 1, the IC_{50}s of celecoxib on human COX-1/2 activity as well as its selectivity in different studies are summarized.

876

Experimental system	IC_{50} (μM)		COX-2 selectivity	Reference
	hCOX-1	hCOX-2		
Human recombinant enzymes	15	0.04	375	[123]
	-	0.01	-	[128]
	-	0.08	-	[129]
	-	<<10	-	[130]
	-	<1	-	[131]
	<100	<1	-	[132]
Human macrophage	0.039	0.005	8.3	[133]
Human monocytes	82	6.8	12	[134]
CHO cells transfected with hCOX-1/2	13.5	0.036	375	[135]
U-937 cells (COX-1) / 143982 cells (COX-2)	5.1	0.079	64.6	[136]
Human lymphoma cell (COX-1) / IL-1β-stimulated dermal fibroblast (COX-2)	2.8	0.0091	31	[137]
Human Whole Blood Assay (WBA)	1.2	0.83	1.45	[100]
	-	1	-	[131]
	-	1	-	[132]
	-	<1	-	[136]
William Harvey Human Modified Whole Blood Assay (WHMA)	-	0.34	-	[100]

877

878 **Table 1. IC_{50} value on COX-1/2 activities and selectivity of celecoxib**
879 **determined in different studies.**

880

1.2.4.4 **Structure-activity relationship studies of celecoxib**

The structure-activity relationship (SAR) study of celecoxib and its analogs illustrated that the 1,5-diarylpyrazole structure was essential for their inhibitory potency on COX-2 activity. The researchers made various modifications to different positions on the chemical skeleton of celecoxib and performed a comprehensive SAR study [123]. The substitution of *p*-sulfamoylphenyl at position 1 of the pyrazole ring is fundamental to the selectivity towards COX-2, because it helps to occupy the side pocket which is in COX-2 but absent in COX-1. Meanwhile, the substitutions at position 1 of the pyrazole can only be *p*-sulfamoylphenyl or *p*-methylsulfonylphenyl to keep both the potency and selectivity in COX-2 inhibition.

At position 3 of the pyrazole, replacement of the trifluoromethyl by other groups such as difluoromethyl, fluoromethyl and methyl et al. will generate a series of compounds with comparable or decreased potency in inhibiting COX-2. When celecoxib is accommodated in the binding channel of COX-2, the trifluoromethyl is oriented toward the opening of the channel, which may render fewer interactions with amino acid residues and allow more flexible substituents to this site.

With respect to the *para*-methylphenyl attached to position 5 of the pyrazole, remarkably various modifications can be made to it without altering the potency and selectivity toward COX-2 significantly. For example, the 4-methyl can be substituted by hydrogen, 2-methyl, 3-methyl, 2-chloro, 3-chloro, 4-chloro, 2-fluoro, 3-fluoro, 4-fluoro, and 4-methoxy. However, hydrophilic substitutions such as hydroxyl and carboxyl groups are unfavorable and diminish potency. Also, if the substituents are bulky, the binding affinity between the inhibitor and COX-2 will be decreased due to steric hindrance. It should be noted that the analogs of celecoxib with halogen substitutions to this phenyl ring usually possess an incredibly long half-life (hundreds of hours) *in vivo* which is unacceptable for a drug candidate.

1.2.4.5 **Absorption, metabolism and excretion of celecoxib**

Celecoxib can be classified as a biopharmaceutic classification system (BCS) class II drug due to its low aqueous solubility and high permeability [127]. In dogs, when administrated in a solution, celecoxib was absorbed rapidly and reached the peak concentration in the plasma in 1 hour, while administrated as a solid, the absorption was delayed for 1 or 2 hours. Administration of celecoxib in a solution also resulted in higher oral bioavailability than as a solid. The absorption of celecoxib as a solid was limited by its dissolution rate [126, 138]. When the same doses of celecoxib were administrated intragastrically or into the duodenum, jejunum, or colon directly through a chronic intestinal access port in dogs, the absorption rate of celecoxib was slower in the colon than in the other segments of GI tract [138]. However, the $AUC_{0-\infty}$ values of celecoxib in the systemic circulation were found to be similar after dosing celecoxib to the four sites, indicating that the extent of celecoxib absorption was similar. All these results have illustrated that celecoxib is a highly permeable drug which can be absorbed through the GI tract in dogs. Fat-containing diet delayed the absorption of celecoxib given in a gelatin capsule in dogs, but significantly increased the oral bioavailability and $AUC_{0-\infty}$ of celecoxib by 300-500%. However, only a slight (11%) increase in $AUC_{0-\infty}$ was observed in human after celecoxib administrated with a high fat meal, which was considered as clinically irrelevant [138].

In humans and rats, the metabolism pathways of celecoxib are similar. In previous studies, orally administered celecoxib was demonstrated to be well absorbed and appeared in the plasma quickly, featuring a concentration much higher than its IC_{50} value against COX-2 [139]. The phase I metabolism of celecoxib comprises of two steps (Figure 11) [140, 141], where celecoxib is initially oxidized to hydroxycelecoxib (M3), and then further oxidized to carboxycelecoxib (M2). In humans, these two steps are catalyzed by CYP2C9 and alcohol dehydrogenase, respectively [142, 143]. In subsequent phase II metabolism, M3 and M2 can be conjugated with glucuronic acid on the carboxyl or hydroxyl group to form the glucuronides M1 and M5,

930 respectively. The UGTs are responsible for the glucuronidation. It is also notable that as 1-*O*-
931 acyl glucuronide, M1 is unstable at physiological pH and isomers can be formed via the acyl
932 migration process [144]. M1 can be converted to M2 by β-glucuronidase, while the acyl
933 migration products are resistant to hydrolysis [145]. In previous studies, multiple positional
934 isomers of M1 were observed in the *in vivo* samples [141].

935 In male human volunteers, after oral administration of 300 mg celecoxib, 50%~60% of the dose
936 was recovered in the feces as M2, while less than 5% of the dose was excreted as unmetabolized
937 celecoxib [140]. In the urine, approximately 20% of the dose was excreted as M2, and less than 2%
938 of the dose was excreted as either unmetabolized celecoxib, M1 or M3 [140]. In rats, after oral
939 administration of 1mg/kg celecoxib, approximately 75% and 10% of the dose was recovered as
940 M2 in the feces and urine, respectively. Besides that, 5% of the dose was recovered as M3 in
941 urine [141]. Larger oral doses of celecoxib (20, 80 and 400 mg/kg) in rats resulted in increased
942 percentages of the dose recovered as unmetabolized celecoxib in the feces, perhaps due to
943 inadequate absorption in the GI tract. Analysis of the rat bile extract also revealed that the major
944 metabolite in the bile was M2, while M1 and M5 were also found as the minor metabolites [141].
945 M1 and M5 were susceptible to hydrolysis by bacterial glucuronidases in the rat colon. The
946 hepatobiliary and renal excretion of M2 was proved to be mediated by BCRP [146, 147].

947

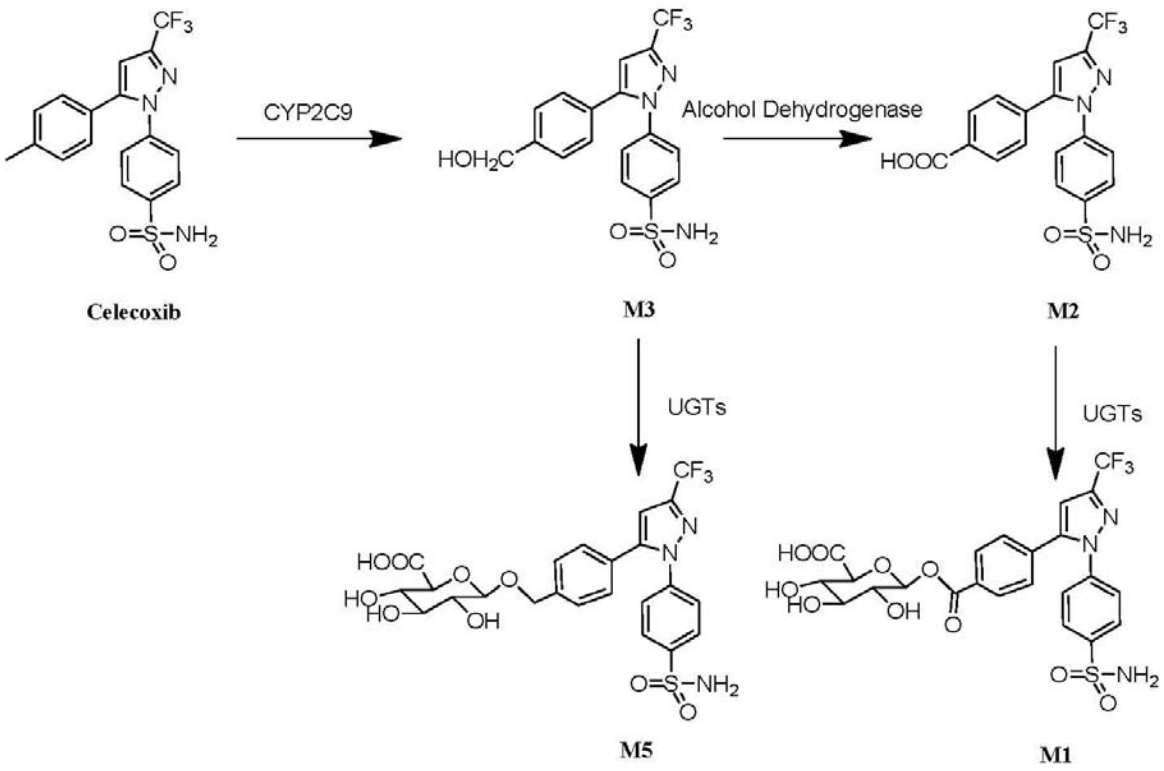

948

949 **Figure 11. The metabolism pathways of celecoxib in human.**

950 The phase I metabolism of celecoxib comprises of two steps. Celecoxib is initially oxidized to
951 hydroxycelecoxib (M3), and then further oxidized to carboxycelecoxib (M2). In humans, these
952 two steps are catalyzed by CYP2C9 and alcohol dehydrogenase, respectively. In subsequent
953 phase II metabolism, M3 and M2 can be conjugated with glucuronic acid on the carboxyl or
954 hydroxymethyl group to generate the glucuronides M1 and M5, respectively. The UGTs are
955 responsible for the glucuronidation (derived from Paulson et al.).

956

957

1.2.5 The other selective COX-2 inhibitors

1.2.5.1 **Rofecoxib**

Rofecoxib (Figure 8, **3**) is another famous selective COX-2 inhibitor besides celecoxib. It was classified into the group of NSAIDs with highest selectivity in the inhibition of COX-2 activity [100]. Similar to celecoxib and the other selective COX-2 inhibitors, rofecoxib is with a diaryl heterocyclic backbone in its chemical structure. The methylsulfonyl substitution on one of the aryl rings is inherited from DuP-697. It was marketed by Merck under the brand name Vioxx in 1999. After the APPROVe trial showed the increased risk of the cardiovascular events in patients by rofecoxib, the drug was withdrawn from the market in 2004.

Rofecoxib was usually available as tablets or in oral suspensions. The oral bioavailability is higher than 90% when a dose of 12.5, 25 or 50 mg rofecoxib was given to healthy subjects, but the oral bioavailability of rofecoxib is much lower in cholecystectomy patients, indicating that the bile facilitates the absorption of rofecoxib [148]. The absorption of rofecoxib in the gastrointestinal tract of humans is rapid and the peak concentration in the plasma is achieved in 3 hours. The elimination half-life of rofecoxib in human plasma is 17 hours [149]. The metabolism of rofecoxib in humans is more complicated than that of celecoxib and involves multiple enzymes including CYPs and UGTs [149, 150]. At least 8 metabolites of rofecoxib have been detected and characterized in humans [148]. The majority of metabolites are excreted in urine [148].

1.2.5.2 **Valdecoxib and parecoxib**

Valdecoxib (Figure 8, **4**) is another selective COX-2 inhibitor which was once on the market with the brand name Bextra by G. D. Searle & Company. The chemical structure of valdecoxib is featured with a 3,4-diarylisoxazole, which is very similar to that of celecoxib. On November 20, 2001, celecoxib is approved by FDA for the treatment of OA, adult RA, and primary dysmenorrhea. It was also used off-label for controlling acute pain and various types of surgical

pain. Valdecoxib was available by prescription in the United States as tablets until 2005, and then it was withdrawn from the market due to concerns about increased cardiovascular events and also serious skin side effects in patients.

Parecoxib (Figure 8, **5**) is the amide of propanoic acid and valdecoxib. It was developed as a water soluble and injectable prodrug of valdecoxib for those patients unable to receive oral administration of drugs. Following parenteral administration in patients, parecoxib is stable in the whole blood and plasma, but rapidly converted to valdecoxib and propanoic acid by hepatic carboxyesterases. It is successfully marketed as Dynastat in European Union for use in perioperative pain control, but not approved by FDA in the United States.

1.2.5.3 **Etoricoxib**

Etoricoxib (Figure 8, **6**), with the brand name Acroxia, is a selective COX-2 inhibitor which has been approved in more than 80 countries but not in the United States. A *p*-(methylsulfonyl)phenyl and a bipyridine are included in the chemical structure of etoricoxib, which make it similar to the other selective COX-2 inhibitors. Etoricoxib is used in the treatment of inflammatory diseases such as RA, OA, psoriatic arthritis and ankylosing spondylitis, as well as in the control of chronic low back pain, acute pain, and gout.

1.2.5.4 **Lumiracoxib**

Lumiracoxib (Figure 8, **7**) is an analog of diclofenac and its structure is largely different from those mentioned above. Unlike the other selective COX-2 inhibitors with three aryl rings adjacently placed in the structures, lumiracoxib is classified as a member of the arylalkanoic acid class of NSAIDs. It also binds to a different binding site in COX-2 protein, compared with the other selective COX-2 inhibitors. It was once approved in the European Union, Australia, Canada, and other countries for arthritis treatment and pain control, but soon withdrawn from the most countries due to its potential to cause liver adverse events or even liver failure.

Chapter 2 Hypothesis and Specific Aims

2.1 Hypothesis

The selective COX-2 inhibitors have been demonstrated to be effective in the chemoprevention of CRC. However, they can not be used as safe agents in CRC chemoprevention because of their cardiovascular toxicity. The long-term goal of this project is to develop novel selective COX-2 inhibitors without cardiovascular toxicity for CRC chemoprevention. In the current studies, we hypothesize that by taking advantage of phase II metabolism and excretion, locally bioavailable COX-2 inhibitors can be developed as effective agents to inhibit the COX-2 activity in colon, and meanwhile they are not systemically available to avoid the cardiovascular toxicity.

2.2 Specific Aims

2.2.1 Aim 1

To design and synthesize a series of phenolic compounds as potential inhibitors of COX-2 activity. We will use celecoxib as the template to design a series of new compounds with phenolic groups in their structures. After synthesis and purification, the inhibitory effects of the new compound on COX-2 cells will be assessed in different cell lines or by human recombinant COX-2 enzyme.

2.2.2 Aim 2

To characterize the metabolic properties of the new compounds by the *in vitro* tools and models, as well as in pharmacokinetics studies in rats. In this aims, the new compounds will be put into *in vitro* characterization and their phase II metabolism rates will be compared. The one which is the most likely to have a low systemic bioavailability will be selected as the lead

compound. PK studies will be also conducted to confirm the results from the *in vitro* characterization.

2.2.3 Aim 3

To evaluate of the efficacy of the new compounds in inhibiting colonic COX-2 activity in inflamed rat colon. In this aim, in rat colon with acute inflammation, we will conduct *in situ* perfusion studies to verify the efficacies of the new compounds in inhibiting colonic COX-2 activity. Also, the metabolism, absorption and excretion of the representative new compound in rats will be also investigated in the perfusion studies.

Chapter 3 The Design and Synthesis of Phenolic Compounds as COX-2 Inhibitors

3.1 Abstract

Totally 8 new COX-2 inhibitors were successfully synthesized and purified. They have either different substitutions on one of the aryl rings (R_1) or different phenolic groups (R_2) in their structures. Their efficacies to inhibit the production of COX-2-derived prostaglandins was tested in Raw264.7 cells and HCA-7 cells. In Raw264.7 cells, among all the 8 compounds, **6a3**, **6b3** and **6a3** were identified as the most potent ones to inhibit PGD_2 potent, while the other compounds were found to be much weaker. However, in HCA-7 cells, the differences in IC_{50} values between **6a3** and the other three compounds (**6a1**, **6a2**, and **6a4**) were much less than those in Raw264.7 cells. The metabolic stability of **6a1**, **6a2** and **6a3** were investigated and the results showed that the rapid glucuronidation and excretion of these compounds in Raw264.7 cells decreased their potency. Meanwhile, no significant difference in potency were observed among **6a1**, **6a2** and **6a3** when their inhibitory effects on the activity of human recombinant COX-2 enzyme were assessed. The *in silico* docking of the new compounds to the crystal structure of COX-2 protein revealed that the binding orientations of these compounds were similar to that of celecoxib in the active pocket of COX-2. Although the new compounds are much less potent inhibitors of COX-2 compared with celecoxib, they still have IC_{50} values lower than 0.2 μM and a local concentration higher than that is quite achievable in the colon.

3.2 Introduction

Besides the role of COX-2 in the inflammation, its involvement in human neoplasia, tumorigenesis, tumor angiogenesis and metastasis has also attracted a lot of attention. With extensive studies *in vitro* or in animal models, COX-2 has been validated as an effective target in the therapy and chemoprevention of cancer, primarily CRC. In clinical trials, oral administration of either celecoxib or rofecoxib has been demonstrated to be effective in decreasing the recurrence of adenomas in CRC patients after surgery. The existing COX-2 inhibitors, either in the market now or withdrawn from the market, have a very good oral bioavailability. After oral administration, the drugs can be rapidly absorbed in the intestine, and they enter the systemic circulation without notable first-pass effects. With half-lives longer than 8 hours, the drug concentrations in the plasma are usually much higher than their IC_{50}s on COX-2 activity, in order to guarantee the efficacies in the treatment of acute pain and inflammatory arthritis in patients. However, the high drug levels in the systemic circulation may also inhibit the physiological role of vascular COX-2 and lead to the increased risk of the cardiovascular events.

In contrast to the existing COX-2 inhibitors, it has long been recognized that phenolic drugs (e.g., raloxifene) or natural chemicals (e.g., flavonoids) usually have a low oral bioavailability due to the extensive first-pass effects. These compounds can be excellent substrates of phase II enzymes expressed in the intestinal epithelium and liver, including the UGTs and SULTs. Before the phenolic compounds can reach the systemic circulation, they are rapidly conjugated as hydrophilic glucuronides or sulfates. The ABC transporters embedded on the membrane of enterocytes or hepatocytes facilitate excretion of the phase II metabolites. The functional coupling of the phase II enzymes and transporters largely decreases the chance of the phenolic compounds entering the systemic circulation and results in a low oral bioavailability.

Hence, the extensive experiences in studying the absorption, disposition, metabolism and excretion of the phenolic drugs and natural compounds inspired the researchers in Dr. Ming Hu's lab to invent novel selective COX-2 inhibitors with phenolic groups built in their structures. The novel COX-2 inhibitors are supposed to be active locally to inhibit colonic COX-2. However, different from the existing COX-2 inhibitors, the novel ones will be conjugated as phase II metabolites and excreted before they enter the systemic circulation, resulting in negligible or even no plasma concentration. In this way, the physiological role of vascular COX-2 can be protected from disruption, and thus the side effects in the cardiovascular system can be avoided. The long-term objective in this project is to develop drug candidates to target COX-2 activity in related colonic diseases (e.g., CRC chemoprevention) with no side effects.

In this chapter, a series of phenolic compounds as novel COX-2 inhibitors were designed and synthesized. The structure of celecoxib, the only selective COX-2 inhibitor in the market now, was selected as a prototype for the development of new compounds. Modifications were made in the structure to generate new compounds with binding affinity and selectivity to COX-2. Like most other selective COX-2 inhibitors, celecoxib possesses a central heterocycle with two aryl substitutions. Based on the SAR studies of celecoxib, it is inappropriate to introduce hydroxyl groups to the two aryl rings, or the binding affinity with COX-2 will be lost or largely reduced. However, certain modifications made to the pyrazole can be tolerated. Thus, the structure of celecoxib was modified to generate phenolic compounds by substituting the 3-trifluoromethyl group on the pyrazole ring. A previously reported route for the synthesis of celecoxib derivatives was modified in the present project. In this route, different phenolic groups were conjugated to the skeleton of celecoxib.

After the structures of the new compounds were certified, their inhibitory effects on COX-2 activity were determined in different cell lines with inducible or constitutive COX-2 expression, as well as by *in vitro* assays using recombinant human COX-2 enzyme. The cell lines included:

Raw264.7 cells, a murine macrophage cell line with COX-2 expression upon LPS induction and HCA-7 cells, a human CRC cell lines with constitutive COX-2 expression. After the new compounds were confirmed as selective COX-2 inhibitors, they were further characterized for their metabolism and excretion in the next chapter.

3.3 Materials and Methods

3.3.1 Materials

4'-Methoxyacetophenone (CAS 100-06-1), 4′-methylacetophenone (CAS 122-00-9), acetophenone (CAS 98-86-2), sodium hydride (NaH, CAS 7646-69-7), 1,2-dihydroxybenzene (CAS 120-80-9), resorcinol (CAS 108-46-3), hydroquinone (CAS 123-31-9), 3,7-dihydroxyflavone (3,7-DHF), tetrahydrofuran anhydrate (THF), sodium hydroxide (NaOH), lithium aluminum hydride ($LiAlH_4$), anhydrous magnesium sulfate ($MgSO_4$), hydrogen chloride (HCl), sodium carbonate (K_2CO_3), ethylenediaminetetraacetic acid (EDTA), L-glutathione reduced (GSH), hematin (porcine), phenol, formic acid, lipopolysaccharides (LPS), methyl sulfoxide (DMSO), DMSO-d_6, methanol-d_4 (CD_3OD) and chloroform-d ($CDCl_3$) were purchase from Sigma-Aldrich (St Louis, MO). Diethyl oxalate (CAS 95-92-1) and 4-hydrazinobenzenesulfonic acid hemihydrate (CAS 98-71-5) were purchased from TCI chemicals (Portland, OR). PGE_2, PGD_2, PGE_2-d_4, PGD_2-d_4, AA, recombinant human COX-2 protein, and the cation ionophore A23187 were purchased from Cayman Chemicals (Ann Arbor, MI). In the chemical synthesis, ACS grade acetonitrile, ethyl acetate (EtOAc), methylene chloride (CH_2Cl_2), methanol, and ethanol were purchased from EMD Millipore (Billerica, MA).

Raw264.7 cells were purchased from the American Type Culture Collection (ATCC, Manassas, VA). HCA-7 cells were obtained as a kind gift from Dr. Raymond DuBois in University of Texas MD Anderson Cancer Center. Phosphate-buffered saline (PBS), Dulbecco's modified eagle medium (DMEM), McCoy's 5A medium, and fetal bovine serum (FBS) were purchased from

Life Technologies (Carlsbad, CA). In the ultra-performance liquid chromatography - tandem mass spectrometer (UPLC-MS/MS) analysis, MS grade formic acid, acetonitrile, H_2O, and methanol were purchased from EMD Millipore (Billerica, MA).

3.3.2 Chemistry

3.3.2.1 General

The thin-layer chromatography (TLC) was performed on EMD TLC Silica Gel 60 F_{254}, and the compounds were visualized by UV detection. Flash chromatography (FC) was performed on silica gel. Liquid-gel partition chromatography was performed on Sephadex™ LH-20 column using methanol as the solvent.

Analytical UPLC was performed on a Waters Acquity™ UPLC (Waters, Milford, MA) equipped with a diode array detector (DAD). The conditions were: column, Waters BEH C18, 1.7μm, 50 mm × 2.1 mm (Waters, Milford, MA); mobile phase A, 100% water; mobile phase B, 100% acetonitrile; gradient, 0-0.5min, 20% B, 0.5-5.5min, 20-29% B, 5.5-6min, 29-70% B, 6min-6.5min, 95% B, 6.5-7.0min, 95% B, 7.0-7.5min, 95-20% B, 7.5-8min, 20% B; flow rate, 0.5mL/min; column temperature, 45 °C.

The structures were certified by ^{1}H-NMR at 500 MHz on a JEOL ECA-500 spectrometer or at 400 MHz on a JEOL ECX-400 spectrometer. Chemical shifts (δs) are reported in ppm downfield from tetramethylsilane, and *J* values are in hertz. The splitting patterns are described as: s = singlet, d = doublet, t = triplet, q = quartet, quint = quintet, dd = doublet of doublets, dt = doublet of triplets, td = triplet of doublets, m = multiplet and br = broad signal. ESI (electrospray ionization) mass spectra were acquired on an API 5500-Qtrap triple quadrupole mass spectrometer (Applied Biosystem/MDS SCIEX, Foster City, CA).

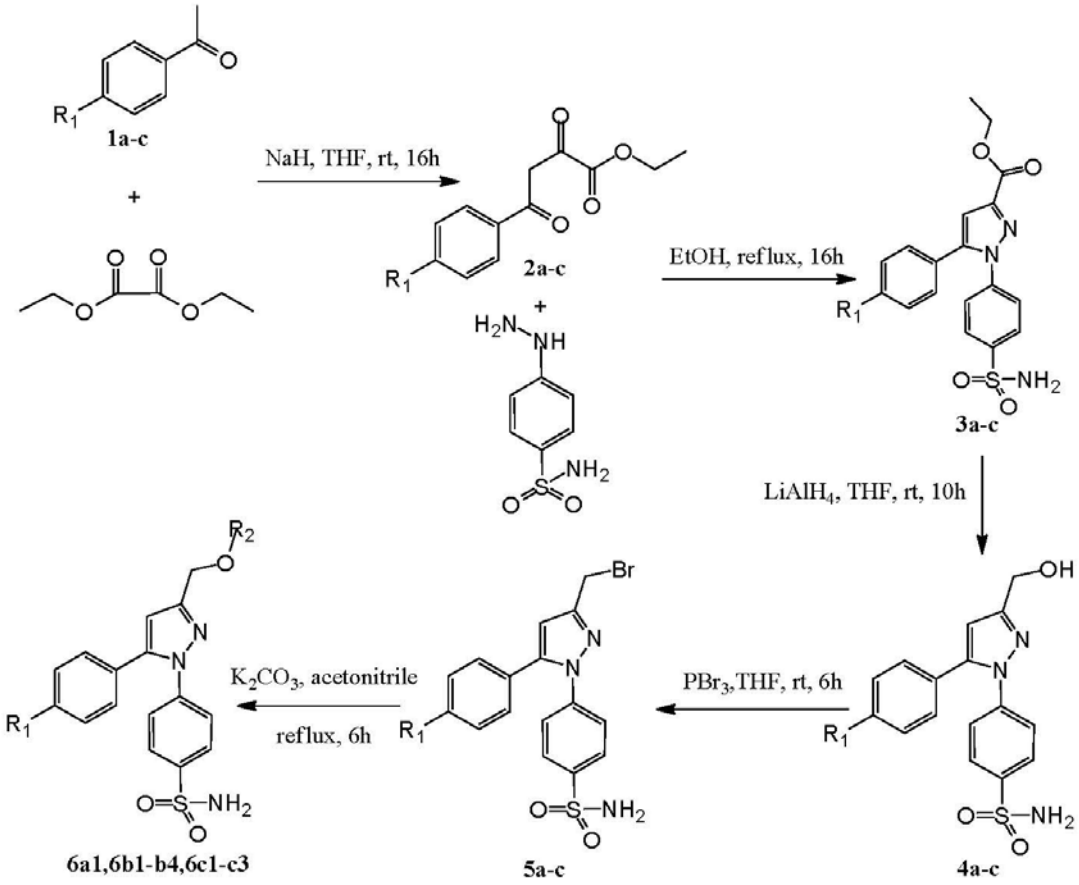

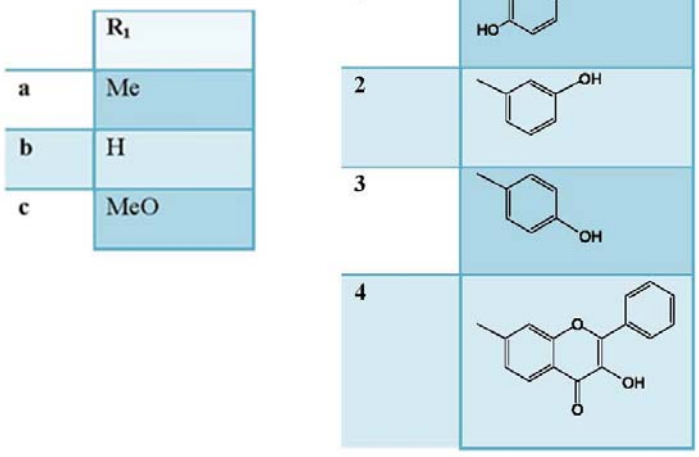

Scheme 2. The synthesis of locally bioavailable COX-2 inhibitors.

3.3.2.2 **Preparation of 2a-c**

Ethyl 2,4-dioxo-4-(*p*-tolyl)butanoate (2a). NaH (15.0g, 625 mmol) was suspended in 250 mL anhydrous THF at 0°C, and then 4-methyl-acetophenone (**1a**, 30.0 g, 224 mmol) was added in portions. The mixture was stirred at 0 °C for 30 minutes before ethyl oxalate (40.0 g, 274 mmol) was added. The reaction was allowed to stir at room temperature for another 8 hours. After the reaction, THF in the reaction mixture was evaporated and the excessive NaH was quenched by ice-water. The mixture was acidified to pH = 6 by 1 N HCl and extracted by EtOAc (150 mL × 3). The combined extract was washed with water, dried over anhydrous $MgSO_4$ and evaporated under reduced pressure to provide a yellow oil. The crude product was purified by an LH-20 Sephadex column using methanol as eluant to give **2a** as a light yellow solid (43.2 g, 83%). ^{1}H NMR (500 MHz, $CDCl_3$) δ 7.90 (d, *J* = 8.3 Hz, 2H), 7.30 (d, *J* = 8.1 Hz, 2H), 7.06 (s, 1H), 4.39 (q, *J* = 7.3 Hz, 2H), 2.44 (s, 3H), 1.41 (t, *J* = 7.1 Hz, 3H). MS (ESI-) m/z: 233.2 (M - H^+).

Ethyl 2,4-dioxo-4-phenylbutanoate (2b). Compound **2b** was prepared from acetophenone (**1b**) and ethyl oxalate by the procedures described in the preparation of **2a**. **2b** was provided as a pale solid in 80% yield. ^{1}H NMR (400 MHz, $CDCl_3$) δ 7.98 (d, *J* = 7.2 Hz, 2H), 7.63 – 7.57 (m, 1H), 7.52 – 7.47 (m, 2H), 7.07 (s, 1H), 4.39 (q, *J* = 7.1 Hz, 2H), 1.40 (t, *J* = 7.1 Hz, 3H). MS (ESI-) m/z: 219.2 (M - H^+).

Ethyl 4-(4-methoxyphenyl)-2,4-dioxobutanoate (2c). Compound **2c** was prepared from 4-methoxyl-acetophenone (**1c**) and ethyl oxalate by the procedures described in the preparation of **2a**. **2c** was provided as a light brown solid in 87% yield. ^{1}H NMR (400 MHz, $CDCl_3$) δ 7.98 (d, *J* = 7.1 Hz, 2H), 7.02 (s, 1H), 6.97 (d, *J* = 8.9 Hz, 2H), 4.38 (q, *J* = 7.1 Hz, 2H), 3.88 (s, 3H), 1.40 (t, *J* = 7.1 Hz, 3H). MS (ESI-) m/z: 249.1 (M - H^+).

3.3.2.3 **Preparation of 3a-c**

Ethyl 1-(4-sulfamoylphenyl)-5-(*p*-tolyl)-1*H*-pyrazole-3-carboxylate (3a). Compound **2a** (20.0 g, 85.4 mmol) and 4-hydrazinobenzenesulfonamide hydrochloride (20.0 g, 89.6 mmol) was added in 1 L ethanol. The mixture was stirred and heated to reflux for 10 hours. After ethanol was evaporated under reduce pressure, the reaction mixture was reconstituted in 500 mL EtOAc, washed with water and 1N $NaHCO_3$, and dried over anhydrous $MgSO_4$. Then EtOAc was evaporated and the crude product was purified by an LH-20 Sephadex column using methanol as eluant to give **3a** as a light yellow solid (25.0 g, 76%). ^{1}H NMR (400 MHz, $CDCl_3$) δ 7.88 (d, J = 8.9 Hz, 2H), 7.48 (d, J = 8.9 Hz, 2H), 7.15 (d, J = 7.9 Hz, 2H), 7.08 (d, J = 8.2 Hz, 2H), 7.00 (s, 1H), 4.95 (s, 2H), 4.45 (q, J = 7.1 Hz, 2H), 2.36 (s, 3H), 1.42 (t, J = 7.1 Hz, 3H). MS (ESI-) *m/z*: 384.1 (M - H^+).

Ethyl 5-phenyl-1-(4-sulfamoylphenyl)-1*H*-pyrazole-3-carboxylate (3b). Compound **3b** was prepared from **2b** and 4-hydrazinobenzenesulfonamide hydrochloride by the procedures described in the preparation of **3a**. **3b** was provided as a white solid in 81% yield. ^{1}H NMR (400 MHz, $CDCl_3$) δ 7.88 (d, J = 8.9 Hz, 2H), 7.47 (d, J = 8.9 Hz, 2H), 7.40-7.32 (m, 3H), 7.23-7.18 (m, 2H), 7.04 (s, 1H), 4.97 (s, 2H), 4.45 (q, J = 7.1 Hz, 2H), 1.42 (t, J = 7.1 Hz, 3H). MS (ESI-) *m/z*: 370.1 (M - H^+).

Ethyl 5-(4-methoxyphenyl)-1-(4-sulfamoylphenyl)-1*H*-pyrazole-3-carboxylate (3c). Compound **3c** was prepared from **2c** and 4-hydrazinobenzenesulfonamide hydrochloride by the procedures described in the preparation of **3a**. **3c** was provided as a light yellow solid in 85% yield. ^{1}H NMR (500 MHz, $CDCl_3$) δ 7.89 (d, J = 8.7 Hz, 2H), 7.49 (d, J = 8.7 Hz, 2H), 7.13 (d, J = 8.8 Hz, 2H), 6.98 (s, 1H), 6.87 (d, J = 8.8 Hz, 2H), 4.92 (s, 2H), 4.45 (q, J = 7.1 Hz, 2H), 3.82 (s, 3H), 1.42 (t, J = 7.1 Hz, 3H). MS (ESI-) *m/z*: 400.1 (M - H^+).

3.3.2.4 **Preparation of 4a-c**

4-(3-(Hydroxymethyl)-5-(*p*-tolyl)-1*H*-pyrazol-1-yl)benzenesulfonamide (4a). $LiAlH_4$ (6.00 g, 158 mmol) was added to 300 mL anhydrous THF at 0 °C. The suspension was stirred for 10 minutes and then compound **3a** (15.0 g, 38.9 mmol) dissolved in 100 mL anhydrous THF was added in portions at 0 °C. The reaction was allowed to stir for 8 hours at room temperature. Then the reaction mixture was evaporated under reduced pressure and excessive $LiAlH_4$ was quenched with ice-water. The pH was adjusted to 7 by 1 N HCl and the reaction mixture was extracted by EtOAc (150 mL × 3). The combined extract was washed with water, dried over anhydrous $MgSO_4$, and evaporated under reduced pressure. The crude product was purified by an LH-20 Sephadex column using methanol as eluant to give **4a** as a light yellow solid (12.7 g, 95%). ^1H NMR (400 MHz, CD_3OD) δ 7.85 (d, J = 8.6 Hz, 2H), 7.38 (d, J = 8.7 Hz, 2H), 7.18 – 7.05 (m, 4H), 6.57 (s, 1H), 4.65 (s, 2H), 2.31 (s, 3H). MS (ESI-) *m/z*: 342.1 ($M - H^+$).

4-(3-(Hydroxymethyl)-5-phenyl-1*H*-pyrazol-1-yl)benzenesulfonamide (4b). Compound **4b** was prepared from **3b** by the procedures described in the preparation of **4a**. **4b** was provided as a white solid in 90% yield. MS (ESI-) *m/z*: 328.1 ($M - H^+$).

4-(3-(Hydroxymethyl)-5-phenyl-1*H*-pyrazol-1-yl)benzenesulfonamide (4c). Compound **4c** was prepared from **3c** by the procedures described in the preparation of **4a**. **4c** was provided as a white solid in 94% yield. MS (ESI^-) *m/z*: 358.1 ($M - H^+$).

3.3.2.5 **Preparation of 5a-c**

4-(3-(Bromomethyl)-5--(*p*-tolyl)-1*H*-pyrazol-1-yl)benzenesulfonamide (5a). Compound **4a** (10.0 g, 29.1 mmol) was dissolved in 40 mL anhydrous THF. The solution was stirred and cooled to 0 °C on ice before PBr_3 (4.05 g, 15.0 mmol) was slowly added in drops. The reaction was allowed to stir for 6 hours at room temperature. Then the excessive PBr_3 was quenched with ice water and the pH was adjusted to 6 with 1 N NaOH. THF in the reaction mixture was evaporated under reduced pressure and the remaining mixture was extracted by EtOAc (150 mL × 3). The combined extract was dried over anhydrous $MgSO_4$ and evaporated under reduced pressure. The

crude product was purified by an LH-20 Sephadex column using methanol as eluant to give **5a** as a yellow solid (4.37 g, 37%). ^{1}H NMR (500 MHz, DMSO-d_6) δ 7.80 (d, J = 8.6 Hz, 2H), 7.46 (s, 2H), 7.41 (d, J = 8.6 Hz, 2H), 7.17 (d, J = 8.1 Hz, 2H), 7.12 (d, J = 8.1 Hz, 2H), 6.70 (s, 1H), 4.67 (s, 2H), 2.28 (s, 3H). MS (ESI-): *m/z*: 404.0, 405.8 (M - H^+).

4-(3-(Bromomethyl)-5-phenyl-1*H*-pyrazol-1-yl)benzenesulfonamide (5b). Compound **5b** was prepared from **4b** by the procedures described in the preparation of **5a**. **5b** was provided as a white solid in 44% yield. ^{1}H NMR (500 MHz, DMSO-d_6) δ 7.82 (d, J = 8.2 Hz, 2H), 7.49 – 7.21 (m, 9H), 6.74 (s, 1H), 4.68 (s, 2H). MS (ESI-) *m/z*: 390.0, 391.8 (M - H^+).

4-(3-(Bromomethyl)-5-(4-methoxyphenyl)-1*H*-pyrazol-1-yl)benzenesulfonamide (5c). Compound **5c** was prepared from **4c** by the procedures described in the preparation of **5a**. **5c** was provided as a yellow solid in 47% yield. ^{1}H NMR (500 MHz, DMSO-d_6) δ 7.83 (d, J = 8.6 Hz, 2H), 7.47 (s, 2H), 7.42 (d, J = 8.7 Hz, 2H), 7.17 (d, J = 11.5 Hz, 2H), 6.92 (d, J = 8.8 Hz, 2H), 6.66 (s, 1H), 4.66 (s, 2H), 3.73 (s, 3H). MS (ESI-) *m/z*: 420.0, 421.8 (M - H^+).

3.3.2.6 **Preparation of 6a1-4, 6b2-3, and 6c2-3**

4-(3-((2-Hydroxyphenoxy)methyl)-5-(*p*-tolyl)-1*H*-pyrazol-1-yl)benzenesulfonamide (6a1). Compound **5a** (400 mg, 0.988 mmol) and 1,2-dihydroxybenzene (750 mg, 6.82 mmol) was dissolved in 15 mL acetonitrile. K_2CO_3 (140 mg, 1.01 mmol) was also added to the solution and the mixture was stirred and heated to reflux for 12 hours. Then the reaction mixture was evaporated under reduced pressure and washed by water to remove inorganic salts and excessive 1,2-dihydroxybenzene. After the remaining water was removed under vacuum, the crude product was purified by FC with CH_2Cl_2/MeOH 15:1 to give **6a1** was a white solid (373 mg, 87%). ^{1}H NMR (500 MHz, DMSO-d_6) δ 8.98 (s, 1H), 7.80 (d, J = 8.7 Hz, 2H), 7.45 – 7.39 (m, 4H), 7.20 – 7.05 (m, 5H), 6.80 – 6.67 (m, 4H), 5.08 (s, 2H), 2.28 (s, 3H). ^{13}C NMR (126 MHz, DMSO-d_6) δ

150.63, 147.51, 147.18, 144.40, 143.24, 142.50, 138.91, 129.97, 128.99, 127.29, 127.26, 125.57, 122.13, 119.80, 116.53, 114.91, 109.03, 64.80, 21.35. MS (ESI-) *m/z*: 434.2 (M - H^+).

4-(3-((3-Hydroxyphenoxy)methyl)-5-(*p*-tolyl)-1*H*-pyrazol-1-yl)benzenesulfonamide (6a2). Compound **6a2** was prepared from **5a** and resorcinol by the procedures described in the preparation of **6a1**. **6a2** was provided as a white solid in 83% yield. ^{1}H NMR (500 MHz, DMSO-d_6) δ 9.44 (s, 1H), 7.80 (d, *J* = 8.7 Hz, 1H), 7.47 – 7.40 (m, 4H), 7.19 – 7.10 (m, 4H), 7.04 (t, *J* = 8.1 Hz, 1H), 6.70 (s, 1H), 6.48 – 6.33 (m, 2H), 5.02 (s, 1H), 2.28 (s, 2H). ^{13}C NMR (126 MHz, DMSO-d_6) δ 160.04, 159.12, 150.27, 144.47, 143.27, 142.47, 138.90, 130.48, 129.94, 129.03, 127.22, 125.63, 108.84, 108.73, 105.82, 102.51, 63.75, 21.34. MS (ESI-) *m/z*: 434.2 (M - H^+).

4-(3-((4-Hydroxyphenoxy)methyl)-5-(p-tolyl)-1H-pyrazol-1-yl)benzenesulfonamide (6a3).

Compound **6a3** was prepared from **5a** and hydroquinone by the procedures described in the preparation of **6a1**. **6a3** was provided as a white solid in 78% yield. ^{1}H NMR (500 MHz, DMSO-d_6) δ 8.94 (s, 1H), 7.79 (d, *J* = 8.8 Hz, 2H), 7.48 – 7.38 (m, 4H), 7.17 (d, *J* = 8.4 Hz, 4H), 7.12 (d, *J* = 8.2 Hz, 2H), 6.85 (d, *J* = 9.0 Hz, 2H), 6.70 – 6.63 (m, 3H), 4.98 (s, 2H), 2.28 (s, 3H). ^{13}C NMR (126 MHz, DMSO-d_6) δ 151.97, 151.67, 150.58, 144.43, 143.21, 142.48, 138.88, 129.93, 129.01, 127.25, 127.21, 125.61, 116.29, 116.19, 108.78, 64.43, 21.33. MS (ESI-) *m/z*: 434.2 (M - H^+).

4-(3-(((3-hydroxy-4-oxo-2-phenyl-4*H*-chromen-7-yl)oxy)methyl)-5-(p-tolyl)-1*H*-pyrazol-1-yl)benzenesulfonamide (6a4). Compound **6a4** was prepared from **5a** and 3,7-DHF by the procedures described in the preparation of **6a1** except that the reflux time was prolonged to 24 hours. **6a4** was provided as a yellow solid in 72% yield. ^{1}H NMR (500 MHz, DMSO-d_6) δ 10.89 (s, 1H), 7.98 – 7.88 (m, 3H), 7.76 (d, *J* = 8.6 Hz, 2H), 7.48 – 7.40 (m, 5H), 7.25 (d, *J* = 8.7 Hz, 2H), 7.15 (d, *J* = 8.0 Hz, 2H), 6.99 – 6.88 (m, 4H), 6.37 (s, 1H), 5.11 (s, 2H), 2.27 (s, 3H). ^{13}C NMR (126 MHz, DMSO-d_6) δ 173.80, 163.40, 157.24, 155.90, 149.78, 144.04, 143.17, 142.31,

139.07, 138.78, 131.19, 131.00, 129.86, 129.03, 128.93, 128.81, 127.32, 127.13, 125.48, 116.88, 115.71, 109.14, 102.76, 67.30, 21.33. MS (ESI-) *m/z*: 578.1 (M - H^+).

4-(3-((3-Hydroxyphenoxy)methyl)-5-phenyl-1*H*-pyrazol-1-yl)benzenesulfonamide (6b2). Compound **6b2** was prepared from **5b** and resorcinol by the procedures described in the preparation of **6a1**. **6b2** was provided as a white solid in 77% yield. ^{1}H NMR (500 MHz, DMSO-d_6) δ 9.44 (s, 1H), 7.82 (d, *J* = 8.6 Hz, 2H), 7.48 – 7.42 (m, 4H), 7.38-7.25 (m, 3H), 7.28 – 7.22 (m, 2H), 7.06 (t, *J* = 8.1 Hz, 1H), 6.75 (s, 1H), 6.52 – 6.44 (m, 2H), 6.39 – 6.36 (m, 1H) 5.04 (s, 2H). ^{13}C NMR (126 MHz, DMSO-d_6) δ 160.05, 159.13, 150.33, 144.44, 143.33, 142.40, 130.51, 130.13, 129.37, 129.17, 127.24, 125.65, 109.15, 108.77, 105.84, 102.54, 63.75. MS (ESI-) *m/z*: 420.2 (M - H^+).

4-(3-((4-Hydroxyphenoxy)methyl)-5-phenyl-1*H*-pyrazol-1-yl)benzenesulfonamide (6b3). Compound **6b3** was prepared from **5b** and hydroquinone by the procedures described in the preparation of **6a1**. **6b3** was provided as a white solid in 88% yield. ^{1}H NMR (500 MHz, DMSO-d_6) δ 8.94 (s, 1H), 7.79 (d, *J* = 8.7 Hz, 2H), 7.45 – 7.40 (m, 4H), 7.38 – 7.35 (m, 3H), 7.27 – 7.23 (m, 2H), 6.86 (d, *J* = 9.0 Hz, 2H), 6.74 (s, 1H), 6.66 (d, *J* = 9.0 Hz, 2H), 4.99 (s, 2H). ^{13}C NMR (126 MHz, DMSO-d_6) δ 151.99, 151.66, 150.62, 144.36, 143.29, 142.38, 130.16, 129.36, 129.31, 129.15, 127.20, 125.62, 116.28, 116.19, 109.08, 64.43. MS (ESI) *m/z*: 420.2 (M - H^+).

4-(3-((3-Hydroxyphenoxy)methyl)-5-(4-methoxyphenyl)-1*H*-pyrazol-1-yl)benzenesulfonamide (6c2). Compound **6c2** was prepared from **5c** and resorcinol by the procedures described in the preparation of **6a1**. **6c2** was provided as a white solid in 85% yield. ^{1}H NMR (500 MHz, DMSO-d_6) δ 9.44 (s, 1H), 7.85 (d, *J* = 8.6 Hz, 2H), 7.67 – 7.31 (m, 4H), 7.18 (d, *J* = 8.6 Hz, 2H), 7.06 (t, *J* = 8.0 Hz, 1H), 6.93 (d, *J* = 8.7 Hz, 2H), 6.67 (s, 1H), 6.53 – 6.36 (m, 3H), 5.05 (s, 2H), 3.73 (s, 3H). ^{13}C NMR (126 MHz, DMSO-d_6) δ 160.07, 160.05,

159.15, 150.24, 144.34, 143.19, 142.57, 130.55, 130.52, 127.25, 125.57, 122.35, 114.80, 108.77, 108.63, 105.84, 102.56, 63.80, 55.73. MS (ESI) *m/z*: 450.2 (M - H^+).

4-(3-((4-Hydroxyphenoxy)methyl)-5-(4-methoxyphenyl)-1*H*-pyrazol-1-yl)benzenesulfonamide (6c3). Compound **6c3** was prepared from **5c** and hydroquinone by the procedures described in the preparation of **6a1**. **6c3** was provided as a white solid in 80% yield. ^{1}H NMR (500 MHz, DMSO-d_6) δ 8.95 (s, 1H), 7.78 (d, J = 16.9 Hz, 2H), 7.48 – 7.37 (m, 4H), 7.16 (d, J = 8.6 Hz, 2H), 6.92 (d, J = 8.7 Hz, 2H), 6.85 (d, J = 8.9 Hz, 2H), 6.70 – 6.62 (m, 3H), 4.97 (s, 2H), 3.73 (s, 3H). ^{13}C NMR (126 MHz, DMSO-d_6) δ 151.99, 151.66, 150.62, 144.36, 143.29, 142.38, 130.16, 129.36, 129.31, 129.15, 127.20, 125.62, 116.28, 116.19, 109.08, 64.43. MS (ESI) *m/z*: 450.2 (M - H^+).

3.3.3 Experiments in Raw264.7 cells

Raw264.7 cells were maintained in DMEM supplemented with 10% FBS. To test the inhibitory effects of the new compounds on COX-2 activity, the cells were seeded to 24-well cell culture plate at a suitable density. When the cells reached 80% confluence, the medium was aspirated and the cells were washed twice with PBS pre-warmed to 37 °C. The cells in each well were then incubated with 0.5 mL fresh DMEM containing 1 μg/mL LPS and different concentrations of the compound of interest at 37 °C for 14 hours. At the end of incubation, 200 μL medium was transferred from each well to an Eppendorf tube. After spiked with 25 ng/mL PGD_2-d_4, the samples were extracted with 600 μL EtOAc twice. The extract was combined and dried by nitrogen. Before the UPLC-MS/MS analysis, the samples were reconstituted with 200 μL 25% methanol containing 0.1% formic acid. 40 μL supernatant was injected to the column for each sample after 15 minutes of centrifuge at 15,000 × g.

3.3.4 Experiments in HCA-7 cells

HCA-7 cell lines were maintained in McCoy's 5A medium supplemented with 10% FBS. To test the inhibitory effects of the new compounds on COX-2 activity, the cells were seeded to 24-well cell culture plate at a suitable density. When the cells reached 95% confluence, the medium was aspirated and the cells were washed twice with PBS pre-warmed to 37 °C. Then, the cells in each well were incubated with 0.25 mL fresh DMEM containing different concentrations of the compound of interest at 37 °C for 30 minutes. Then, to each well, 0.25 mL DMEM containing 100 μM A23187 and the same concentration of drug was added. The cell culture plate was gently shaken to mix the medium and then incubated at 37 °C for another 30 minutes.

At the end of incubation, the whole volume of medium in each well was transferred to an Eppendorf tube. After spiked with 5 ng/mL PGE_2-d_4, the samples were extracted with 1.5 mL EtOAc twice. The extract was combined and dried by nitrogen. Before the UPLC-MS/MS analysis, the samples were reconstituted with 100 μL 25% methanol containing 0.1% formic acid. 40 μL supernatant was injected to the column for each sample after 15 minutes of centrifuge at 15,000 × g.

3.3.5 Recombinant human COX-2 assay

Recombinant human COX-2 (1 unit) was incubated with 1 μM hematin, 5 mM GSH, 5 mM phenol, 10 mM EDTA and different concentrations of inhibitors or vector (0.1% DMSO) in 200 μL 50 mM potassium phosphate (KPi) buffer (pH 8.0) at 37 °C for 15 minutes. Then 10 μM AA was introduced in the samples to start the reaction. The samples were incubated at 37 °C for another 15 minutes and then put on ice to stop the reaction. After spiked with 25 ng/mL PGE_2-d_4, the samples were extracted with 600 μL EtOAc twice. The extract was combined and dried by nitrogen. Before the UPLC-MS/MS analysis, the samples were reconstituted with 200 μL 25% methanol containing 0.1% formic acid. 40 μL supernatant was injected to the column for each sample after 15 minutes of centrifuge at 15,000 × g.

3.3.6 PGs quantitation by UPLC-MS/MS

The quantitation of PGE_2 or PGD_2 was analyzed on a Waters Acquity^{TM} ultra-performance liquid chromatography coupled with an API 5500-Qtrap triple quadrupole mass spectrometer equipped with a TurboIonSpray^{TM} source. The UPLC conditions were: column, Waters BEH C18, 1.7μm, 100mm × 2.1mm (Waters, Milford, MA, USA); mobile phase A, 0.1% formic acid in water; mobile phase B, 0.1% formic acid in acetonitrile; gradient, 0-0.5 min, 5% B, 0.5-1.0 min, 5-37% B, 1.0-4.5 min, 37% B, 5.0-5.5 min, 95% B, 5.5-6.0 min, 95-5% B, 6.0-7.0 min, 5% B; flow rate, 0.5mL/min; column temperature, 45 °C; injection volume, 40 μL. As isomers, PGE_2 and PGD_2 were separated chromatographically with the retention times as 3.8 and 4.0 minutes, respectively. For either PGE_2 or PGD_2, the deuterated internal standard was eluted simultaneously.

The MS analysis was conducted at the negative ion mode by multiple reaction monitor (MRM) scan type. As isomers, PGE_2 and PGD_2 share common product ions, and the mass transition 351.2/271.2 was used for both of them. Similarly, for PGE_2-d_4 and PGD_2-d_4, the mass transition 355.2/275.2 was used. The compound-dependent parameters were shown in Table 2, and the main instrument-dependent parameters were set as follows: ionspray voltage, -4500 V; ion source temperature, 700 °C; nebulizer gas, 20 psi; turbo gas, 30 psi; curtain gas, 30 psi.

	Q1 (m/z)	Q3 (m/z)	Dwell Time (msec)	DP (V)	EP (V)	CE (V)	CXP (V)
PGE_2/PGD_2	351	271	100	-65	-10	-24	-15
PGE2-d_4/PGD2-d_4	355	275					

Table 2. Compound-dependent parameters of PGE_2, PGD_2, PGE_2-d_4, and PGD_2-d_4 in MS analysis.

3.3.7 Data analysis

The inhibition-concentration curves were established for celecoxib and the new compounds to study their inhibitory effects on COX-2 activity in the cell-based assays. The half maximal inhibitory concentration (IC_{50}) values were obtained by fitting the experimental data into the following equation:

$$\text{Inhibition}(\%) = \frac{100}{1 + \frac{\text{IC}_{50}}{\text{Concentration}}}$$

3.4 Results

3.4.1 Chemistry

The synthesis route of the new compounds was design based on that of celecoxib described previsouly (Scheme 2) [123]. Acetophenone (**1b**) and many of its derivatives are commercially available. Among these compounds, we selected 4′-methylacetophenone (**1a**), acetophenone and 4'-methoxyacetophenone (**1c**) as the starting materials according to the SAR studies of celecoxib. Instead of ethyl trifluoroacetate, dimethyl oxalate was used as another starting material. After the condensation of the dione and (4-sulfamoylphenyl)hydrazine hydrochloride, the 1,5-diarylpyrazoles **3a-c** were synthesized as the analogs of celecoxib. As ethyl esters, **3a-c** were reduced by $LiAlH_4$ to alcohols **4a-c.** Then **4a-c** were brominated by PBr_3, yielding the alkyl bromides **5a-c**. The reaction of the alkyl bromides with various phenolic compounds including 1,2-dihydroxybenzene, resorcinol, hydroquinone, 3,7-DHF in the presence of K_2CO_3 in refluxed acetonitrile, yielding the final products as **6a1**, **6a2**, **6a3**, **6a4**, **6b2**, **6b3**, **6c2**, and **6c3**.

3.4.2 The inhibitory effects of the new compounds on COX-2 in Raw264.7 cells

Upon LPS induction, the predominant PG produced from overexpressed COX-2 in the Raw64.7 cells was determined as PGD_2. Thus the PGD_2 concentrations in the cell culture medium were used as the indicators of COX-2 activity. The PGD_2 production in the Raw264.7 cells was inhibited by celecoxib and all the new compounds tested, but with different potencies (Figure 12). The IC_{50} of celecoxib was as low as 0.003 μM, which revealed that celecoxib is a very potent inhibitor on COX-2 activity. The modifications in the structure of celecoxib more or less reduced its inhibitory effect on COX-2 activity (Table 3). At high concentrations (> 10 μM), all the new compounds tested potently inhibited PGD_2 production in Raw264.7 cells, but their inhibitory effects differed at concentrations lower than 10 μM. Among the new compounds, the ones with a 4-phenol group (**6a3**, **6b3**, and **6a3**) were much more potent than the others, and their IC_{50} values

were lower than 0.05 μM. In contrast, the IC_{50} values of the ones with 2- or 3-phenol groups were higher than 1 μM, implying that the efficacy of celecoxib was perhaps largely impaired by the structural modifications. Meanwhile, the IC_{50} values of the new compounds with the same phenolic group species were comparable, although the compounds were with different R_1 groups.

1409

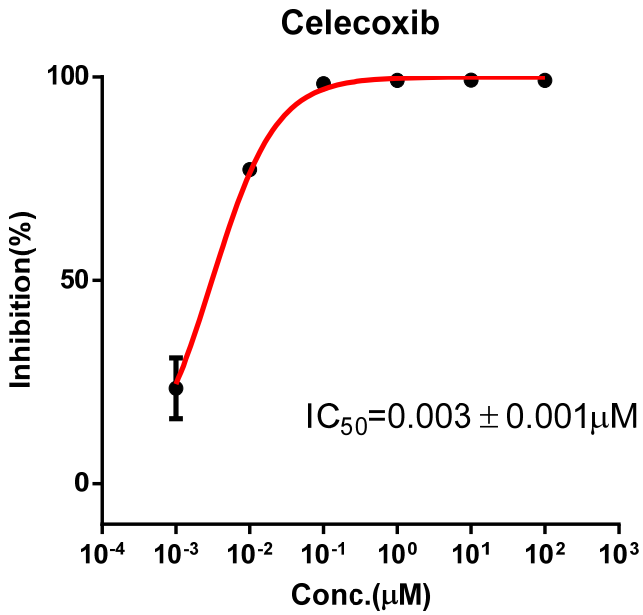

1410

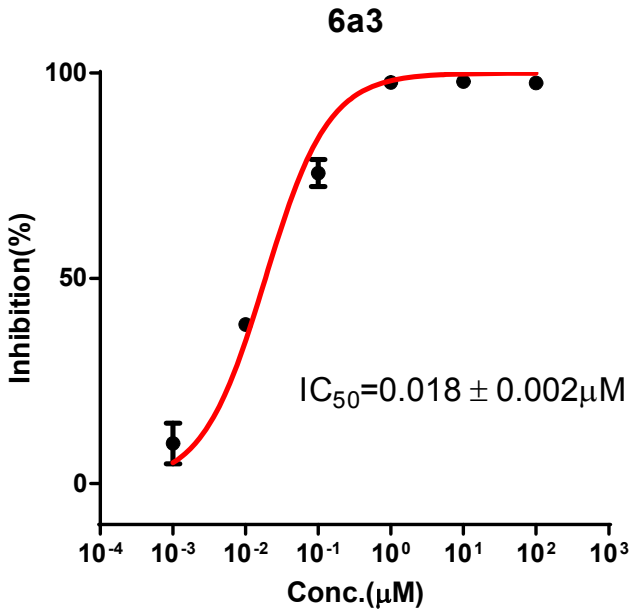

1411

1412 **Figure 12. The concentration-inhibition curves of celecoxib and 6a3 in**

1413 **Raw264.7 cells.**

1414

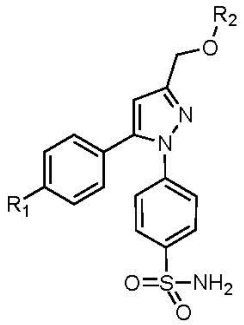

Compound	R_1	R_2	M.W.	c Log P	IC_{50}
6a1	$-CH_3$	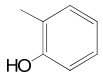	435.1	4.64[a]	1.387±0.384
6a2	$-CH_3$	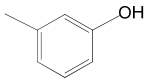	435.1	4.64[a]	4.618±1.342
6a3	$-CH_3$	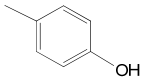	435.1	4.64[a]	0.019±0.002
6a4	$-CH_3$	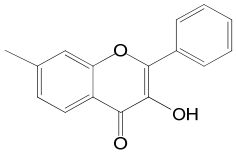	579.6	4.90[a]	0.303±0.055
6b2	-H	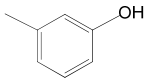	421.5	4.15[a]	4.311±0.629
6b3	-H	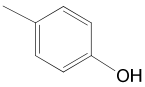	421.5	4.15[a]	0.033±0.004
6c2	$-OCH_3$	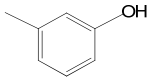	451.1	4.02[a]	2.379±0.502
6c3	$-OCH_3$	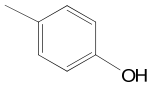	451.1	4.02[a]	0.019±0.002
celecoxib	-	-	381.4	4.01[b]	0.003±0.001

M.W., Molecular Weight.
ND, Not Determined.
[a], predicted with ChemDraw Software.
[b], from http://www.drugbank.ca/drugs/DB00482

Table 3. IC_{50} values of the new compounds on PGD_2 production in Raw264.7 cells.

3.4.3 The inhibitory effects of the new compounds on COX-2 in HCA-7 cells

The inhibitory effects of celecoxib, **6a1**, **6a2**, **6a3** and **6a4** on COX-2 activity were also investigated in HCA-7 cells, a human CRC cell line with constitutive COX-2 expression [151]. The cells were pre-incubated with the compound of interest before AA release inside the cells was stimulated by the calcium ionophore A23187. PGE_2 is the predominant product derived from COX-2 in this cell line, and at the end of incubation its content in the medium indicated the COX-2 activity.

As well as in the Raw264.7 cells, celecoxib potently inhibited COX-2 activity in the HCA-7 cells with an IC_{50} of 0.003 μM. The new compounds tested also inhibited COX-2, but with much lower potencies. The $IC50_s$ of the new compounds were determined to be between 0.05 and 0.2 μM (Figure 13). Although **6a3** was still more potent than the other three compounds, however, the difference between their IC_{50} values was much smaller than what was observed in Raw264.7 cells. The IC_{50}s of **6a1**, **6a2**, and **6a4** were only 2 to 3 folds higher than that of **6a3**. Considering the unavoidable variation between different experiments, **6a3** may be only slightly superior to the other compounds in the potency when serving as COX-2 inhibitors. The selection criteria of a lead compound for the following studies included not only the IC_{50} value on COX-2 but also other characteristics, especially metabolism rates. To remove any bias impacting the selection of a lead compound, the divergence between the results from the two cell lines was further investigated in 2.4.4.

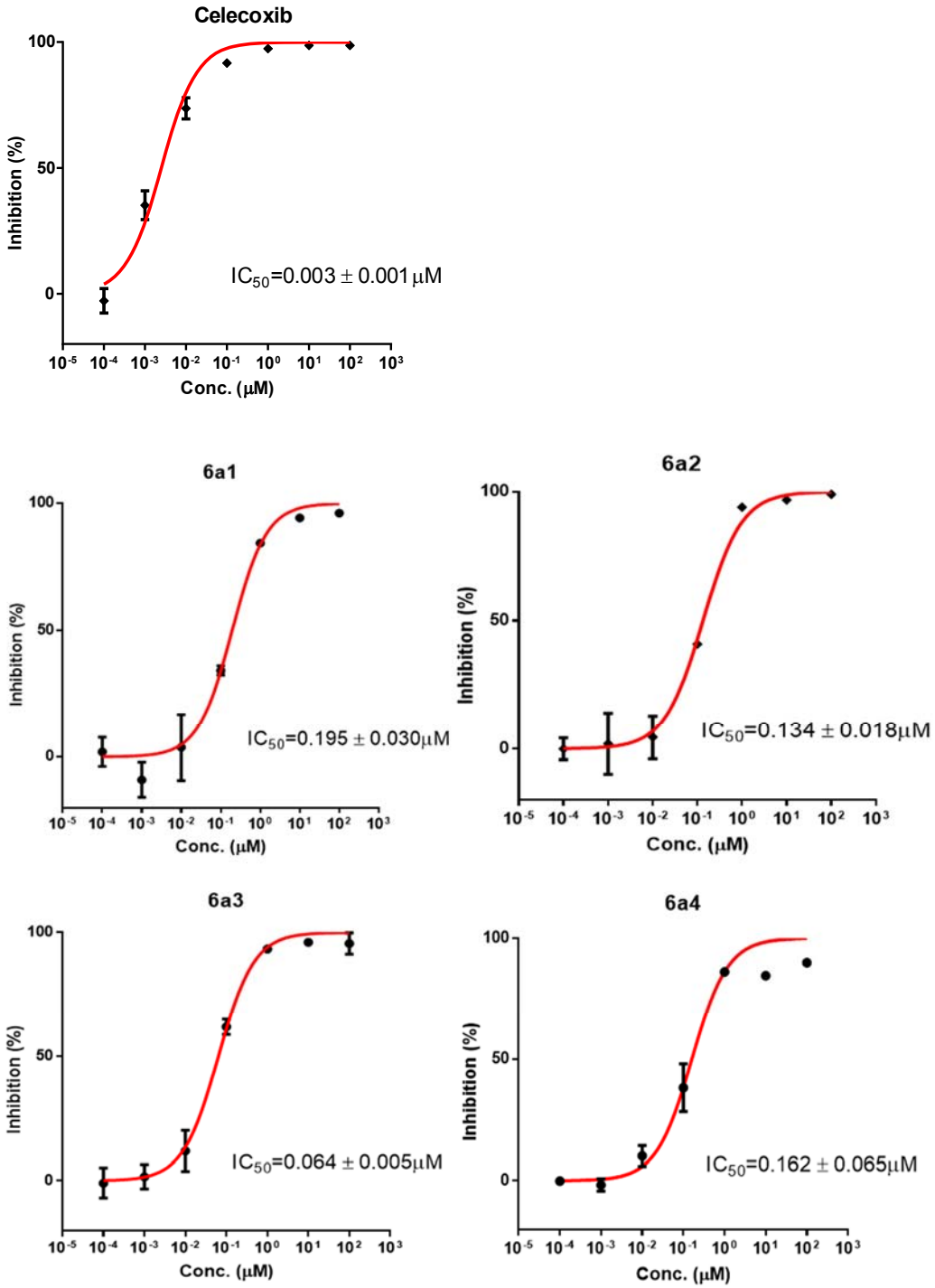

Figure 13. Inhibition of celecoxib and 6a1-4 on PGE_2 production in HCA-7 cells.

3.4.4 The metabolism of the new compounds in Raw264.7 cells

To investigate why **6a1** and **6a2** were much less potent than **6a3** in inhibiting COX-2 activity in the Raw264.7 cells, the metabolism of these new compounds were examined in the incubation with Raw264.7 cells.

Firstly, 1 μM of each compound was incubated with the cells respectively and the content of each compound in the cell culture medium was examined after the 14 hour incubation. The results indicated that at the end of the incubation period, **6a1** and **6a2** were recovered exclusively as their glucuronides, while the majority of **6a3** remained as unconjugated aglycone (Figure 14, A, upper). Meanwhile, we found that PGD_2 production by the cells incubated with 1 μM **6a1** or **6a2** was only slightly reduced, while 1 μM **6a3** thoroughly inhibited PGD_2 production (Figure 14, A, lower).

Further, to figure out whether the ability of Raw264.7 cells to conjugate substrates was induced by LPS or not, 1 or 10 μM **6a1** was incubated in the Raw264.7 cells with or without LPS induction. The results showed that **6a1** was extensively conjugated in Raw264.7 cells and the glucuronidation of **6a1** was not altered by LPS (Figure 14, B, upper). The UGT activity in Raw264.7 cells was constitutive. Meanwhile, 1 μM **6a1** had only minimal effects on PGD_2 production in LPS-induced Raw264.7 cells, while 10 μM **6a1** inhibited >90% PGD_2 production (Figure 14, B, lower).

Then, we introduced β-glucuronidase into the cell culture medium when 1 μM **6a1** was incubated with the Raw264.7 cells in the presence of LPS. At the end of incubation, the majority of **6a1** in the culture medium was recovered as unconjugated aglycone (Figure 14, C, upper) and the inhibitory effects of **6a1** on PGD_2 production was largely restored (24.3% of control with glucuronidase versus 67.5% of control without glucuronidase) (Figure 14, C, lower).

1473 A

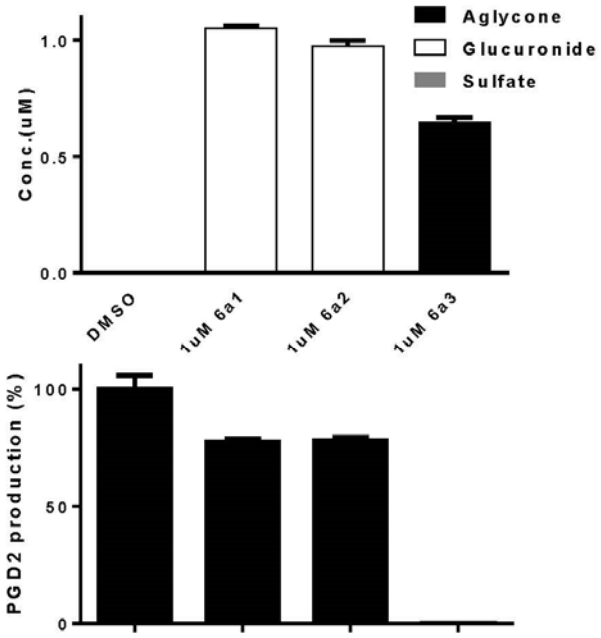

1474

1475 B

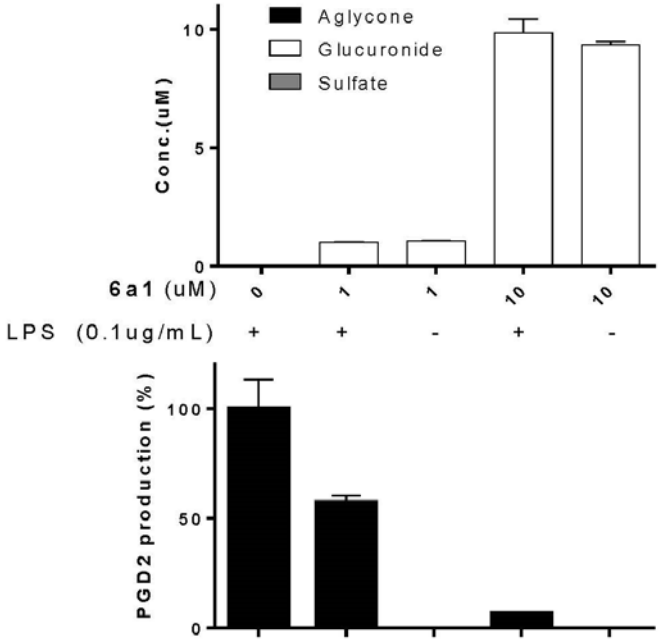

1476

1477

C

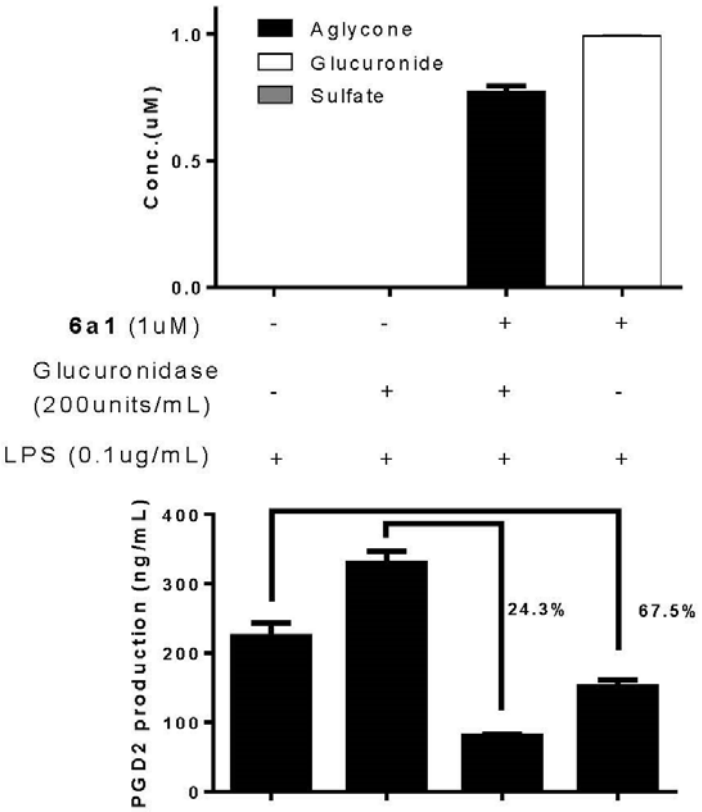

Figure 14. Metabolism of the new compounds in Raw264.7 cells.

(A) 1 μM **6a1**, **6a2** or **6a3** was incubated with Raw264.7 cells for 14 hours in the presence of 1 μg/mL LPS. (B) 1 or 10 μM **6a1** was incubated with Raw264.7 cells for 14 hours. With or without 1 μg/mL LPS in the cell culture medium, **6a1** was recovered as glucuronide in all the samples at the end of incubation. (C) When 1 μM **6a1** was incubated with Raw264.7 cells in the presence of 1 μg/mL LPS, 200 units/mL β-glucuronidase was introduced into the cell culture medium. The inhibitory effects of 6a1 was enhanced by β-glucuronidase.

3.4.5 Recombinant human COX-2 assay

Besides the cell-based assays, we also confirmed the inhibitory effects of the new compounds on recombinant human COX-2 enzyme activity (Figure 15). The result indicated that in the presence of 1 μM **6a1**, **6a2**, or **6a3**, the PGE_2 production by COX-2 enzyme were inhibited to lower than 25% compared to the control group. 0.1 μM **6a1** or **6a3** could inhibit approximately 50% percent of PGE_2 production by COX-2 enzyme. 0.1 μM **6a2** was even more potent.

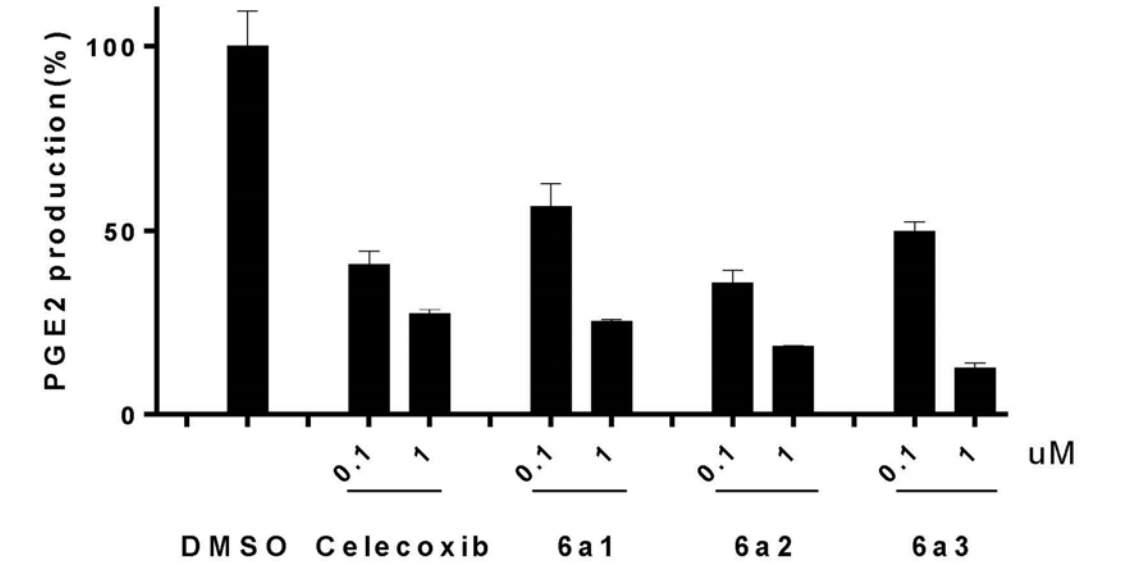

Figure 15. The inhibitory effects of celecoxib and 6a1-6a3 on recombinant human COX-2 activity.

3.5 Discussion

The selective COX-2 inhibitors including rofecoxib and celecoxib became blockbuster drugs in the treatment of inflammatory arthritis at the end of last century. In human clinical trials, the two drugs were also investigated for their efficacy in CRC therapy and chemoprevention. These clinical trials successfully demonstrated the anti-CRC effectiveness of rofecoxib and celecoxib, but also revealed their adverse effects in the human cardiovascular system. Since then, the long-term and high dose use of the selective COX-2 inhibitors was considered as dangerous to the cardiovascular health of patients. All the selective COX-2 inhibitors were withdrawn from the market except celecoxib. To improve the safety of selective COX-2 inhibitor usage in human, researchers were trying to employ different approaches to reduce their cardiovascular toxicity. For example, one approach was to release protective nitric oxide (NO). Velázquez et al. designed and synthesized a series of hybrid COX-2 inhibitor/NO donor agents which could release NO to rescue the cardiovascular system from platelet aggregation and adhesion [152]. However, more efforts are required to demonstrate the effectiveness of this approach before any clinical use of these NO donor agents.

Here in the current study, a novel strategy has been proposed to develop new selective COX-2 inhibitors which are devoid of cardiovascular toxicity. The new selective COX-2 inhibitors were developed as phenolic compounds with poor oral bioavailability, extensive first-pass effects and extremely low blood concentrations in systemic circulation. In contrast to the previous studies, this strategy could be considered as pharmaceutical rather than pharmacological, because it took advantage of rapid phase II metabolism and excretion to make COX-2 inhibitors only locally bioavailable. As the only selective COX-2 inhibitor in the market, celecoxib was selected as the template to design new compounds. The inhibitory effect of celecoxib on COX-2 activity should be appropriately retained when phenolic groups are incorporated in its chemical structure. Meanwhile, previous structure-activity relationship studies of celecoxib revealed that hydroxyl

group substitutions on either aryl ring resulted in complete loss of the anti-COX-2 potency [123]. Thus we decided to substitute the $-CF_3$ group on the central pyrazole ring of celecoxib with phenolic groups (R_2). Also, the methyl group of celecoxib on one aryl ring was substituted by other hydrophobic groups including –H and –OMe (R_1).

After synthesis and purification, eight new compounds were obtained. The inhibitory effects of celecoxib and the new compounds were firstly assessed and compared in the murine macrophage cell line Raw264.7. Celecoxib was identified as a very potent inhibitor of COX-2. Among all the new compounds, the IC_{50} values of **6a1**, **6a2**, **6b2** and **6c2** were found to be at least 20-fold higher than those of **6a3**, **6b3** and **6a3**. Based on the results in Table 3，it seemed that we should select lead compounds from **6a3**, **6b3** and **6b3** for the following studies. However, in human CRC cell line HCA-7, the IC_{50} values of **6a1** and **6a2** on COX-2 activity were determined to be at most 3-fold higher than that of **6a3**. The divergence between the results obtained in different cell lines attracted our attention and the reason was further investigated. The long incubation time of the new compounds with Raw264.7 cells prompted us to check their chemical and metabolic stability. Surprisingly, **6a1** and **6a2** were recovered exclusively as glucuronides in the cell culture medium, and the majority of **6a3** was still unconjugated when the incubation ended. After the introduction of β-glucuronidase into the cell culture medium, the efficacy of **6a1** to inhibit PGD_2 production largely improved. The inhibitory effects of **6a1** and **6a2** on COX-2 activity were impaired by metabolism in Raw264.7 cells, because the conjugation and excretion decreased their concentrations inside the cells. Also, the glucuronidation activity in Raw264.7 cells was constitutive because **6a1** was conjugated by this cell line either with or without LPS induction. Due to the high hydrophilicity of glucuronides, the efflux transporters expressed on the cell membrane were probably involved in their excretion from the cells to the cell culture medium. These results also indicate that in the screening of drug candidates with a cell-based assay, the stability and possible biotransformation of the compounds should be considered as important

factors which can influence the results, especially when the incubation time is very long. In additions, for **6a1**, **6a2** and **6a3**, no significant differences was observed in their inhibitory effects on human recombinant COX-2 enzyme activity. Taken together, the results from different experiments clearly illustrated that if only based on the IC_{50} values of the new compounds in Raw264.7 cells, the selection of lead compounds for the following studies would be largely biased. In this project, anti-COX-2 potency is necessary but not enough for developing a locally bioavailable COX-2 inhibitor. An eligible compound should be with extensive first-pass effects as well. Thus, it was not appropriate to select a leading compound before the metabolic properties of these new compounds were investigated.

The new compounds were designed using celecoxib as a template. With an interpretation of its SAR, we tried to make modifications to the structure of celecoxib and expected that the anti-COX-2 activity was impacted as less as possible. However, compared with celecoxib, all the new compounds were found to be much less potent in inhibiting COX-2 activity. The substitution of $–CF_3$ by the other groups weakened the binding affinity between the inhibitor and COX-2 protein, although substitutions of any position on the two aryl rings by a hydroxyl group would lead to a greater or even complete loss in potency. When the active site of COX-2 protein is occupied by celecoxib, the two aryl rings interact with the amino acid residues deep inside the binding pocket, and the $–CF_3$ group was near the opening of the binding pocket. Judging from the IC_{50} values of celecoxib and the new compounds determined in experiments, the substitution of $-CF_3$ group by a more bulky group unfortunately decreased the binding affinity. The negative effect of such a substitution may be due to a lack of extra space near the pocket opening to accommodate a bulky group. Compared with celecoxib, the new COX-2 inhibitors with increased IC_{50} values will probably have lower efficacies to prevent CRC development *in vivo*, although so far no quantative studies are available for reference. In the following studies, when we wanted to validate the inhibitory effects of **6a1**, **6a2**, and **6a3** on colonic COX-2 in rats, a much higher

concentration than that of celecoxib was required in the perfusate to alter the half-life of PGE_2 attenuation. Thus, in the future development of locally bioavailable COX-2 inhibitors, perhaps it is quite necessary for the researchers to obtain next-generation compounds which are superior to the current ones before the efficacy studies are conducted in certain CRC chemoprevention model.

Chapter 4 *In Vitro* Characterization of the Metabolic Properties of the New Compounds and Pharmacokinetics (PK) Studies

4.1 Abstract

Besides the potency in inhibiting COX-2 activity, a poor systemic bioavailability is another essential property of an eligible locally bioavailable COX-2 inhibitor. After the new compounds were confirmed as COX-2 inhibitors in the last chapter, their metabolic properties were characterized by the *in vitro* tools and models, as well as in the PK studies in rats.

The phase II metabolism rates of the new compounds was determined by employing the subcellular fractions including microsomes and S9 fractions prepared from different organs of rats or human. For either glucuronidation or sulfation, the conjugation rates of the new compounds were shown to be largely determined by the phenolic group species (R_2), while the substitutions on one of the aryl rings (R_1) had an only slight influence. Based on the IC_{50} values on COX-2 activity and the phase II metabolism rates characterized *in vitro*, **6a1** was selected as a lead compound in the following studies. **6a1** was put into the Caco-2 monolayer model to study its absorption, metabolism and excretion in colonic epithelium. **6a1** was easily absorbed into the cells and rapidly metabolized. The predominant metabolite was **6a1**-sulfates and the majority of sulfates were excreted to the apical side. Less metabolites were found to be **6a1**-glucuronide.

Besides *in vitro* characterization, we also conducted PK studies in Sprague Dawley (SD) rats of after oral administration of 20 mg/kg celecoxib or **6a1**. The peak blood concentration of celecoxib in the systemic circulation was 3000-fold higher than its IC_{50} on COX-2 activity and the half-life was 5.7 hours. The cardiovascular system was exposed to very high blood levels of celecoxib. In contrast, the blood concentration of **6a1** and its phase II metabolites never exceeded

0.015 μM, which was much lower than its IC_{50}. The PK study of **6a3** was also conducted at the same dose, and peak blood concentration of **6a3** was found to be higher than 1.5 μM, which was 20-fold higher than its IC_{50}. The significant difference in PK profiles between **6a1** and **6a3** illustrated that the poor oral bioavailability of **6a1** was probably caused by extensive first-pass effects.

4.2 Introduction

In Chapter 2 we successfully designed and developed a series of new compounds as selective COX-2 inhibitors. With phenolic groups in their structures, these compounds were built as substrates of the phase II enzymes including UGTs and SULTs. It has long been know that the systemic bioavailability of certain phenolic compounds can be dramatically decreased by the first-pass effects after oral administration. The aim of the current project is to develop COX-2 inhibitors only locally bioavailable in colon by taking advantage of the extensive first-pass metabolism and excretion. Hence, the new compounds were characterized for their absorption, metabolism and excretion properties by *in vitro* tools or in rats.

In this chapter we will first characterize the *in vitro* phase II metabolism by subcellular fractions including microsomes and S9 fractions. The microsomes prepared from human and animal tissues contain various membrane-bound drug metabolizing enzymes such as CYP450s, UGTs, and carboxylesterases. The microsomes were employed as an enzyme resource of UGTs in the *in vitro* glucuronidation of the new compounds. The S9 fractions obtained from organ or tissue homogenates by centrifuging at 9000 × g contain both cytosolic and microsomal enzymes. In the *in vitro* sulfation of the new compounds, the S9 fractions were employed as an enzyme resource of cytosolic SULTs. The microsomes or S9 fractions prepared from small intestine, colon and liver were employed for comparing the conjugation rates of the new compounds by different organs. The locally bioavailable COX-2 inhibitors are supposed to be relatively stable in the colon but metabolized and excreted efficiently in the liver. Among the new compounds, the ones efficiently conjugated by the liver subcellular fractions were the most promising to be only locally bioavailable. Also, the ideal compound should also be relatively slowly conjugated by the colon subcellular fractions, because the inhibitory effect on colonic COX-2 may be impaired by the rapid metabolism in the colon. Two phenolic compounds, raloxifene and genistein, were used

as controls in glucuronidation and sulfation, because both of them undergo extensive first-pass effects and have low oral bioavailability *in vivo*.

Besides the microsomes and S9 fractions, Caco-2 cell monolayer was also employed in the *in vitro* characterization. The Caco-2 cell monolayer is a well-established model to study the absorption, metabolism and transport of drugs in the human gastrointestinal tract [153]. The model may help us to better predict the disposition of the new compounds in colonic epithelium which is undergoing carcinogenesis, because Caco-2 is a human CRC cell line.

After the *in vitro* characterization, *in vivo* pharmacokinetics studies were also conducted in rats for the prototype drug celecoxib, as well as the new compounds. The blood concentrations in the systemic circulation were determined at different time points after oral administration. Celecoxib has been reported as a drug with rapid absorption and excellent oral bioavailability in both human and rats. Here, the pharmacokinetics of celecoxib in rats was validated, and the result was also compared to that of the new compounds. Among the new compounds, the one showing ideal metabolism rates in the *in vitro* characterization was selected as the lead compound and given to rats in the pharmacokinetics study. Besides the lead compound, another new compound which was not metabolized very rapidly *in vitro* was also investigated for its pharmacokinetics in rats. Comparing the blood concentrations of these two new compounds would help to determine whether the *in vitro* metabolism rates could be effectively extrapolated *in vivo* or not. If so, in the future, the *in vitro* characterization of metabolism rates will be employed to identify compounds which are only locally bioavailable, especially when a much larger number of new compounds are synthesized than at the current stage.

4.3 Materials and Methods

4.3.1 Materials

All the materials were analytical grade or better. Celecoxib was purchased from LC laboratory (Woburn, MA). Genistein was purchased from Indofine Chemicals (Somerville, NJ). Raloxifene, UDPGA, magnesium chloride ($MgCl_2$), alamethicin, D-saccharic-1,4-lactone monohydrate, PAPS, dithiothreitol (DTT), KH_2PO_4, K_2HPO_4, HCl, sodium chloride (NaCl), and Hanks' balanced salt solution (HBSS, powder) were purchased from Sigma-Aldrich (St Louis, MO). The cloned Caco-2 cell line (TC7) was a kind gift from Dr. Moniqué Rousset of Institut National de la Santé et de la Recherche Médicale U178 (Villejuit, France). DMEM and FBS for Caco-2 cell culture were purchased from Life Technologies (Carlsbad, CA). The pooled human liver and intestine microsomes were purchased from BD Biosciences (Woburn, MA). The pooled human liver and intestine S9 fractions were purchase from Xenotech (Lenexa, KS). The rat liver and colon microsomes/S9 fractions were prepared from the SD rats as previously described [154].

4.3.2 Animals

Male SD rats (approximately 250g) were purchased from Harlan Laboratory (Indianapolis, IN). They had been kept in the animal facilities for at least one week before any experiment.

4.3.3 *In vitro* glucuronidation by microsomes

The glucuronidation rates of the new compounds were determined *in vitro* by using the microsomes from various sources. In 200 μL 50 mM KPi (pH 7.4), the microsomes (final protein concentration approximately between 0.01-0.05 mg/mL), $MgCl_2$ (0.88 mM), D-Saccharic acid 1,4-lactone monohydrate (4.4 mM), alamethicin (0.022 mg/mL), and 10 μM substrate were mixed. The sample was pre-warmed at 37 °C for 5 minutes before UDPGA (final concentration 3.5 mM) was added to start the reaction. After incubation for a pre-determined period of time (typically 15, 30 or 60 minutes) at 37 °C, the reaction was stopped by adding 50 μL 94% acetonitrile/6% formic acid containing 50 μM formononetin or 100 μM testosterone as the internal standard. After 15 minutes of 15,000 × g centrifuge, 10 μL supernatant from each sample was injected for UPLC-

UV analysis. For the substrates in all the samples, less than 15% of the total amount was conjugated when the incubation was ended. For each substrate, the experiment was performed in triplicate. Genistein and raloxifene were employed as positive controls for glucuronidation.

4.3.4 *In vitro* sulfation by S9 fractions

The sulfation rates of the new compounds were determined *in vitro* by using the S9 fractions from various sources. In 150 μL 50 mM KPi (pH 7.4), the S9 fractions (final protein concentration approximately between 0.01-0.05 mg/mL), $MgCl_2$ (5 mM), DTT (10 mM), and 10 μM substrate were mixed. The sample was pre-warmed at 37 °C for 5 minutes, and then PAPS (final concentration 0.1 mM) was added to start the reaction. After incubation for a pre-determined period of time (typically 15, 30 or 60 minutes) at 37 °C, the reaction was stopped by adding 50 μL 94% acetonitrile/6% formic acid containing 50 μM formononetin or 100 μM testosterone as the internal standard. After 15 minutes of 15,000 × g centrifuge, 10 μL supernatant from each sample was injected for UPLC-UV analysis. For the substrates in all the samples, less than 15% of the total amount was conjugated when the incubation was ended. For each substrate, the experiment was performed in triplicate. Genistein and raloxifene were employed as positive controls for sulfation.

4.3.5 Caco-2 monolayer assay

The Caco-2 cells were maintained in DMEM supplemented with 10% FBS. In the present study, the procedures to establish Caco-2 monolayers were performed as they were described previously [155]. In brief, after the cells reached at least 95% confluence in a flask, they were seeded onto the inserts in a 6-well cell culture cluster at a suitable density. After the seeding, the cell culture medium was changed every other day, and the Caco-2 monolayer was ready for experiments in 19-22 days. Before experiments, the cell culture medium was aspirated and the Caco-2 cell monolayers were washed three times with blank HBSS, pH 7.4, at 37 °C. The trans-epithelial

electrical resistance (TEER) values were measured, and the monolayers with TEER lower than 500 ohms/cm^2 were discarded.

After the Caco-2 monolayer was incubated with blank HBSS (pH 7.4) for 1 hour, 2.5 mL HBSS (pH 7.4) containing 10 μM **6a1** in was applied to either apical side or basolateral side, and 2.5 mL blank HBSS (pH 7.4) was loaded to the other side to receive **6a1** and its phase II metabolites after trans-epithelial transport or excretion. The absorbed, metabolized and excreted amounts of **6a1** were monitored as a function of time. 0.25, 0.5, 1, 2, 4, 6 and 8 hours after the experiment began, 200 μL of sample was collected from the donor and receiver sides, respectively. Each time after the samples were taken, 200 μl of donor solution was added to the donor side, and the receiver side was supplemented with 200 μl of blank HBSS as well. The samples were immediately mixed with 25 μL 94% acetonitrile/6% formic acid containing 50 μM formononetin as the internal standard. After 15 minutes of 15,000 × g centrifuge, 10 μL supernatant from each sample was injected for UPLC-UV analysis.

4.3.6 Quantitation of the new compounds and their phase II metabolites by UPLC-UV

The new compounds and their metabolites were quantitated on a Waters Acquity^{TM} UPLC equipped with a DAD. The conditions were: column, Waters BEH C_{18}, 1.7 μm, 50 mm × 2.1 mm (Waters, Milford, MA, USA); mobile phase A, 2.5mM NH_4Ac in water, pH 7.4; mobile phase B, 100% acetonitrile; gradient, 0-2.0 min, 10-20% B, 2.0-3.0 min, 20-40% B, 3.0-3.5 min, 40-50% B, 3.5-4.0 min, 50-90% B, 4.0-4.5 min, 90% B, 4.5-5.0 min, 90-10% B; flow rate, 0.5mL/min; column temperature, 45 °C; detect wavelength, 254nm; injection volume, 10 μL.

4.3.7 Pharmacokinetics study in SD rats

The procedures for animal experiment were approved by University of Houston Institutional Animal Use and Care Committee (IACUC). The rats (n=6 in each group) were fasted for

approximately 14 hours with free access to water before the experiment. Celecoxib, **6a1**, or **6a3** dispersed in Ora-Plus® suspension vehicle was administrated to rats by oral gavage at the dose of 20mg/kg. At each time point, approximately 50μL blood was collected in heparinized tubes from the rats by tail tip snipping (1-2 mm cut) after the rat was anesthetized by isoflurane. The blood samples were frozen immediately after collection and stored at -80 °C until analysis.

4.3.8 Blood sample preparation

40 μL blood sample was initially mixed with 40 μL saturated NaCl solution (pH 1.5, adjusted by HCl). Then 300 μL acetonitrile containing 0.1 μM 1-(4-sulfamoylphenyl)-5-(*p*-tolyl)-1*H*-pyrazole-3-carboxylic acid (internal standard) was added and the mixture was vigorously vortexed for 1 min. The addition of the inorganic salt to blood sample made it immiscible with acetonitrile and the extraction was referred to as "salting-out liquid-liquid extraction" [156]. After 10 minutes of 15,000 × g centrifugation, the supernatant was transferred to a new tube. The extraction was repeated once and the extract was combined and evaporated to dryness under nitrogen flow. Before analysis the samples were reconstituted in 100μL 25% acetonitrile containing 0.1% formic acid and centrifuged at 15,000 × g for 15 minutes. 10μL supernatant was injected for UPLC-MS/MS analysis.

4.3.9 Quantitation of celecoxib, 6a1, 6a1-glucuronide, 6a1-sulfate, 6a3, 6a3-glucuruonide, 6a3-sulfate by UPLC-MS/MS

UPLC-MS/MS analysis was conducted with an API 5500-Qtrap triple quadrupole mass spectrometer (Applied Biosystem/MDS SCIEX, Foster City, CA, USA) equipped with a TurboIonSpray^{TM} source at the negative ion mode. The analyte concentrations were determined by MRM scan type. The compound-dependent parameters for all the analytes were listed in Table 3, and the main instrument-dependent parameters were set as follows: ionspray voltage, -4500 V; ion source temperature, 700 °C; nebulizer gas, 20 psi; turbo gas, 30 psi; curtain gas, 30 psi.

	Q1 (m/z)	Q3 (m/z)	Dwell Times (msec)	DP (V)	EP (V)	CE (V)	CXP (V)
Celecoxib	380	316	100	-265	-10	-32	-21
6a1 / 6a3	434	108	100	-50	-10	-24	5
6a1-glucuronide / 6a3-glucuonide	610	113	100	-100	-10	-30	-11
6a1-sulfate / 6a3-sulfate	514	187	100	-100	10	-30	-11
I.S.	356	312	100	-10	-10	-22	-17

Table 4. Compound-dependent parameters in the analysis of the rat blood samples by MS.

4.4 Results

4.4.1 *In vitro* metabolism by microsomes or S9 fraction

The *in vitro* metabolism rates can be used for predicting the *in vivo* metabolic clearance and bioavailability. The new compounds were built with phenolic groups in their structures, in order to make them excellent substrates in phase II metabolism. Before any *in vivo* studies, the metabolism of the new compounds were first characterized by *in vitro* tools. With abundant phase II metabolic enzymes expression, the microsomes or S9 fractions prepared from different organs of human or rats were employed. The results from the *in vitro* assays were helpful for the investigators to select a lead compound which was most likely can be only locally bioavailable.

The effects of R_1 and R_2 groups on the metabolism rates were firstly investigated. For the substrates with the same R_2, the glucuronidation or sulfation rates were found to be similar in the incubation with rat liver microsomes and S9 fractions (Figure 16, A and B). In other words, the variety of R_1 groups did not have significant impact on the metabolism rates. Also, a substrate with a 2- or 3-phenol group was more favored by the phase II metabolic enzymes than that with a 4-phenol group. In either glucuronidation or sulfation by rat liver subcellular factions, **6a1**, **6a2**, **6b2**, and **6c2** were more rapidly conjugated than raloxifene and genistein. The results indicate that it is quite possible for these 4 compounds to undergo extensive first-pass metabolism in rat liver.

The locally bioavailable COX-2 inhibitors are proposed to be adequately stable in colon to inhibit COX-2, but rapidly conjugated and excreted in liver. Although it is quite doubtful that we can obtain a compound without any conjugation in colon, the ideal compound should at least be conjugated much more rapidly in the liver than in the colon. Hence, we also compared the abilities of rat colon and liver to conjugate the new compounds. For both glucuronidation and sulfation, microsomes or S9 fractions prepared from rat liver were usually much more efficient in

conjugating **6a1**, **6a2**, **6a3**, and **6a4** than those prepared from rat colon (Figure 16, C and D). Due to the differences between the colonic epithelium and liver in size and weight, it can be expected that the liver will exhibit a much greater capacity in conjugating these compounds than the colonic epithelium.

To figure out whether the results obtained in rat model could be reasonably extrapolated to humans, microsomes and S9 fractions prepared from human liver and intestine were also characterized for their abilities to conjugate the new compounds. Here the human intestine subcellular fractions were used because the human colon subcellular fractions were not commercially available. **6a1** was the most rapidly conjugated as glucuronide by the human liver microsomes among all the substrates. The glucuronidation rate of **6a1** by the human intestinal microsomes was much lower than that by the human liver microsomes (Figure 16, E). For **6a2** and **6a3**, the glucuronidation rates by different microsomes were similar. However, similar to raloxifene and genistein, **6a4** was more efficiently conjugated as a glucuronide by the human intestine microsomes, indicating that it was perhaps not suitable to be developed as a locally bioavailable drug in colon. Surprisingly, the sulfation rates of the new compounds by human intestine S9 fractions were found to be tens of fold higher than those by human liver S9 fractions (Figure 16, F), which was quite different from what we observed in the subcellular fractions of rats. It is still not clear whether the human colon S9 fractions can conjugate these new compounds to sulfates as efficiently as the human intestine S9 fractions. The relevant species difference in phase II metabolism between rats and human should be considered in the further studies of the locally bioavailable COX-2 inhibitors.

A

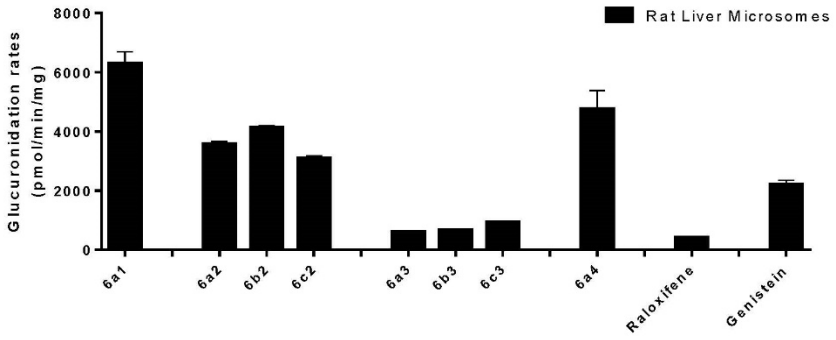
Rat Liver Microsomes
Glucuronidation rates (pmol/min/mg)
8000
6000
4000
2000
0
6a1
6a2
6b2
6c2
6a3
6b3
6c3
6a4
Raloxifene
Genistein

B

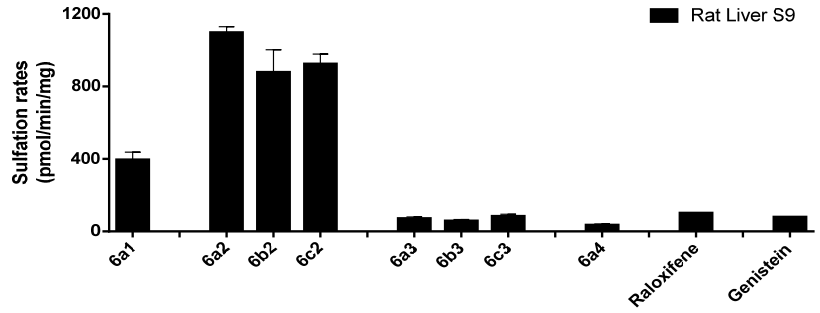
Rat Liver S9
Sulfation rates (pmol/min/mg)
1200
800
400
0
6a1
6a2
6b2
6c2
6a3
6b3
6c3
6a4
Raloxifene
Genistein

C

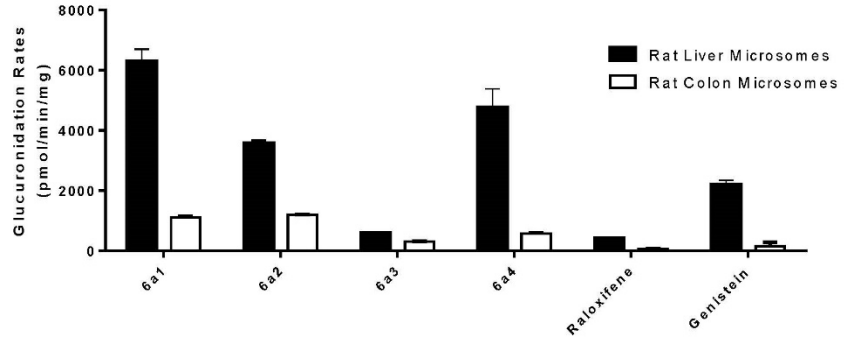
Rat Liver Microsomes
Rat Colon Microsomes
Glucuronidation Rates (pmol/min/mg)
8000
6000
4000
2000
0
6a1
6a2
6a3
6a4
Raloxifene
Genistein

D

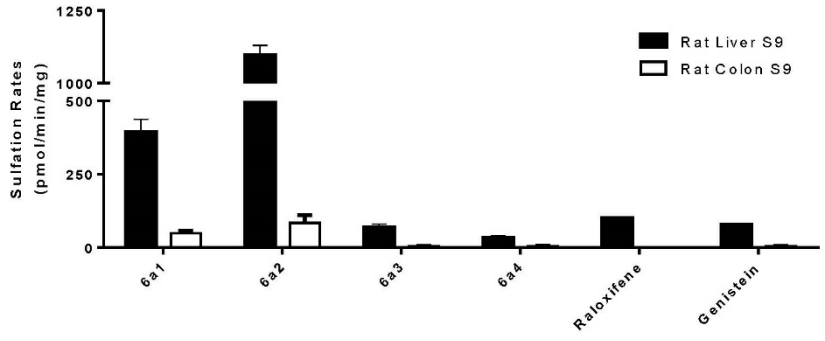
Rat Liver S9
Rat Colon S9
Sulfation Rates (pmol/min/mg)
1250
1000
500
250
0
6a1
6a2
6a3
6a4
Raloxifene
Genistein

E

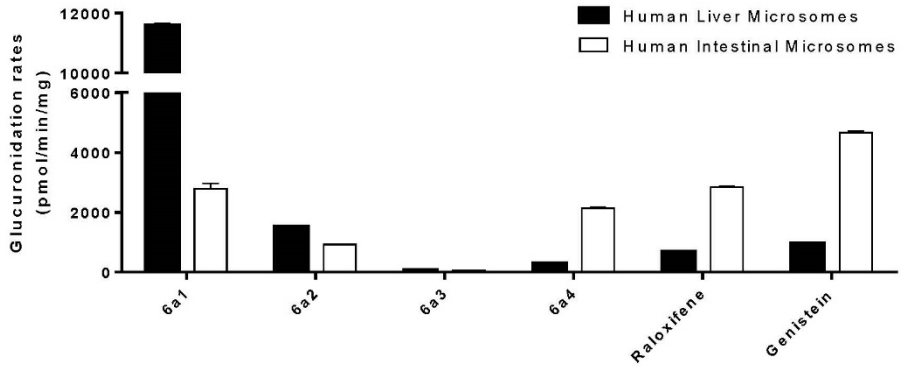

F

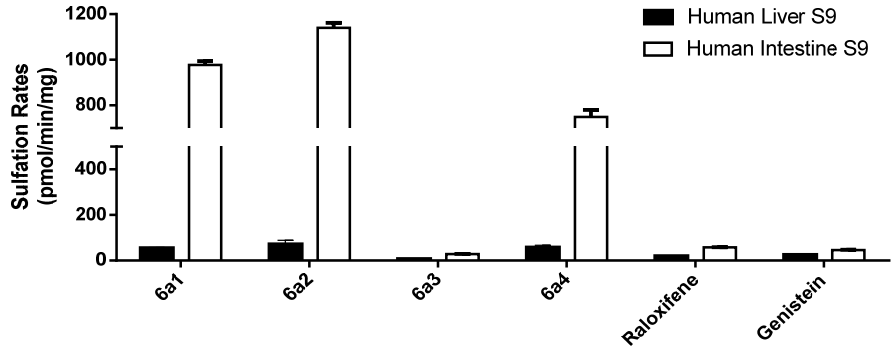

Figure 16. The phase II metabolism rates of the new compounds characterized by *in vitro* tools.

(A) Glucuronidation rates of all the new compounds by rat liver microsomes. (B) Sulfation rates of all the new compounds by rat liver S9 fractions. (C) Glucuronidation rates of **6a1-6a4** by rat liver and colon microsomes. (D) Glucuronidation rates of **6a1-6a4** by rat liver and colon S9 fractions. (E) Glucuronidation rates of **6a1-6a4** by human liver and intestine microsomes. (F) Sulfation rates of **6a1-6a4** by human liver and intestine S9 fractions.

4.4.2 6a1 in Caco-2 monolayer assay

After 10 μM **6a1** was applied to the apical or basolateral side of the Caco-2 monolayer model, the concentrations of **6a1** and its phase II metabolites, glucuronide and sulfate, were monitored at the both the donor and receiver sides. The results showed that **6a1** penetrated the cell membrane easily and was rapidly conjugated by UGTs and SULTs inside the Caco-2 cells. The dominant metabolites were found to be sulfates. The majority of **6a1**-sulfate was effluxed to the apical side, while less was transported to the basolateral side (Figure 17, A and B). The amount of **6a1**-glucuronide produced by Caco-2 cells was much less than that of **6a1**-sulfate. **6a1**-glucuronide was also transported to both sides of the Caco-2 monolayer. However, unlike **6a1**-sulfate, **6a1**-gulcuronide was preferentially effluxed to the basolateral sides. When 10 μM **6a1** was applied to the basolateral side of the Caco-2 monolayer, similar results were observed in the production and excretion of the **6a1** phase II metabolites (Figure 17, C and D).

A

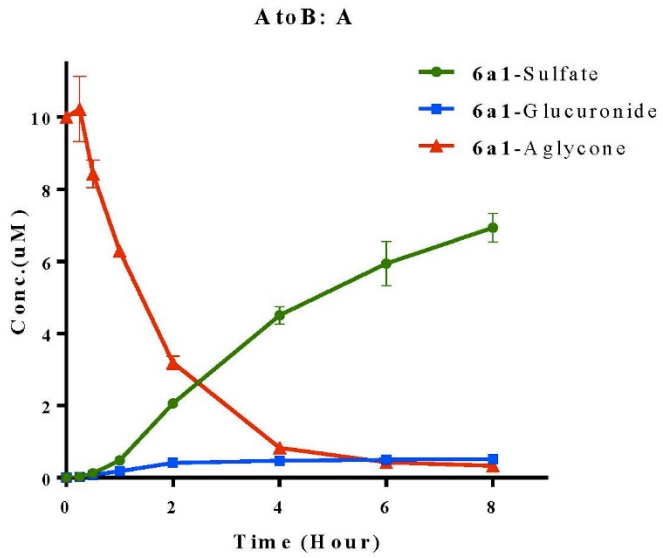
A to B: A
6a1-Sulfate
6a1-Glucuronide
6a1-Aglycone
Conc.(uM)
Time (Hour)
0
2
4
6
8
10

B

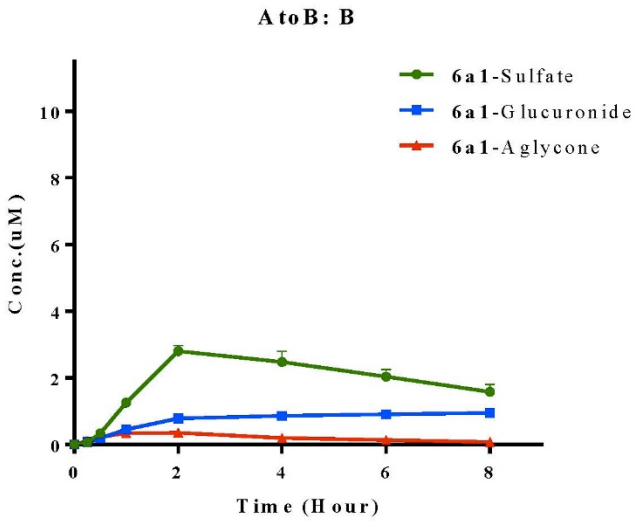
A to B: B
6a1-Sulfate
6a1-Glucuronide
6a1-Aglycone
Conc.(uM)
Time (Hour)
0
2
4
6
8
10

C

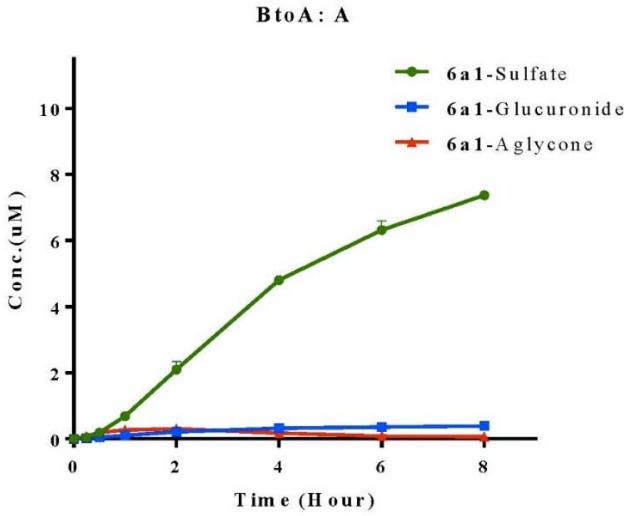

D

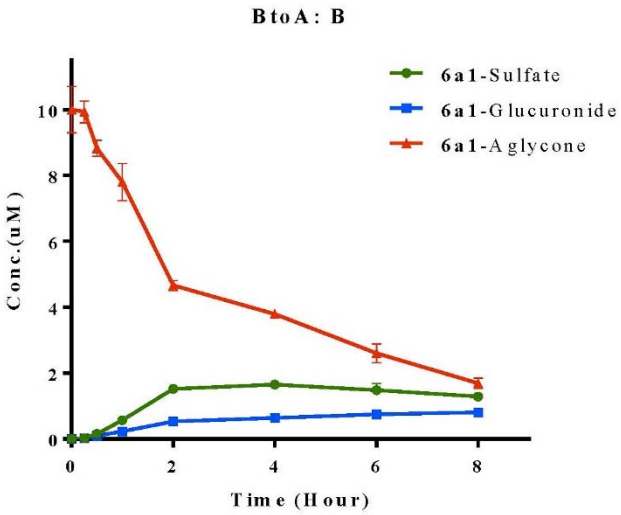

Figure 17. The metabolism and excretion of 6a1 in Caco-2 cell monolayer assay.

10 μM **6a1** was applied to the apical (A and B) or basolateral (C and D) side of the Caco-2 cell monolayer. The concentrations of **6a1** and its phase II metabolites in the both sides were determined at different time points.

4.4.3 Pharmacokinetics study in SD rats

After the characterization of drug metabolism by *in vitro* tools, the pharmacokinetics of celecoxib, **6a1** and **6a3** was investigated and compared with each other in SD rats after oral administration.

After an oral dose of 20 mg/kg celecoxib in SD rats, the drug was rapidly absorbed and the blood concentration exceeded 1μM in 30 minutes. 8 hours after the oral administration, celecoxib achieved its peak blood concentration as high as 15.40 ± 4.01 μM, which was more than 1000 folds higher than its IC_{50} value against COX-2 (Figure 18, A). In contrast, after an oral dose of 20 mg/kg **6a1** in SD rats, only trace concentrations of **6a1** and its metabolites could be detected in the blood during the pharmacokinetics studies (Figure 18, B). 24 hours after the administration, the blood concentrations of **6a1** and its metabolites never exceeded 0.02 μM, indicating that only a marginal amount of **6a1** entered the systemic circulation in rats.

To clarify the reason of the low bioavailability of **6a1**, we also conducted the pharmacokinetic study of **6a3** and compared the result with that of **6a1**. After an oral dose of 20 mg/kg **6a3** in SD rats, the peak blood concentration of **6a3** was 1.69 ± 0.69 μM, and the blood levels of the two phase II metabolites of **6a3** were much lower than that of the parent (Figure 18, C).

1879 A

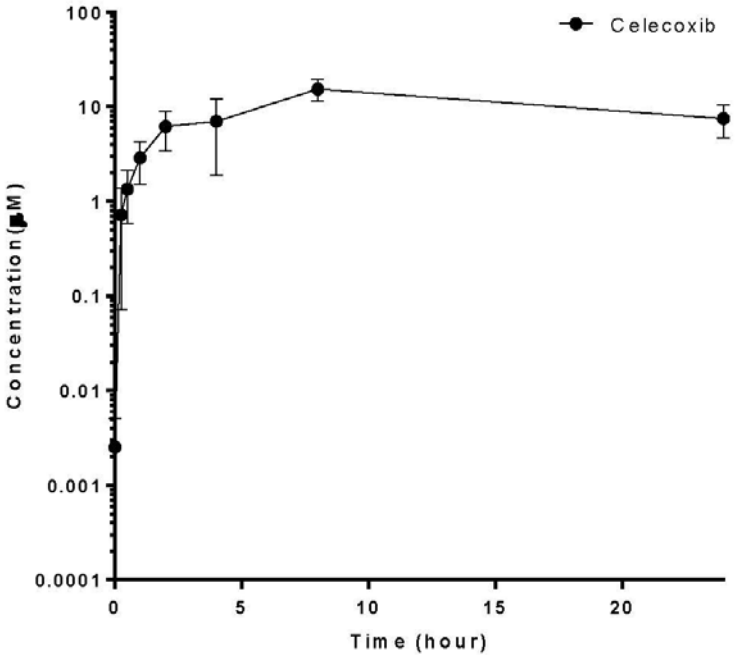

1880

1881 B

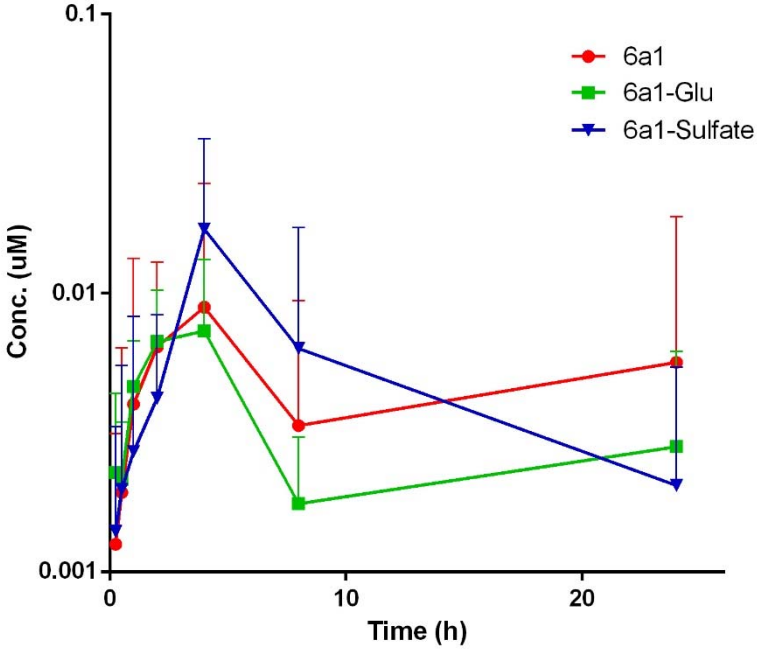

1882

1883

C

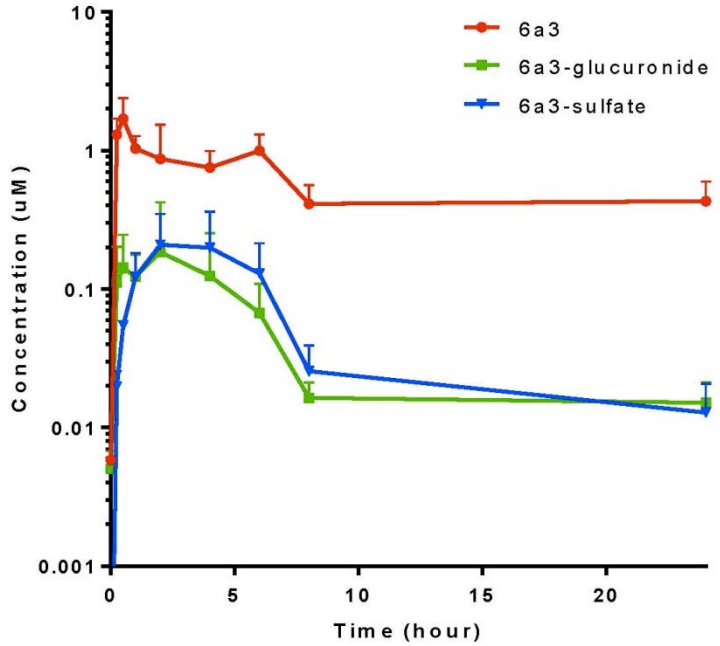

Figure 18. The PK studies of celecoxib, 6a1 and 6a3 in SD rats.

The concentrations of (A) celecoxib (B) **6a1** and its phase II metabolites (C) **6a3** and its metabolites in the blood withdrawn from the rat tail tip after an oral dose of 20 mg/kg.

4.5 Discussion

Before *in vitro* characterization, we hypothesized that for the new compounds, their phase II metabolism rates are determined by their phenolic group species (R_2), which were designed as the kinetophore. As the pharmacophore, the R_1 groups will not significantly impact the metabolism rates of these phenolic compounds because it is located far away from the metabolism position in the structure. This hypothesis was verified when the rat liver microsomes and S9 fractions were used to conjugate the new compounds as glucuronides and sulfates, respectively. The compounds with the same R_2 groups had similar conjugation rates in either glucuronidation or sulfation, although their R_1 groups were different from each other. Meanwhile, among all the new compounds, **6a3**, **6b3** and **6c3** were identified as relatively poor substrates in both glucuronidation and sulfation. Then, **6a1**, **6a2**, **6a3** and **6a4** were selected as the representatives of all the new compounds for further investigation. Their phase II metabolism rates by subcellular fractions from rat liver and colon were determined and compared. An ideal locally bioavailable COX-2 inhibitor should be metabolically stable enough in colonic epithelium to inhibit COX-2, and it is also required to be metabolized and excreted in liver as rapidly as possible. Thus the compounds with high conjugation rates by liver subcellular fractions and low conjugation rates by colon subcellular fractions are favored. Among the four compounds, **6a1** and **6a2** were identified as the most susceptible substrates of phase II metabolic enzymes in rat liver, and also the rat liver subcellular fractions conjugated **6a1** and **6a2** more efficiently than the rat colon subcellular fractions. **6a4** was an excellent substrate of the Ugts but not the Sults in rat liver. **6a3** was slowly conjugated in either rat liver or colon. To figure out whether the metabolic properties of the new compounds in rats could be extrapolated to human, we also use the subcellular fractions from human liver and intestine to conjugate the new compounds. Because human colon microsomes and S9 fractions were not commercially available, we used human intestine microsomes and S9 fractions instead. Among the four compounds, the glucuronidation of **6a1** by

human liver microsomes were the most rapid and the rate was also higher than that by human intestine microsomes. However, the human intestine S9 fractions exhibited a much higher ability to conjugate **6a1**, **6a2** and **6a4** as sulfates than the human liver S9 fractions, showing the species difference between human and rats. In the future when the design of locally bioavailable COX-2 inhibitors is translated from rats to human, the species differences should be considered, especially for avoiding the possible extensive sulfation in human colon. Most importantly, now we know that the metabolism of the new compounds can be manipulated by altering the phenolic group species in their structures. *In vitro* screening among various phenolic groups can help find new compounds with appropriate metabolic properties in human. On the other hand, a locally bioavailable COX-2 inhibitors can be designed as a specific substrate of certain UGT or SULT isoforms expressed in human liver but not colon, which will prevent the systemic bioavailability but protect the local bioavailability.

Here, for the following studies *in vitro* or in rats, **6a1** was selected as a lead compound. The rapid phase II metabolism and active apical efflux of the metabolites in the intestinal epithelium have been observed in the intestinal disposition of a number of phenolic phytochemicals, especially flavonoids [157]. Caco-2 cell monolayer is a commonly used model in which the absorption, metabolism and excretion of substances in the intestinal epithelium can be simulated [155]. As a hydrophobic compound, **6a1** can penetrate the Caco-2 cellular membrane from either side by passive diffusion. The predominant metabolite was found to be **6a1**-sulfate, and less metabolite was **6a1**-glucuronide. The results in Caco-2 cell monolayer model also revealed that human colon may generate a lot of **6a1**-sulfate *in vivo*. Like the phase II metabolites of the other phenolic compounds, the glucuronide and sulfate of **6a1** are very hydrophilic, and their excretion from the Caco-2 cells probably depends on transporters on the cellular membrane. With respect to the transport of the same substrate, the competition between the apical transporters and the basolateral transporters usually results in the unequal efflux to both sides of the Caco-2

monolayer. The majority of **6a1**-sulfate was excreted to the apical side of the monolayer, while more **6a1**-glucuronide was excreted to the basolateral side. The phase II metabolites effluxed to the intestinal lumen can be hydrolyzed by glucuronidases or sulfatases from the colonic bacteria, and the reproduced aglycones are available for reabsorption[56]. This process termed "enteric circulation" can slow down the decrease of drug concentrations in the intestinal lumen, which may help prolong the exposure of the colonic epithelium to drugs. Thus, in humans, the enteric circulation may promote the effect of **6a1** in inhibiting colonic COX-2 activity and enhance its efficacy in CRC chemoprevention. *In vitro* experiments also revealed that in the presence of β-glucuronidase, the efficacy of **6a1** in inhibiting PGD_2 production was largely enhanced in the LPS-induced Raw264.7 cells (Figure 14, C). In the future, effects of colonic bacteria on the efficacies of locally bioavailable COX-2 inhibitors will also be investigated in the *in vivo* studies.

The result of the pharmacokinetics study of celecoxib validated the conclusion made in the previous studies that celecoxib is rapidly absorbed and has excellent oral bioavailability. The blood concentration of celecoxib exceeded 1 μM in 30 minutes after oral administration and the peak blood concentration was as high as 15 μM. Considering that the IC_{50} of celecoxib on COX-2 activity was determined to be as low as 3 nM, the cardiovascular system of rats was exposed to a blood level of celecoxib which was a thousand-fold higher than its IC_{50}. While in healthy human adults, the peak concentration of celecoxib in the plasma was also higher than 2 μM after a single oral dose of 200 mg celecoxib [140]. The high blood concentration and low IC_{50} on COX-2 activity ensured its therapeutic effect in patients with arthritis, but also result in the increased risk of cardiovascular events [113, 118]. In contrast, the blood concentrations of **6a1** were only marginal (< 0.015 μM) and also much lower than it IC_{50} on COX-2. The extensive first-pass metabolism is likely responsible for the low oral bioavailability of **6a1**, although a limited absorption of **6a1** in the gastrointestinal tract may also be a factor. However, the predicted cLogP value and the permeability of **6a1** shown in Caco-2 cell monolayer suggests that the alternative

explanation is unlikely. Beside the study in Caco-2 cell monolayer, we also conducted the PK study of **6a3** at the same oral dose and compared the result with that in **6a1** PK study. **6a3** shares the same molecular weight with **6a1**, and they have very similar structure and physicochemical properties. However, in the *in vitro* characterizations, **6a3** was identified as a relatively poor substrate of phase II metabolism enzymes in both human and rats. The oral bioavailability of **6a3** was much higher than that of **6a1**, implying that the different first-pass metabolism rates accounted for the difference in pharmacokinetic properties between the two. Later, in the perfused rat colon model, the first-pass metabolism and excretion of **6a1** in SD rats were revealed with more details (See below).

Chapter 5 The Efficacy of the New Compounds in Inhibiting COX-2 Activity in the Inflamed Rat Colon; the Absorption, Metabolism and Excretion of 6a1 during the *In Situ* Perfusion

5.1 Abstract

In the 2,4,6-trinitrobenzenesulfonic acid (TNBS)-treated rat colon with COX-2 overexpression, perfusion with 1 or 10 μM celecoxib in HBSS significantly decreased the half-life of PGE_2 attenuation ($P < 0.05$ and $P < 0.01$, respectively), showing the inhibitory effects of celecoxib on colonic COX-2. However, 0.1 μM celecoxib in HBSS had no significant effects. When the inflamed rat colon was perfused with 10 μM **6a1**, **6a2**, or **6a3** respectively, the half-life of PGE_2 attenuation in the perfusate was not significantly altered. However, after the solubility of **6a1** in HBSS at room temperature was increased to 70 μM with the help of 4 mM β-cyclodextrin (β-CD), the half-life of PGE_2 attenuation was significantly decreased, and the efficacy of 70 μM **6a1** was comparable to that of 1 μM celecoxib.

The blood sample analysis by UPLC-MS/MS revealed that when the inflamed rat colon was perfused with 1 or 10 μM celecoxib, the blood concentration of celecoxib kept increasing during the perfusion and reached concentrations that were at least 30 folds higher than its IC_{50} on human COX-2 activity. In contrast, after the infusion with 70 μM **6a1** in the inflamed rat colon began, the blood concentration of **6a1** soon reached a stable plateau and never exceeds 0.1 μM, which was much lower than its IC_{50} on human COX-2. By comparing **6a1** concentrations in the input and output perfusate, we figured out that the rat colon was efficient in absorbing **6a1** but limited in metabolizing **6a1**. UPLC-UV analysis of the bile samples showed that the majority of **6a1** absorbed in the colon was recovered as glucuronide in bile. We estimate the first-pass metabolism

2001 and excretion of **6a1** in the liver successfully prevented more than 99% of absorbed **6a1** from
2002 entering the systemic circulation.

2003

5.2 Introduction

We synthesized a series of new compounds and demonstrated their efficacies for inhibiting recombinant human COX-2 activity or the production of prostaglandins in cell lines. Also, the phase II metabolism of the new compounds were characterized by *in vitro* tools such as liver or colon microsomes/S9 factions and Caco-2 monolayer model. The results from pharmacokinetics study in SD rats demonstrated that compared with celecoxib and **6a3**, the oral bioavailability of **6a1** was very low, probably due to the extensive first-pass effects. **6a1** has been selected as the lead compound for the following studies.

In this section, we want to validate the efficacies of the new compounds in inhibiting colonic COX-2 in a relevant rat model. However, in healthy rats, COX-2 is not expressed in the normal colon tissue. Thus, an acute inflammatory bowel disease (IBD) model induced by TNBS in rat is employed. In this model, substantial expression of COX-2 protein can be detected in the inflamed rat colon several hours after TNBS administration to the colon from the anus. From 12 to 24 hours after TNBS induction, the COX-2 expression level in the colon is relatively stable and this period of time is selected for the experiment. The inflamed colon will be perfused with HBSS containing vector (0.1% DMSO) or different drugs. As the indicators of colonic COX-2 activity, the concentrations of prostaglandins in the perfusate will be determined by UPLC-MS/MS analysis. Celecoxib is employed as a positive control to validate this model. The inflamed rat colon will be perfused with different concentrations of celecoxib for accessing its inhibitory effect on the colonic COX-2 activity. After that, the new compounds will be tested for their efficacies in inhibiting colonic COX-2 activity.

Meanwhile, the *in situ* colon perfusion in rat can help us investigate the absorption, metabolism and excretion of the new compounds, especially **6a1**. The absorption of **6a1** in colon can be determined by comparing the concentration differences between the input and output perfusate.

To characterize its metabolism and excretion in the liver, the bile samples of rats are collected from the cannulated bile ducts during the *in situ* colon perfusion. Also, blood samples are collected from the tail tip of rats hourly for determining **6a1** concentrations in the systemic circulation during the perfusion. The perfusion study on **6a1** in the inflamed rat colon will reveal its efficacy in inhibiting colonic COX-2, as well as the extensive first-pass metabolism and excretion it undergoes. It will be demonstrated that **6a1** is a locally bioavailable COX-2 inhibitor in colon, while its systemic bioavailability is extremely low. In the future, new chemical entities sharing similar pharmacological and pharmaceutical properties with **6a1** may be developed as safe agents for CRC chemoprevention or to treat other COX-2-related colonic diseases.

5.3 Materials and Methods

5.3.1 Materials

All the materials were analytical grade or better. Celecoxib was purchased from LC laboratory (Woburn, MA). β-glucuronidase, TNBS, β-CD, formic acid, KH_2PO_4, K_2HPO_4, DMSO, NaCl, and HCl were purchased from Sigma-Aldrich (St Louis, MO). Ethanol absolute (suitable for use as excipient) was purchased from EMD Chemicals (Darmstadt, Germany). PGE_2, PGD_2, 6-keto-$PGF_{1\alpha}$, TXB_2, and PGE_2-d_4 were purchased from Cayman Chemicals (Ann Arbor, MI). Acetonitrile, H_2O, and methanol (MS grade) were purchased from EMD Millipore (Billerica, MA).

5.3.2 Animals

Male SD rats (approximately 250g) were purchased from Harlan Laboratory (Indianapolis, IN). They had been kept in the animal facilities for at least one week before any experiment.

5.3.3 TNBS-induced IBD model in SD rats

The enema for colonic COX-2 induction was prepared by mixing equal volumes of 1 M TNBS aqueous solution and 100% ethanol. After the rats were anaesthetized by isoflurane, a polyurethane catheter (OD 2 mm) was gently inserted from the anus into the colon until the tip of catheter was 8 cm apart from the anus, reaching the splenic flexure. Then, 0.2 mL of the enema was injected into the rat colon by a syringe connected to the catheter. After that, the rats were kept for 1 minute in the Trendelenburg position before they were recovered from anesthesia. Then, the rats were kept in the cages with access to food and water as usual before we conducted the perfusion studies.

5.3.4 Preparation of the perfusate

The perfusate containing 0.1, 1, and 10 μM celecoxib was prepared by adding the stock solutions of celecoxib in DMSO to HBSS. The perfusate containing 10 μM **6a1**, **6a2**, and **6a3** was prepared by adding the stock solution of each compound in DMSO to HBSS. The final contents of DMSO in all the perfusate were uniformly 0.1%. The perfusate was sonicated to help the solute dissolve.

Before high concentration solutions were prepared, the solubility of **6a1**, **6a2** and **6a3** in HBSS was assessed as follows: 1 mg **6a1**, **6a2** or **6a3** was added to 10 mL HBSS. The suspensions were sonicated in a 25 °C water bath for 30 minutes and then centrifuged at 15,000 × g for 10 minutes, and the supernatants were analyzed by UPLC-UV.

The perfusate with a high **6a1** concentration was prepared as follows: to HBSS containing 4 mM β-CD, the stock solution of **6a1** in DMSO was added to form a 200 μM suspension. The suspension was sonicated thoroughly and then centrifuged at 15,000 × g for 10 minutes. The concentration of **6a1** in the supernatant was determined as 70 μM by UPLC-UV.

5.3.5 *In situ* single-pass perfusion in inflamed rat colon

The rat surgical procedures were approved by University of Houston Institutional Animal Care and Use Committee. 12 hours after TNBS was administrated to the rat colon, the rats were

anaesthetized by an i.p. injection of 1.2 g/kg urethane and then put on a heating blanket to maintain body temperature. Then, the rat abdominal cavity was opened by incising the midline of abdomen and the cut was approximately 4 cm long. The cecum was carefully removed from the abdominal cavity, and an inlet cannula was inserted into the colon at 2 cm below the junction of the cecum and colon. After the inlet cannula was secured with a sterilized black suture, the colon was flushed with saline pre-warmed to 37 °C. After the fecal residues in the colon was removed. The outlet cannula was inserted into the anus. For the perfusion with 70 μM **6a1**, in addition to the colon cannulation, the rat bile duct located near the duodenum was also cut and cannulated with polyethylene-10 tubing. After all the surgical procedures, the cecum and colon were carefully placed back into the abdominal cavity without any crimping or kinking. During the perfusion, the incised rat abdomen was covered by a paper towel soaked with saline to keep the abdominal cavity moist.

The *in situ* perfusion system is shown in Figure 19. To maintain the temperature of the perfusate, the tubings connected to the inlet cannula were kept warm by a 37 °C circulating water bath. The perfusion was conducted by using an infusion pump (Harvard Apparatus, Cambridge, MA), which provided a constant perfusion rate of 0.5 mL/min. In the first hour, the cannulated rat colon was perfused with blank HBSS After the washout hour to remove all the residual PGs, blank HBSS was substituted by HBSS containing different drugs or vector (0.1% DMSO) and the rat colon was perfused for another 3 hours. The outlet perfusate was continuously collected from the rat anus. In every 20 minutes, approximately 10 mL perfusate was collected in a 15mL plastic tube and then spiked with 2.5 ng/mL PGE_2–d_4. For PGE_2 quantitation by UPLC-MS/MS, the perfusate samples were usually processed and analyzed within 2 hours after the perfusion study ended. In addition, when the rat colon was perfused with 70 μM **6a1** in HBSS, 1 mL was taken out from the inlet perfusate, as well as the outlet perfusate collected in each 15 mL plastic tube. These samples were added 250 μL of 94% acetonitrile/6% formic acid and stored at -20 °C before

they were analyzed by UPLC-UV to quantify the amount of **6a1** absorbed from the colon during the perfusion.

In perfused rats with bile duct cannulations, the bile secreted in each hour was collected in an Eppendorf tube. The bile secretion rates varied among different rats, and were also not constant at different time points for the same rat. In general, the volumes of bile secreted in one hour were usually between 0.4 ~ 1.1 mL. At 0.5, 1.5, 2.5 and 3.5 hours after the perfusion with HBSS containing celecoxib or **6a1** began, the blood samples (~ 50 μL) were collected in hepatized Eppendorf tubes by cutting the rat tail tips. All the bile and blood samples were stored at -80 $^{\circ}$C immediately after collection.

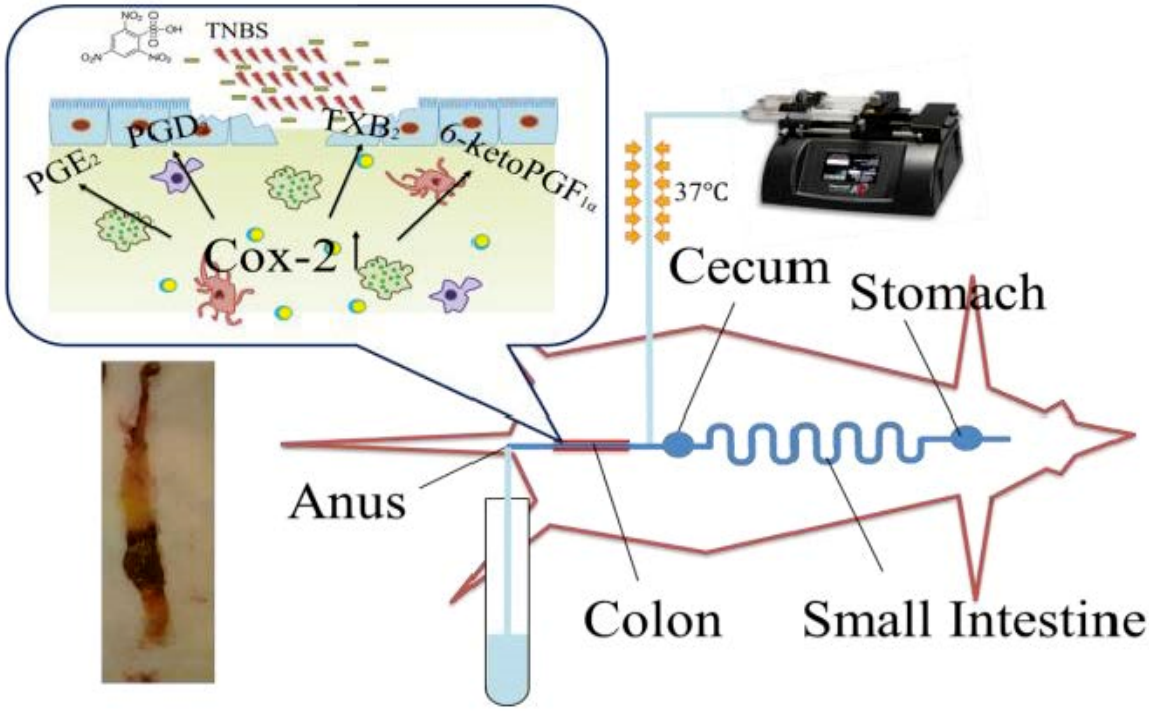

Figure 19. The *in situ* perfusion in TNBS-treated rat colon.

TNBS-induced acute inflammation in rat colon is a common model for IBD studies. In the inflamed colon tissues, TNBS-induced overexpression of COX-2 results in the abundant production of PGs. In the *in situ* production, the cannulated colon was perfused with HBSS containing compounds of interest at different concentrations. The outlet perfusate was collected from the anus. When the inflamed rat colon was perfused with celecoxib or **6a1**, the bile from the cannulated bile duct and the blood samples from the tail tip were also collected for studying drug absorption, metabolism and excretion.

5.3.6 Solid-phase extraction (SPE) of the perfusate and bile samples

The SPE of the perfusate and bile samples collected in the *in situ* perfusion study were conducted with Speedisk® Octadecyl C_{18} 10μm columns (J.T. Baker, NJ) and a Speedisk® 48 Positive Pressure Processor (J.T. Baker, Phillipsburg, NJ). The columns were prepared by washing with 3 mL acetonitrile and then 3 mL H_2O before sample loadings.

For the perfusate, from each 15 mL plastic tube, 3 mL perfusate was loaded to a C_{18} column. The columns were washed with 3 mL H_2O to remove the inorganic salts in HBSS, and then the PGs were eluted with 1 mL acetonitrile. The elute was dried by nitrogen at room temperature and stored at -80 °C until further analysis. The standard curve for quantitating PGE_2 was prepared by adding different concentrations of PGE_2 to HBSS. The standard samples were processed the same as the perfusate collected in the perfusion study.

The weights and volumes of the bile samples were recorded before they were processed. 20 μL bile sample was first diluted in 180 μL 50 mM KPi (pH 7.4). After a vigorous vortex, the 200 uL diluted bile sample was divided to two equal aliquots. One aliquot was mixed with 100 μL β-glucuronidase (200 units/mL) in 50 mM KPi (pH=7.4), while the other was mixed with the same agent but boiled before the mixing. After the samples were incubated at 37 °C for 1 hour, they were loaded onto C_{18} columns. The columns were washed with 3 mL H_2O to remove the inorganic salts in HBSS, and then the analyte(s) were eluted with 1 mL acetonitrile. The elute was dried by nitrogen in room temperature and store at -20 °C.

Also, to prepare the standard curve for quantitating **6a1** in bile, the blank bile was spiked with different concentrations of **6a1**. The standard samples were processed the same as the bile samples collected during the perfusion study.

5.3.7 Quantitation of 6a1 and 6a1-glucuronide in the perfusate and bile samples by UPLC-UV

To characterize the **6a1** absorption during the colon perfusion with 70 μM **6a1**, the concentrations of **6a1** in the input and output perfusate samples were determined. The standard curves were prepared by adding different concentrations of **6a1** to HBSS containing 4 mM β-CD. 1 mL of each standard sample was added 250 μL of 94% acetonitrile/6% formic acid. After 15 minutes of 22,000 × g centrifuge, 10 μL of supernatant from each sample was analyzed by UPLC-UV analysis.

The dried bile extracts, both hydrolyzed and unhydrolyzed, were reconstituted in 200 μL 25% acetonitrile containing 0.1% formic acid. After 15 minutes of 15,000 × g centrifugation, 10 μL supernatant was analyzed by UPLC-UV. The concentrations of **6a1**-glucuronide in the unhydrolyzed bile samples were determined by quantitating **6a1** in the hydrolyzed ones correspondingly.

The UPLC-UV conditions were the same as those described in 4.3.6.

5.3.8 Quantitation of PGE_2 in the concentrated perfusate by UPLC-MS/MS

Before the UPLC-MS/MS, the dried perfusate and standard samples were reconstituted in 200 μL 25% methanol containing 0.1% formic acid. 40 μL of each sample was injected to determine the concentration of PGE_2. The conditions and parameters in the UPLC-MS/MS analysis of PGE_2 were the same as those described in 3.3.6. Three PGs other than PGE_2 were also detected in the concentrated perfusate by UPLC-MS/MS, although their concentrations were not used as the indicator of colonic COX-2 activity. The parameters of these PGs in the MS analysis were shown in Table 2.

5.3.9 Quantitation of celecoxib and 6a1 in the blood samples by UPLC-MS/MS

The blood concentrations of celecoxib and **6a1** in the systemic circulation were determined by salting-out LLE and UPLC-MS/MS. Here, the procedures were the same with those described in 4.3.8. The conditions in UPLC-MS/MS were the same with those described in 4.3.9.

5.4 Results

5.4.1 The PGs in the perfusate

After SPE, the perfusate was concentrated 15 fold and the inorganic salts in HBSS were removed before further analysis. In the UPLC-MS/MS analysis of the concentrated perfusate from the inflamed rat colon, four PGs could be detected as the major products derived from the COX-2 pathway: PGE_2, PGD_2, 6-keto-$PGF_{1\alpha}$ and TXB_2. Among these four PGs, PGE_2 was selected as the indicator of colonic COX-2 activity because its signal was the most abundant among the four (Figure 20). As the internal standard for PGE_2 quantitation, PGE_2-d_4 have the same elution time with PGE_2.

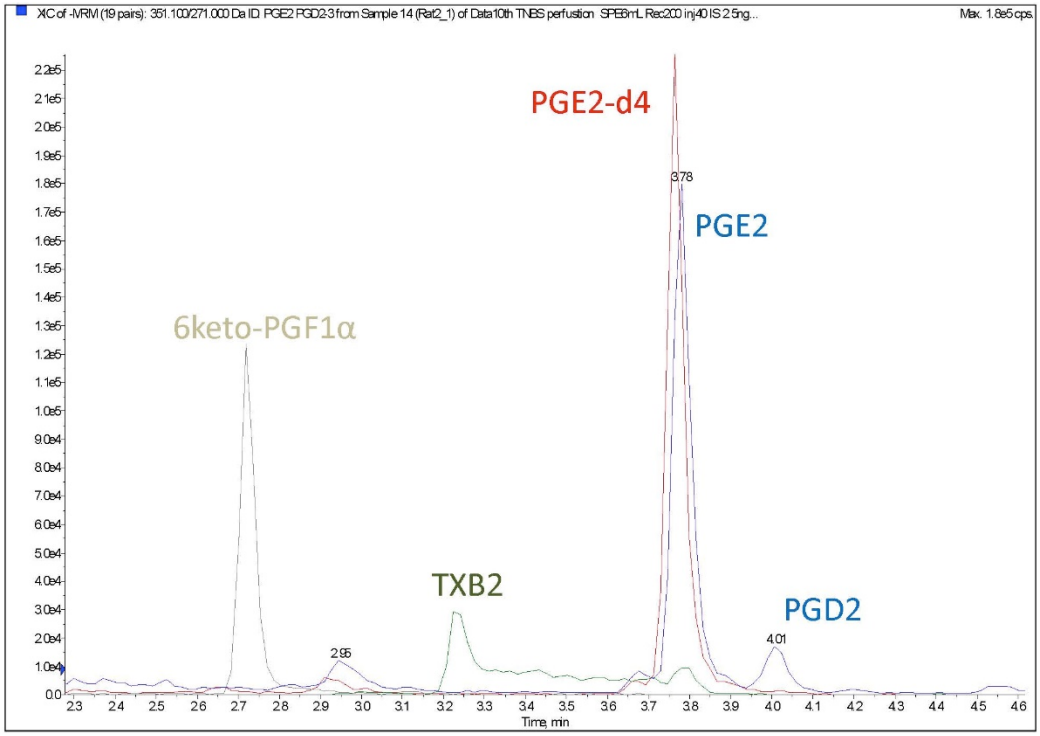

Figure 20. The PGs detected in the perfusate.

After 15-fold concentration by SPE, the PG concentrations in the perfusate was determined by LC-MS/MS. Among the four PGs derived from colonic COX-2, PGE_2 was found to be the most abundant signal. PGE_2-d_4 was employed as the internal standard in the quantitation of PGE_2.

5.4.2 The effects of celecoxib on colonic COX-2 activity

In the control group perfused with HBSS containing 0.1%DMSO, the concentrations of PGE2 in the perfusate decreased during the perfusion period and its attenuation upon time could be appropriately described as a first-order process. The rate constants and half-lives of PGE_2 concentration attenuation were obtained by fitting the results to an exponential equation. In the control group, the average half-life of PGE_2 attenuation was 156 ± 49 minutes, while in the groups perfused with 0.1, 1 and 10 μM celecoxib the half-life was 127 ± 36, 70 ± 19, and 37 ± 4 minutes, respectively. 1 and 10 μM celecoxib significantly decreased the half-life of PGE_2 attenuation in the perfusate, showing the inhibitory effect of celecoxib on colonic COX-2 activity (Figure 21, A). We also found that 0.1 μM celecoxib slightly decreased the half-life of PGE_2 attenuation, but not significantly compared with the control group. The inhibitory effect was dependent on the celecoxib concentrations in the perfusate.

2201 A

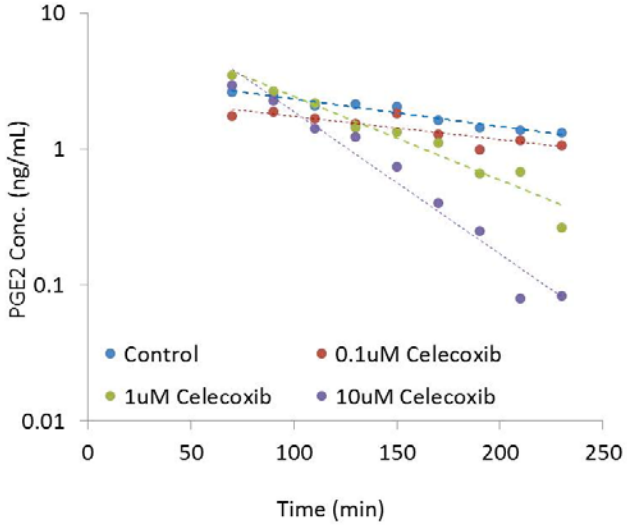

2202

2203 B

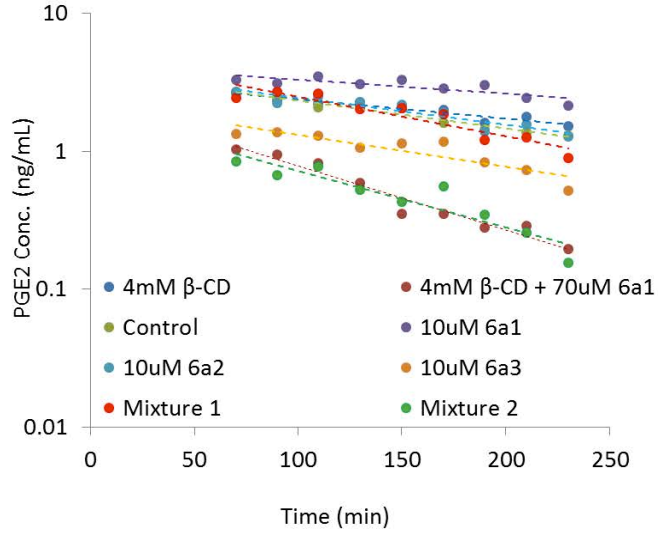

2204

2205 **Figure 21. The inhibitory effects of (A) celecoxib and (B) the new**
2206 **compounds on colonic COX-2 activity.**

2207

2208

5.4.3 The effects of the new compounds on colonic COX-2 activity

After the inhibitory effects of celecoxib on colonic COX-2 were confirmed, the *in situ* perfusion experiments with HBSS containing the new compounds were conducted (Figure 21, B). In the groups perfused with the new compounds, perfusion with 10 μM **6a1**, **6a2** or **6a3** respectively did not significantly alter the half-lives of PGE_2 concentration attenuation. When **6a1**, **6a2**, **6b2** and **6c2** were combined in the perfusate (mixture 1, 10 μM for each), there was mild but still not statistically significant inhibitory effects (P=0.17 with the control group). However, the inhibitory effect of a more comprehensive mixture of **6a1**, **6a2**, **6a3**, **6b2**, **6b3**, **6c2** and **6c3** (mixture 2, 10 μM for each) was found to be similar to that of 1μM celecoxib. Considering that the new compounds were approximately 10~50 fold less potent than celecoxib, we realized that the compound concentrations in the perfusate were critical for exhibiting their efficacy to inhibit colonic COX-2 in the inflamed rat colon model. However, due to the hydrophobic properties of the new compounds, a concentration higher than 15 μM in HBSS could hardly be achieved by simply increasing the amount of solute in the solution. The solubilities of **6a1**, **6a2** and **6a3** in HBSS at 25 °C were determined to be approximately 13.2, 15.0, and 10.9 μM, respectively. Therefore, β-cyclodextrin (β-CD), an excipient often used in pharmaceutical development, was employed to increase the solubility of the new compounds in HBSS [158, 159]. After sonication and subsequent centrifuge to remove undissolved substances, the solubility of **6a1** in HBSS was successfully increased to 70 μM in the presence of 4 mM β-CD. The osmotic pressure of the solution was determined to be 290 mOsm/kg, which was physiologically appropriate for *in situ* perfusion studies in rat colon. Perfusion with β-CD-formulated 70 μM **6a1** in the inflamed rat colon successfully and significantly decreased the half-life of PGE_2 attenuation to 66 ± 7 min, which was comparable to 1 μM celecoxib (Figure 21, B). The perfusion with 4 mM β-CD alone did not have any effects on PGE_2 production in the inflamed rat colon. The results of the efficacy study in the inflamed rat colon were summarized and compared in Figure 22.

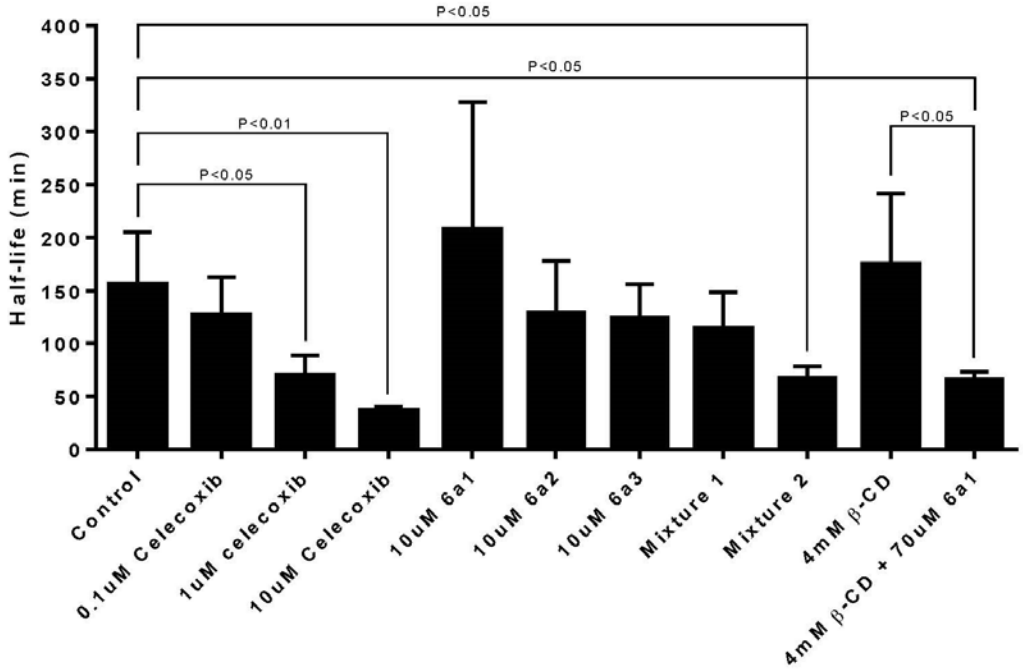

Figure 22. The half-lives of PGE_2 attenuation in different groups of rats.

In the *in situ* perfusion study, the inflamed rat colon was perfused with HBSS containing different compounds. The half-lives of PGE_2 attenuation in different groups of rats are shown. 4-6 rats in each group. P values calculated by T-test.

5.4.4 The absorption, metabolism and excretion of 6a1 in rats during the *in situ* perfusion

The absorption, metabolism and excretion of **6a1** in rats were investigated by quantitating **6a1** and/ or its metabolites in perfusate and bile samples by UPLC-UV analysis. By comparing the **6a1** concentrations in the input (70 μM) and output perfusate, the amounts of **6a1** absorbed from the colon were calculated for each hour during the perfusion period. Approximately 13% of the total **6a1** perfused was absorbed in the colon, illustrating that β-CD-formulated **6a1** could rapidly penetrate the colonic epithelium. No **6a1** glucuronide and sulfate could be detected in the UPLC-UV analysis of the output perfusate.

In the first hour, the inflamed rate colon was perfused with blank HBSS and no **6a1** or its metabolites were detected in blank bile extract (Figure 23, A). In the analysis of bile samples collected after the perfusion with 70 μM **6a1** began, a huge peak was eluted between 2.8 and 2.9 minutes, which was not observed in the analysis of blank bile extract (Figure 23, B). After the extract was hydrolyzed by β-glucuronidase, the peak disappeared and a new peak of **6a1** was shown (Figure 23, C), illustrating that **6a1** could be recovered as glucuronide in bile. **6a1**-glucuronide concentrations in unhydrolyzed bile samples were correspondingly determined by quantitating **6a1** in hydrolyzed bile samples using a standard curve.

Based on **6a1**-glucuronide concentrations and the volumes of the bile samples, the amounts of **6a1** excreted from liver were calculated and compared with the absorption of **6a1** in rat colon (Figure 24). During the 2^{nd} to 4^{th} hour of perfusion, approximately 75% (on average) of the total **6a1** absorbed in colon could be recovered from bile as glucuronide. In the 2^{nd} hour, the amount of **6a1** absorbed from colon was found to be much higher than the amount of **6a1**-glucuronide excreted from liver. In the 3^{rd} and 4^{th} hours, the amount absorbed was found to be approximately equal to that of excretion. The result illustrated that after the absorption, metabolism, and

excretion rates reached the steady state, the first-pass effects in liver prevented almost 100% of **6a1** from entering the systemic circulation.

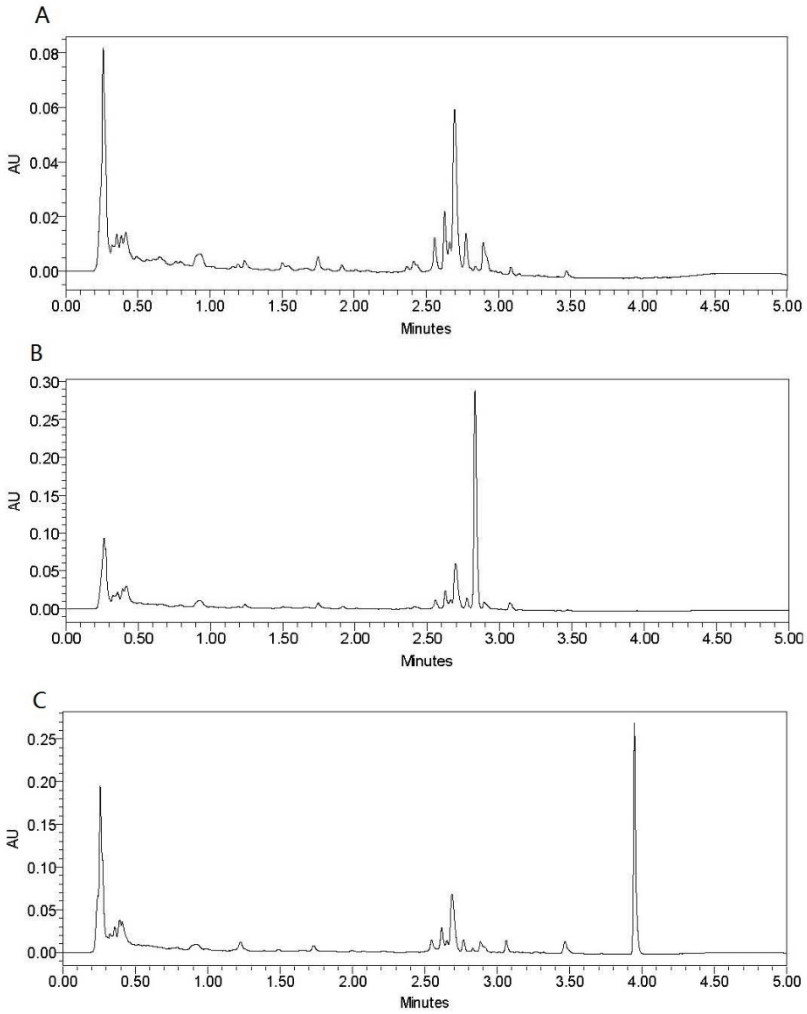

Figure 23. Excretion of 6a1-glucuronide in bile.

The UPLC-UV chromatography of (A) the extract of blank bile (collected during the perfusion with blank HBSS) (B) the extract of a bile sample collected when the inflamed rat colon was perfused with 70 μM **6a1** (C) the extract of the same bile sample in B but after hydrolysis by β-glucuronidase.

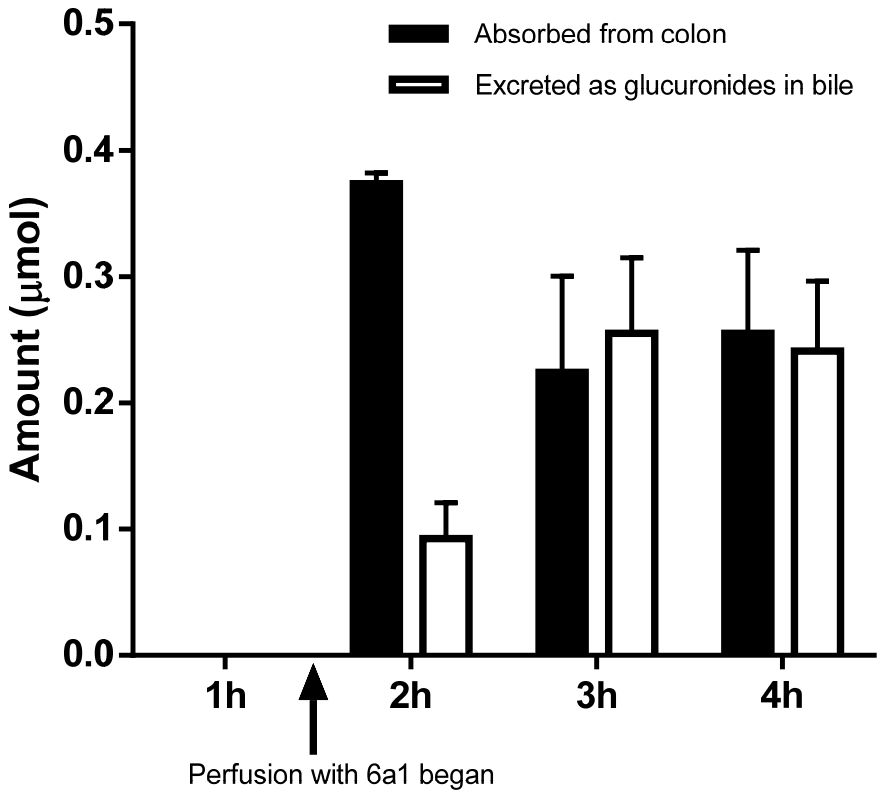

Figure 24. The absorption and excretion of 6a1 in colon-perfused SD rats.

In the 1st hour, the inflamed rat colon was perfused with blank HBSS. From the 2nd hour, perfusion with 70 μM **6a1** began. The amount of **6a1** absorbed in each hour was determined by comparing the **6a1** concentrations in the inlet and outlet perfusate. The amount of **6a1** excreted in bile as glucuronide in each hour was determined as described.

5.4.5 Celecoxib and 6a1 concentrations in the systemic circulation during *in situ* perfusion

Quantitation of celecoxib in the blood samples collected from rat tail revealed that celecoxib were accumulated in the systemic circulation during the perfusion of rat colon with 0.1, 1, and 10 μM celecoxib in HBSS (Figure 25, A). Considering the strong potency of celecoxib in inhibiting COX-2 activity, the blood concentration of celecoxib (0.15μM) was 10~50 fold greater than its IC_{50} value when the rat colon was perfused with 1μM celecoxib which was the lowest concentration required to inhibit colonic COX-2 in our study. In contrast, when the inflamed colon was perfused with 10 μM or 70 μM (β-CD-formulated) **6a1**, the **6a1** blood concentration achieved a plateau soon after the perfusion began (Figure 25, B), and no phase II metabolites of **6a1** were detected in the circulation. β-CD enhanced the solubility and absorption of **6a1**, and also increased its blood concentration. The abundance of **6a1**-glucuronide in bile and the scarcity of **6a1** in the circulation indicated that only less than 0.5% of **6a1** absorbed in the colon escaped first-pass metabolism. When the rat colon was perfused with 70 μM **6a1**, the blood concentration of **6a1** (0.08 μM) was much lower than its IC50 on COX-2 activity. The perfusion with 1 μM celecoxib or 70 μM **6a1** equivalently inhibited COX-2 activity in the inflamed rat colon, but the latter possessed a much lower systemic exposure potentially giving a better safety index for the cardiovascular system.

A

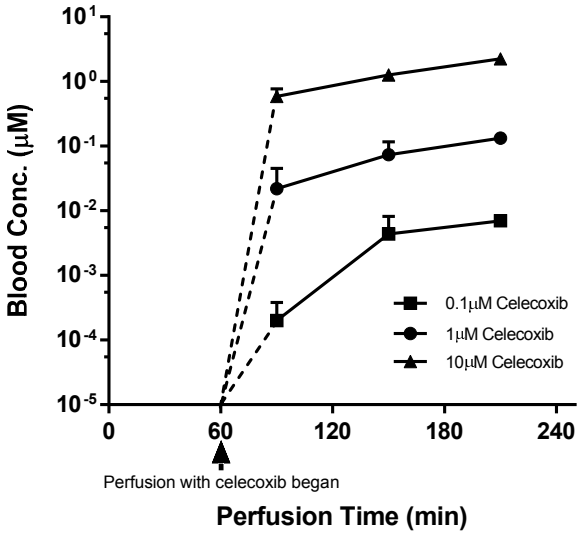

B

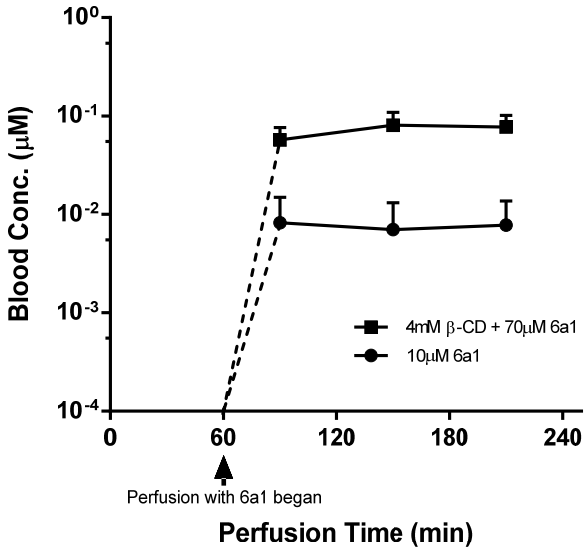

Figure 25. The blood concentration of celecoxib and 6a1 in the systemic circulation during the *in situ* perfusion.

In the 1st hour, the inflamed rat colon was perfused with blank HBSS. From the 2nd hour, perfusion with celecoxib or **6a1** began. At 1.5, 2.5 and 3.5 h, the blood samples were collected from the rat tail tip and the concentrations of celecoxib or **6a1** were determined.

5.5 Discussion

The long-term goal in this project is to develop novel COX-2 inhibitors as effective and safe agents in CRC chemoprevention. In the future, after substantial *in vitro* studies, eventually one or several promising new compounds will be tested for their efficacies to prevent CRC in animal models.

At the current stage of this project, after the *in vitro* characterizations, the inhibitory effects of the new compounds on colonic COX-2 activity was further investigated in rats to fully support the concept of locally bioavailable COX-2 inhibitors. However, in healthy rats, no COX-2 protein was expressed in normal colonic tissues [160]. In this chapter, TNBS was used to induce acute inflammation in rat colon, in which a high level of COX-2 expression can be detected several hours after induction [161].

In pharmaceutical sciences, the *in situ* perfusion studies were often conducted to investigate the drug absorption, metabolism and excretion in the intestine of experimental animals or human [162]. In this project, for the first time, the *in situ* perfusion was performed in the inflamed rat colon to test the pharmacological effects of certain compounds. During the perfusion, the colonic COX-2-derived PGs were released into the perfusate from the inflamed colon. The induced COX-2 activity was sufficient to produce enough PGs, to allow precise quantitation by LC-MS/MS after the perfusate was concentrated 15-fold by SPE.

Before evaluating the new compounds, celecoxib was tested for its inhibitory effects on colonic COX-2 activity in this model as the positive control. When the inflamed rat colon was perfused with blank HBSS, the PGE_2 concentration in the perfusate was shown to decrease over time. The attenuation of PGE_2 in the perfusate could be appropriately described as a first-order process. When the inflamed rat colon was perfused with HBSS containing different concentrations of celecoxib, the PGE_2 concentrations in the perfusate was not influenced immediately, but the

attenuation half-life was significantly shortened by 1 and 10 μM celecoxib in the perfusate. The effect of celecoxib on COX-2 activity in the inflamed rat colon was dependent on its concentration in the perfusate. Although the IC_{50} of celecoxib was only 3 nM in cell-base assays, 0.1 μM celecoxib in the perfusate was still not sufficient to significantly alter the half-life of PGE_2 attenuation.

Considering the divergence in celecoxib potency between the cell-based assays and the *in situ* colon perfusion, it was not surprising for the researchers to see that 10 μM **6a1**, **6a2** or **6a3** in the perfusate did not have significant impacts on the half-life of PGE_2 attenuation. It was recognized that the **6a1**, **6a2** or **6a3** concentrations in the perfusate must be much higher than 10 μM to show their efficacies. However, the concentrations of the new compounds were limited by their solubility in HBSS. With the help of 4 mM β-CD, a concentration of 70 μM was achieved for **6a1** in HBSS and it significantly decreased the half-life of PGE_2 attenuation. The efficacy of 70 μM **6a1** was shown to be similar to that of 1 μM celecoxib, in accordance with the results in cell-based assays in which **6a1** was much less potent than celecoxib.

Simultaneously, the *in situ* perfusion in inflamed rat colon also provided an opportunity for investigating the absorption, metabolism and excretion of the new compounds in rats. When the rats were perfused with β-CD-formulated **6a1**, the **6a1** concentrations in the inlet (70 μM) and outlet perfusates were compared, and the results showed that on average 13% of **6a1** in the inlet perfusate was absorbed in rat colon. No phase II metabolites were detected in the outlet perfusate by UPLC-UV analysis, illustrating that **6a1** were not efficiently metabolized and/or excreted in the colon. When the bile extracts were analyzed by UPLC-UV, a large amount of **6a1** was recovered as **6a1**-glucuronide, showing that **6a1** is an excellent substrate of Ugts in the rat liver. In the 3rd and 4th hours of perfusion, the absorbed and excreted amounts of **6a1** were similar to each other, revealing that the metabolism and excretion of **6a1** in liver were efficient enough to eliminate almost all the **6a1** absorbed before they entered the systemic circulation. These results

were in accordance with the high glucuronidation rate of **6a1** by rat liver microsomes *in vitro*, and also further explained the poor oral bioavailability of **6a1** in the PK study.

When celecoxib was perfused in the rat colon, the blood concentrations of celecoxib in the systemic circulation was always increasing during the perfusion. Celecoxib was accumulated in the blood because its elimination rate was lower than its absorption rate. Thus the blood concentration of celecoxib was 10-fold higher than its IC_{50} even when only 0.1 μM celecoxib was in the perfusate. In contrast, when the rat colon was perfused with either 10 or 70 μM **6a1**, the **6a1** blood concentrations were relatively stable throughout the perfusion period. More importantly, the **6a1** blood concentrations were much lower than its IC_{50}. 1 μM celecoxib and 70 μM **6a1** in the perfusate had similar inhibitory effects on COX-2 activity in the inflamed colon. However, the blood concentrations of celecoxib were 30-fold higher than its IC_{50}. Thus, compared with **6a1**, celecoxib was much more likely to cause severe adverse effects to the cardiovascular systems. The locally bioavailable COX-2 inhibitors like **6a1** are less likely to show the cardiovascular toxicity since its systemic exposure is less.

Although the *in situ* perfusion study has demonstrated **6a1** can inhibit colonic COX-2 activity, more efforts are still required to confirm its efficacy in CRC chemoprevention. In the future, the efficacy of a locally bioavailable COX-2 inhibitor in CRC chemoprevention will be investigated in the rat model and compared with that of celecoxib. This will be a multiple-dose study for both celecoxib and the locally bioavailable COX-2 inhibitors. The concentration in the systemic circulation will be compared between the groups in which similar efficacies are observed for the two agents. Also, factors other than IC_{50} values must be brought into consideration. For example, celecoxib is a drug with extensive plasma protein binding (97%), and the free fraction of celecoxib is more relevant to the inhibition of COX-2 activity in the vascular endothelium [163]. Thus the protein binding of the locally bioavailable COX-2 inhibitors should also be investigated for a more reasonable comparison.

Meanwhile, in the future of this project, based on the current studies, we are going to design new-generation locally bioavailable COX-2 inhibitors. They will inherit the metabolic properties of **6a1**. However, the next-generation inhibitors will be more potent in inhibiting COX-2 activity than **6a1**. Compared with **6a1**, a lower dose will be required for the next-generation inhibitors to inhibit the colonic COX-2 activity. When a lower dose is administrated, less amount of the inhibitor can enter the systemic circulation and the blood concentration can be accordingly decreased, which will further improve the cardiovascular safety.

Chapter 6 Summary

The selective COX-2 inhibitors, especially celecoxib and rofecoxib, were blockbuster drugs in the market. Due to the important role of COX-2 in CRC development, the effectiveness of celecoxib and rofecoxib in CRC therapy and chemoprevention was confirmed in clinical trials. However, these drugs were not used in CRC chemoprevention because of their severe cardiovascular toxicity. The long-term goal in the projects is to develop new selective COX-2 inhibitors which can used as safe agents in CRC chemoprevention. Inspired by the experience in studying the oral bioavailability of phenolic drugs and natural products, we wanted to develop selective COX-2 inhibitors devoid of systemic bioavailability. Thus at the current stage, the objective in this project is to develop new compounds which inhibit colonic COX-2 activity but are not systemic bioavailable.

The approach to reduce the systemic bioavailability is taking advantage of phase II metabolism. Thus, we selected celecoxib as the template and its structure was modified to be substrate of phase II metabolism enzymes. To keep the inhibitory effects on COX-2, we consulted the previous SAR studies of celecoxib and designed a series of new compounds with phenolic groups appropriately incorporated in their structures. Eight compounds were successfully synthesized and purified. Their structures were verified by NMR. The inhibitory effects of the new compounds on COX-2 activity were first assessed in two cell-based assays. We found that the IC_{50} values determined in the cell-base assays may be biased, especially when the cells were incubated with the compound for a long period time and metabolism occurred. We also confirmed the inhibitory effects of the new compounds on recombinant human COX-2 protein. In general, the new compounds are COX-2 inhibitors with IC_{50} values lower than 0.2 μM, although they are much less potent than celecoxib.

Then we studied the metabolic properties of the new compounds. *In vitro* characterization were conducted by employing liver or colon subcellular fractions including microsomes and S9 fractions prepared from rat. The phase II metabolism rates of the new compounds were found to be dependent on the phenolic group species in their structures. Also, the conjugation rates of the new compounds by rat liver subcellular fractions were compared with those by rat colon subcellular fractions. When selecting the lead compound, the new compounds which were conjugated rapidly in rat liver but slowly in rat colon were favored. **6a1** was selected as the lead compound for the following studies in rats. Meanwhile, to see whether the results from rats could be extrapolated to human, we also employed human liver and intestine subcellular fractions to conjugate the new compounds *in vitro*. In the phase II metabolism of these new compounds, the most notable species difference between rats and human was that in human, the colon S9 fractions produced sulfates much more efficiently than liver S9 fractions. When **6a1** was applied to the Caco-2 monolayer model, the predominant metabolite was **6a1**-sulfate, indicating that a lot of **6a1**-sulfate may be generated *in vivo* in human colon. In the future, when the studies in rats are translated to human, the phenolic group species in the structure should be modified to avoid the extensive sulfation in human colon. For example, the neighboring position of –OH of **6a1** will be substituted with various groups (e.g., alkyl groups, ether groups, halogen atoms or other functional groups) and the effects of such substitutions on the phase II metabolism rates will be determined. The aim will be to find a substitution which can largely decrease the sulfation rate of **6a1** in human intestine/colon without impairing its glucuronidation rate in human liver. The subcellular fractions prepared from human tissues will be employed in the *in vitro* screening for such a substitution.

We also verified the inhibitory effect of **6a1** on COX-2 activity in inflamed rat colon. The cannulated rat colon was perfused with HBSS containing compounds of interest at different concentrations after the acute inflammation is induced in rat colon by TNBS. In the perfusate, the

PGE_2 concentration was quantitated as the indicator of colonic COX-2 activity. The inhibitory effects of celecoxib on colonic COX-2 in this model were shown to be dependent on its concentrations in the perfusate. 1 and 10 μM celecoxib significantly accelerated PGE_2 attenuation, while 70 μM **6a1** had similar effects with 1 μM celecoxib. During the perfusion of celecoxib, its blood concentrations in the systemic circulation was always increasing and could be tens of fold higher than its IC_{50} on COX-2 activity. In contrast, the blood concentration of **6a1** was much lower than its IC_{50} during the perfusion of 70 μM **6a1**. The analysis of bile samples of rats illustrated that the extensive glucuronidation and excretion in rat liver prevented almost all the absorbed **6a1** from entering the systemic circulation.

So far, we have provided support for the concept of locally bioavailable COX-2 inhibitors. Also, the results have illustrated that the bioavailability of these compounds can be manipulated by altering the phenolic groups in their structures. In the future, compared with **6a1**, the next-generation locally bioavailable COX-2 inhibitors require improved potency to inhibit COX-2 activity and even lower oral bioavailability. The lead compounds among the next-generation locally bioavailable COX-2 inhibitors will be further investigated for their efficacies in CRC chemoprevention in relevant animal models. Eventually, we wish that the locally bioavailable COX-2 inhibitors can be developed as a class of safe and effective agents which can be used in CRC chemoprevention in human.

APPENDIX A: NMR SPECTRA OF THE FINAL PRODUCTS IN THE CHEMICAL SYNTHESIS

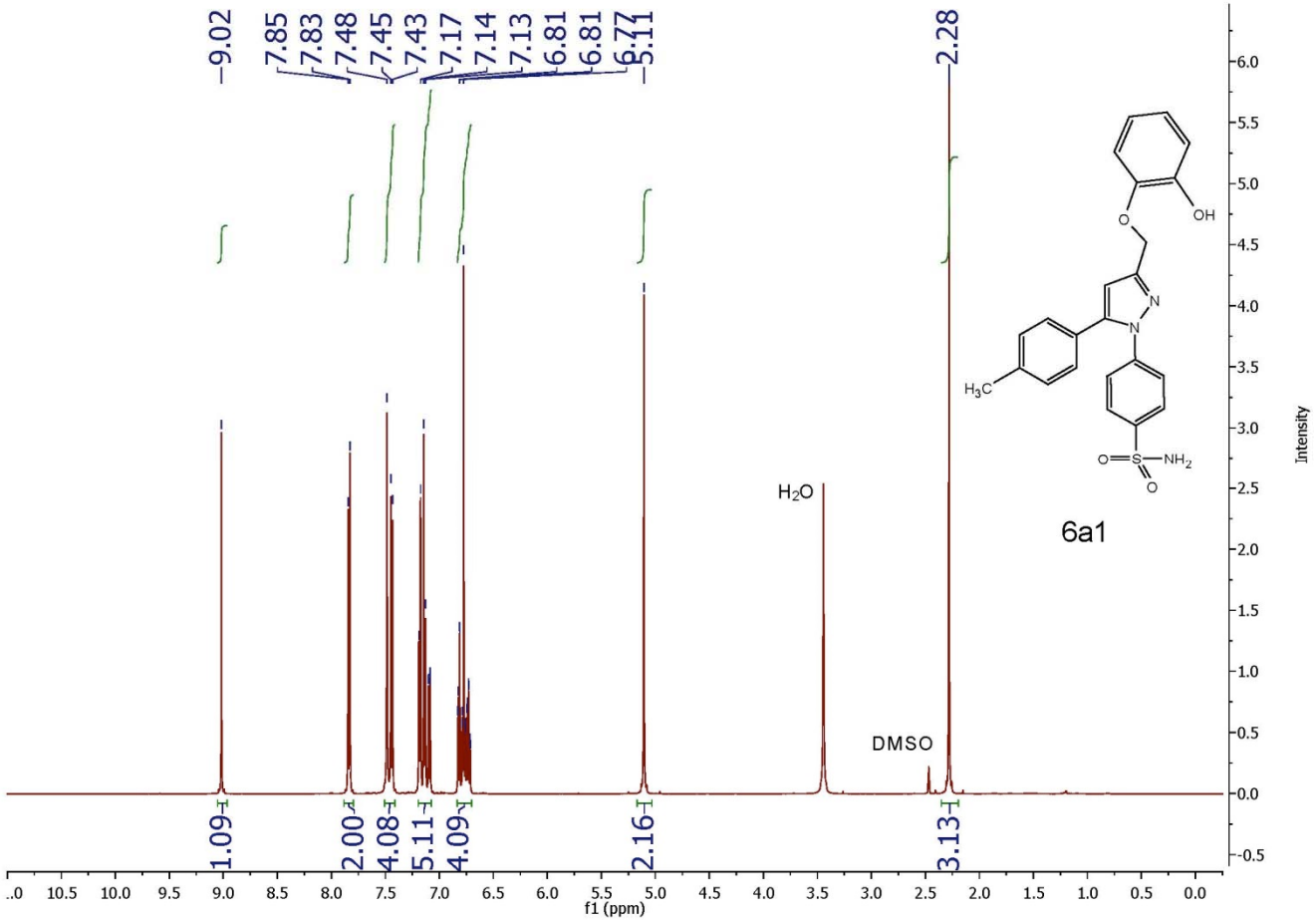

^{1}H-NMR spectra of **6a1**

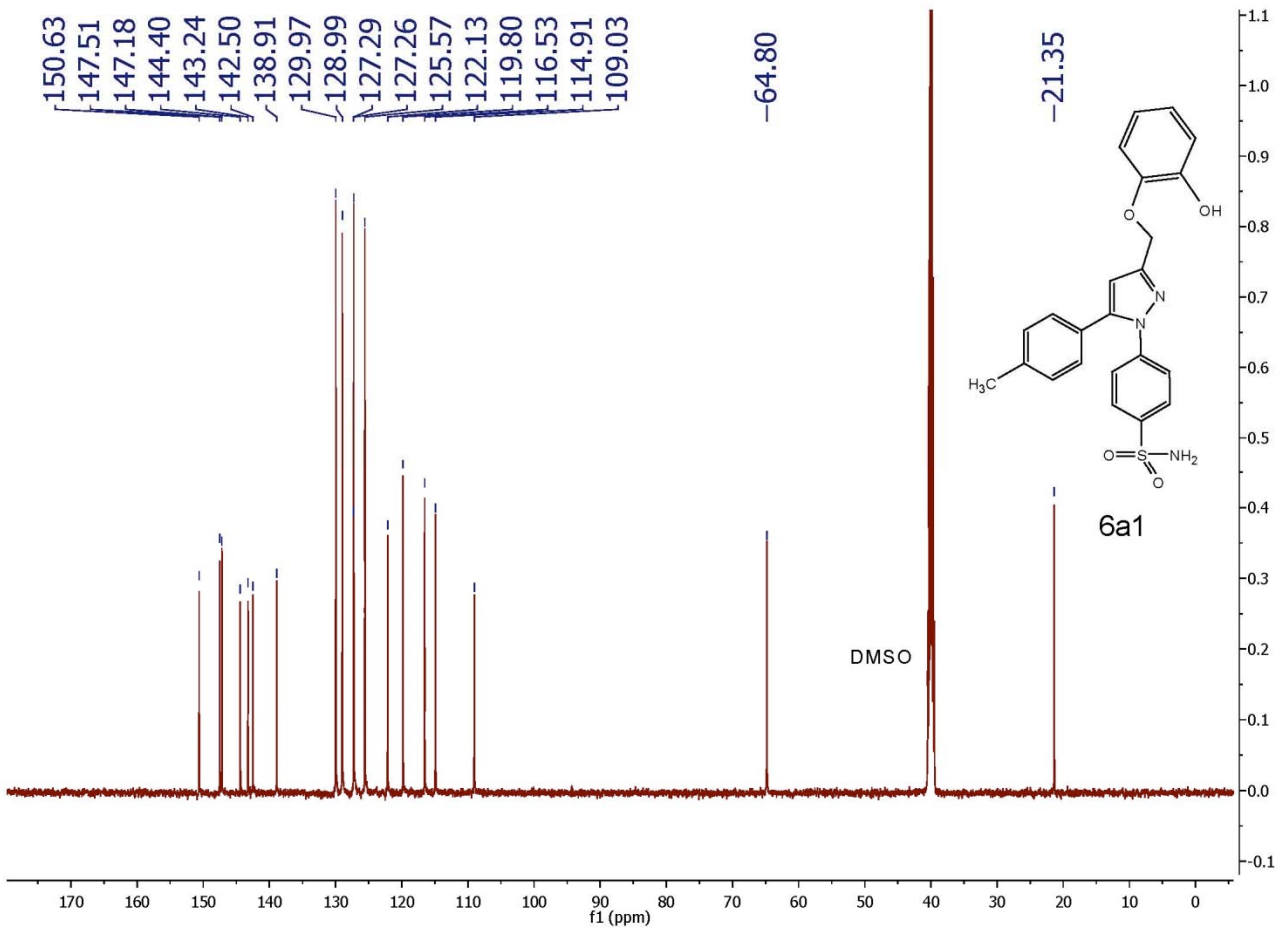

^{13}C-NMR spectra of **6a1**

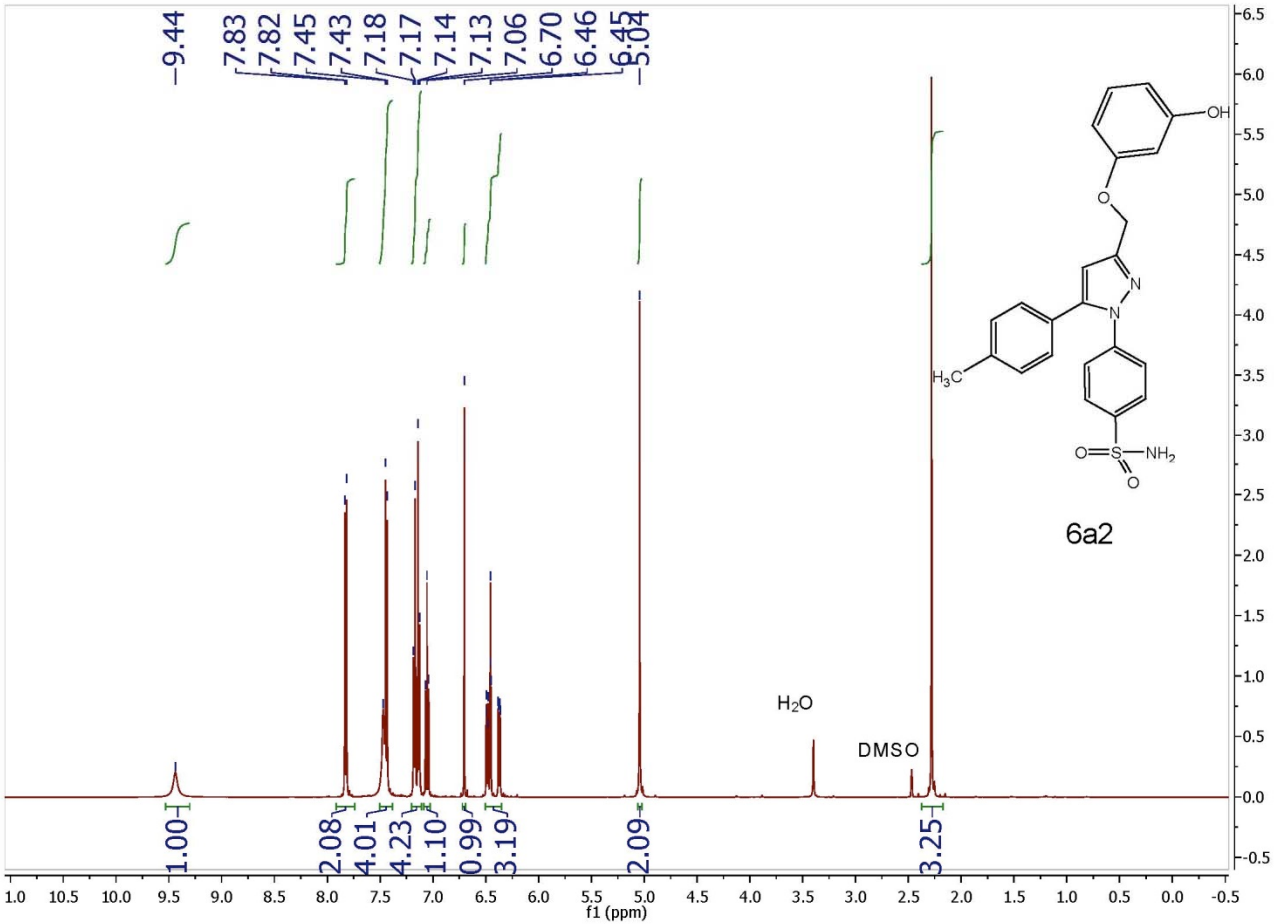

^{1}H-NMR spectra of **6a2**

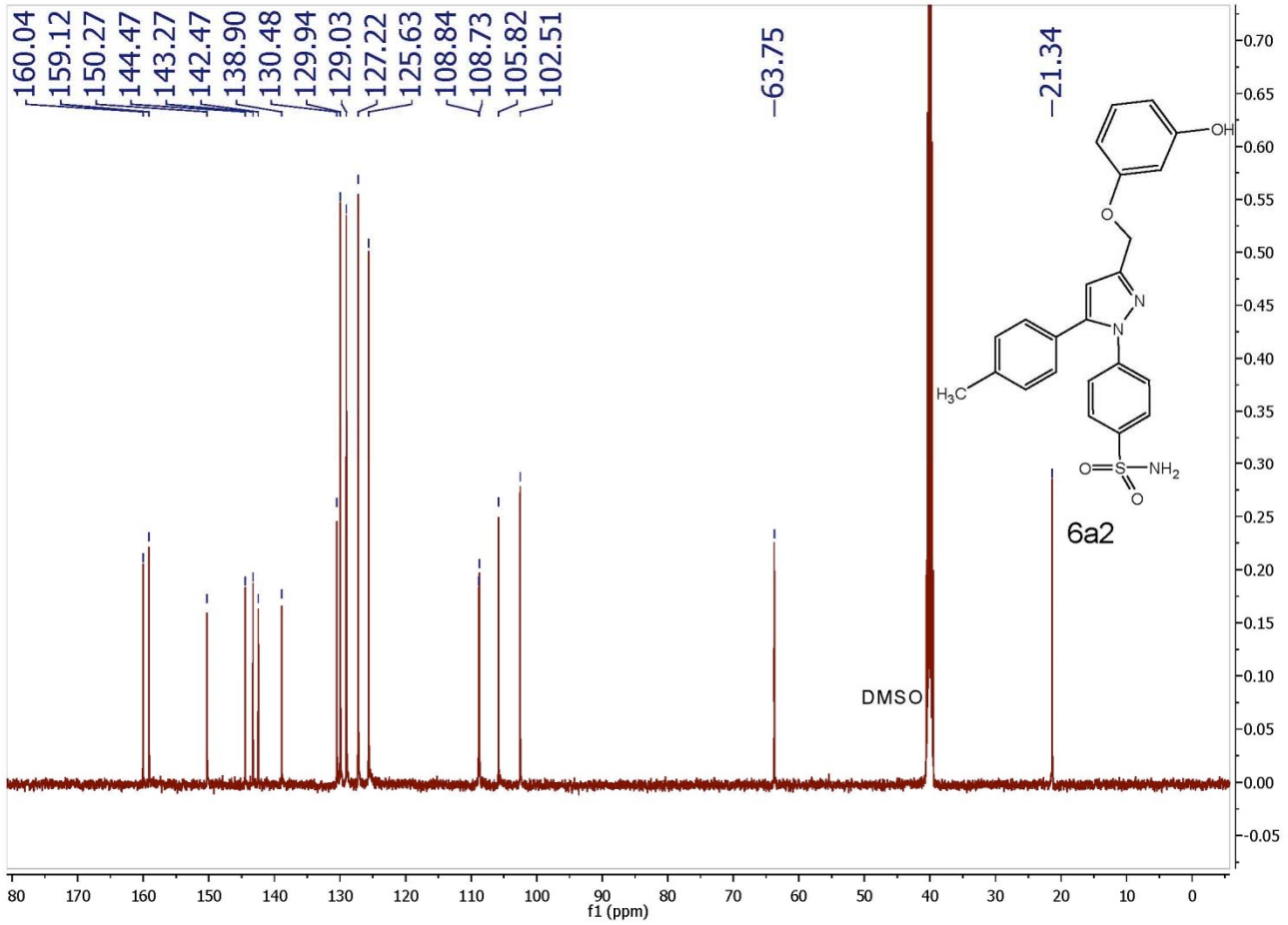

^{13}C-NMR spectra of **6a2**

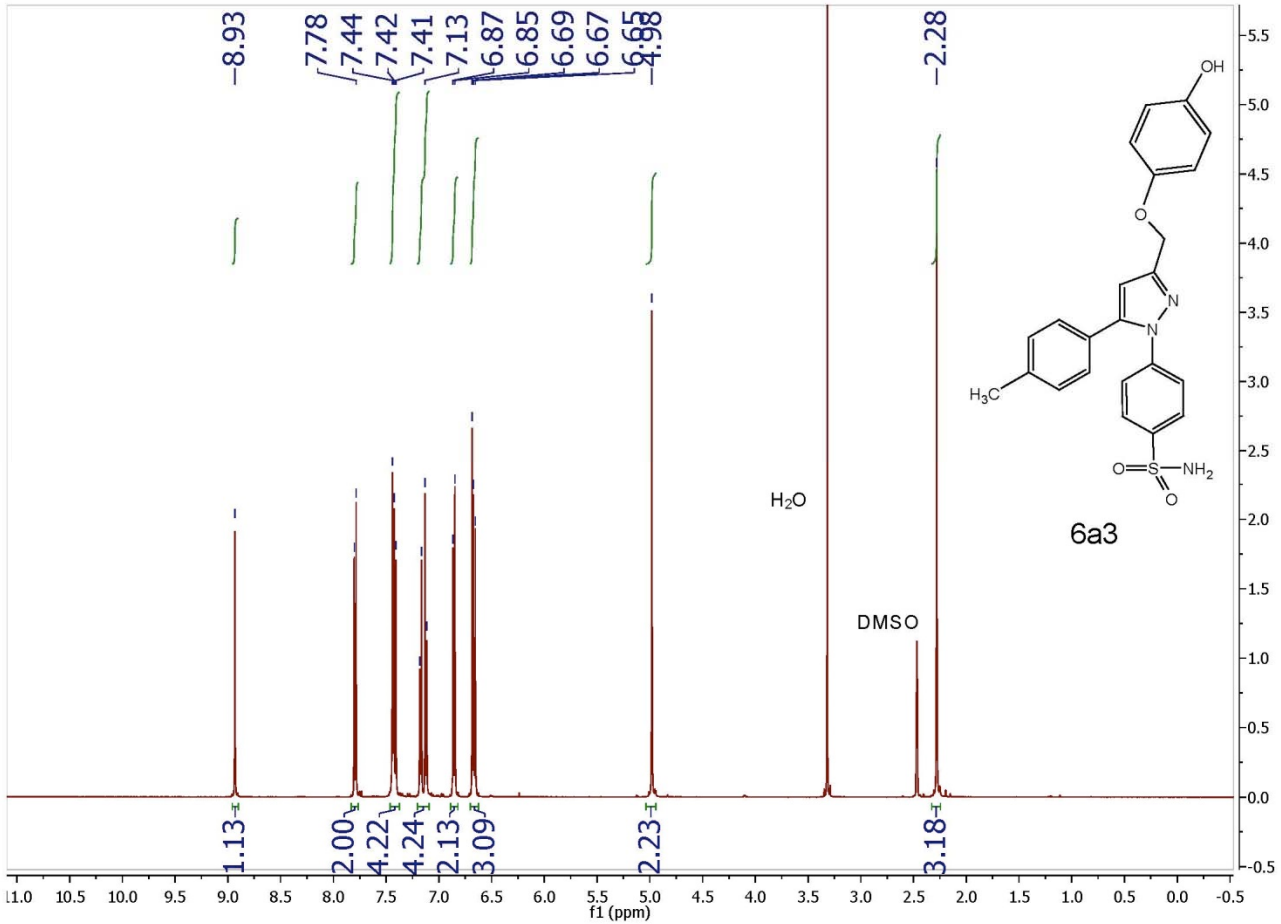

2478

2479 ^{1}H-NMR spectra of **6a3**

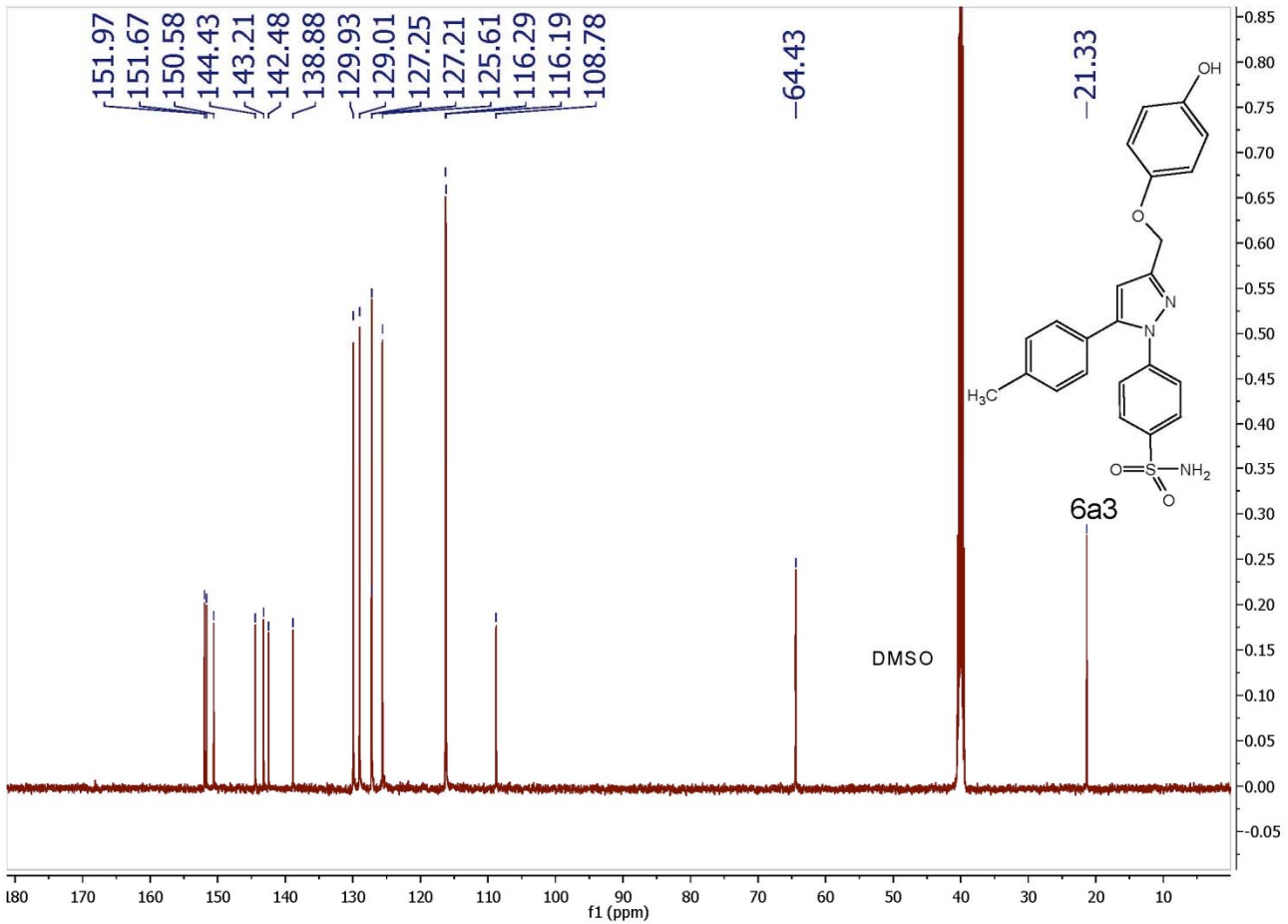

2480

2481 ^{13}C-NMR spectra of **6a3**

2482

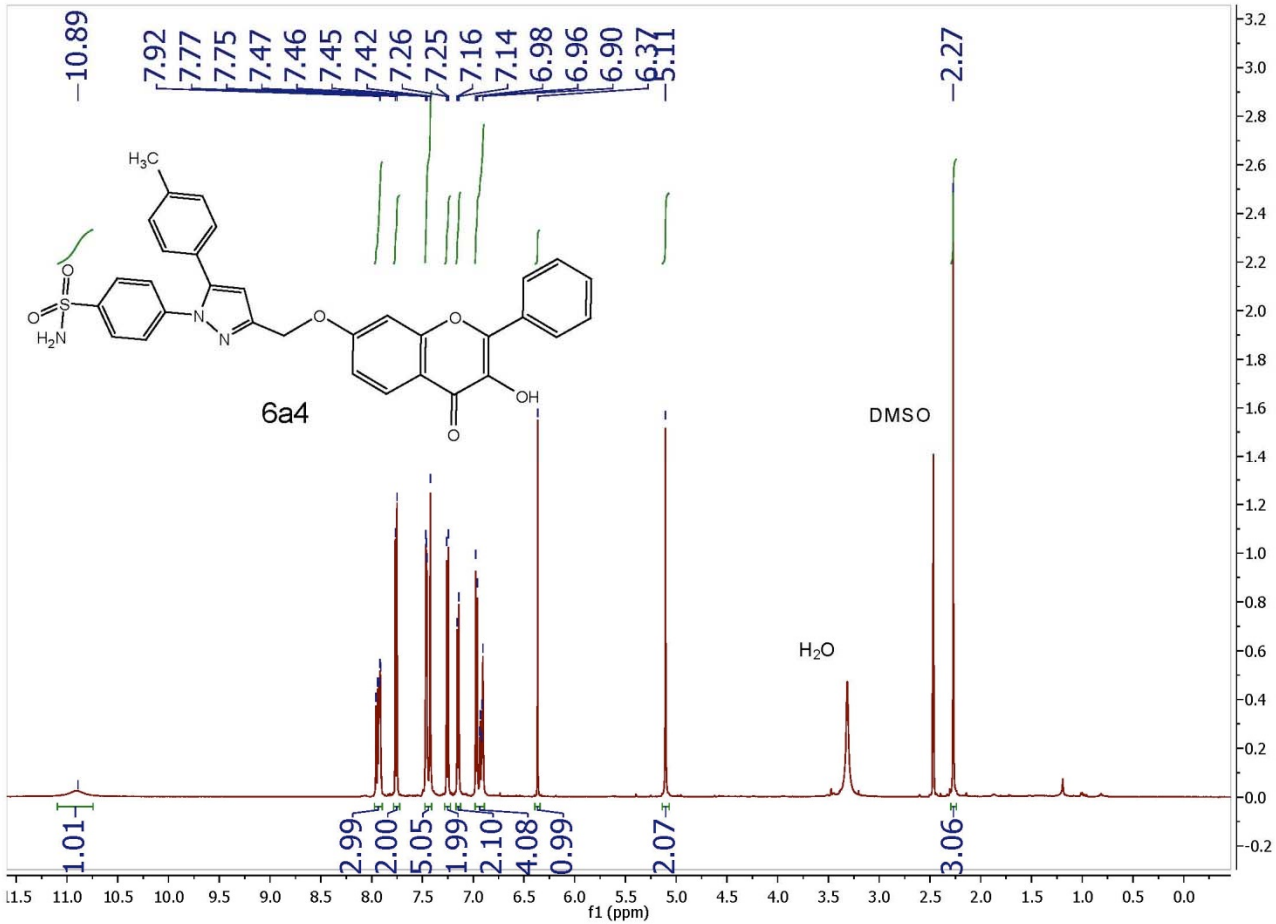

2483

2484 ^{1}H-NMR spectra of **6a4**

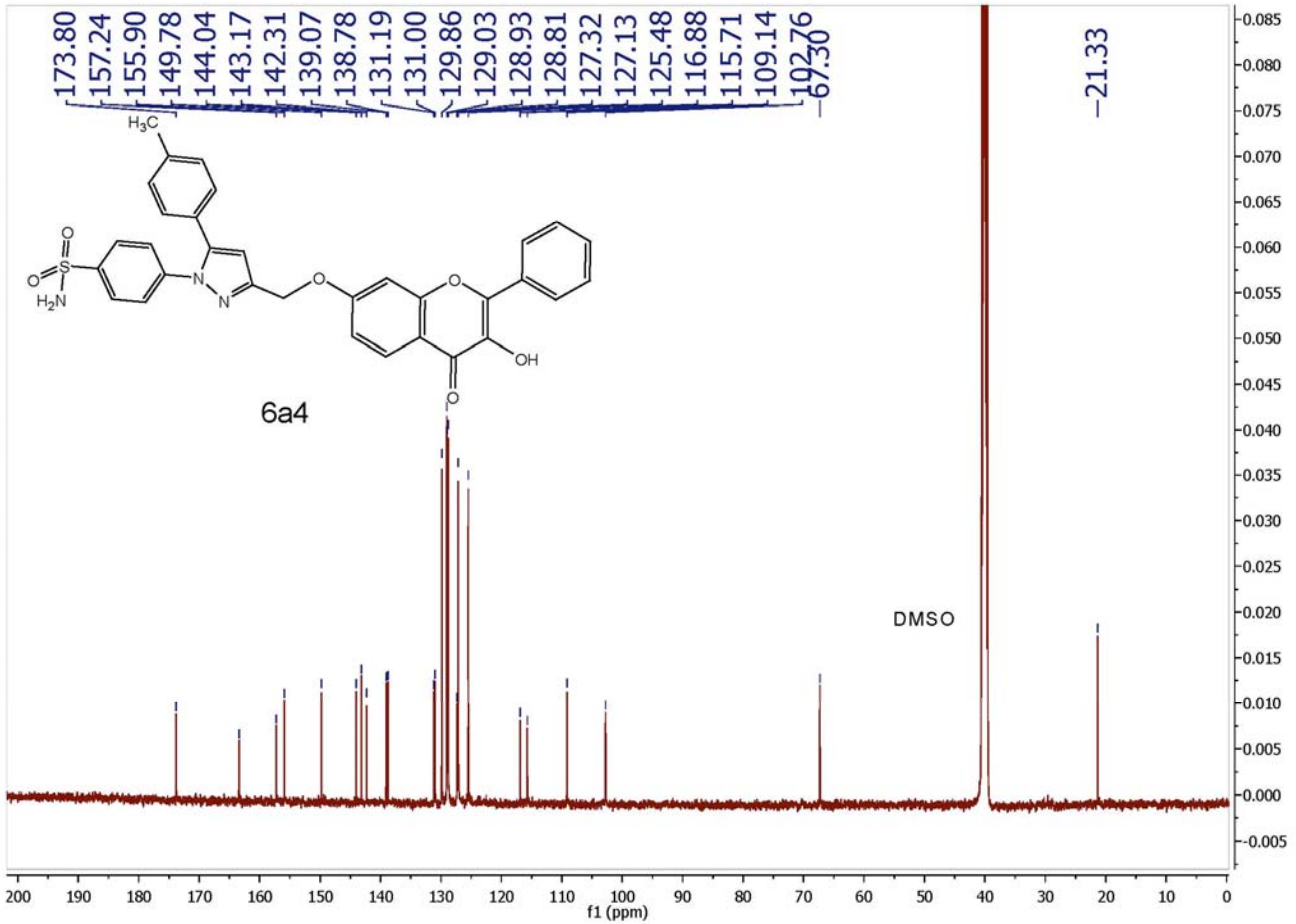

2485

2486 ^{13}C-NMR spectra of **6a4**

2487

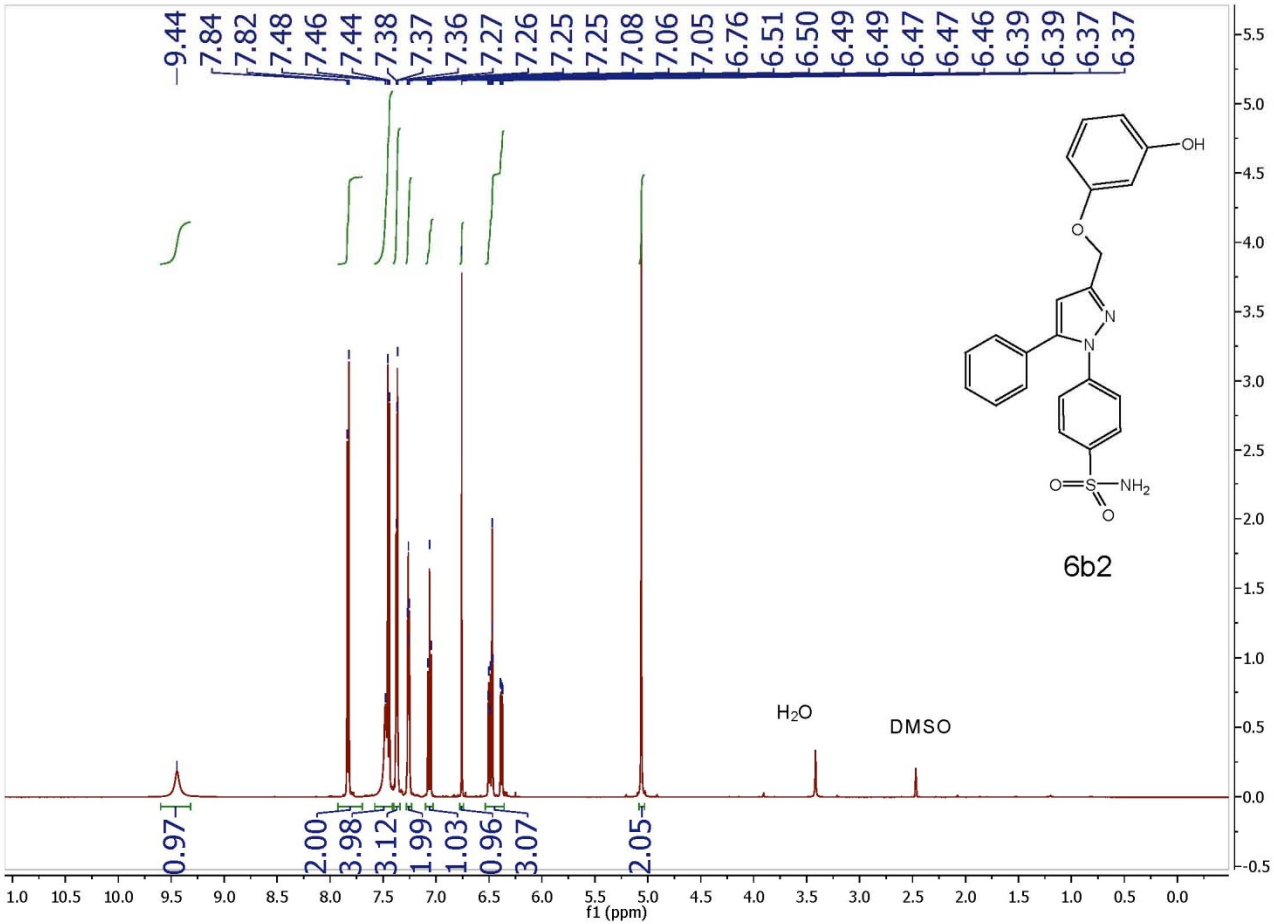

^{1}H-NMR spectra of **6b2**

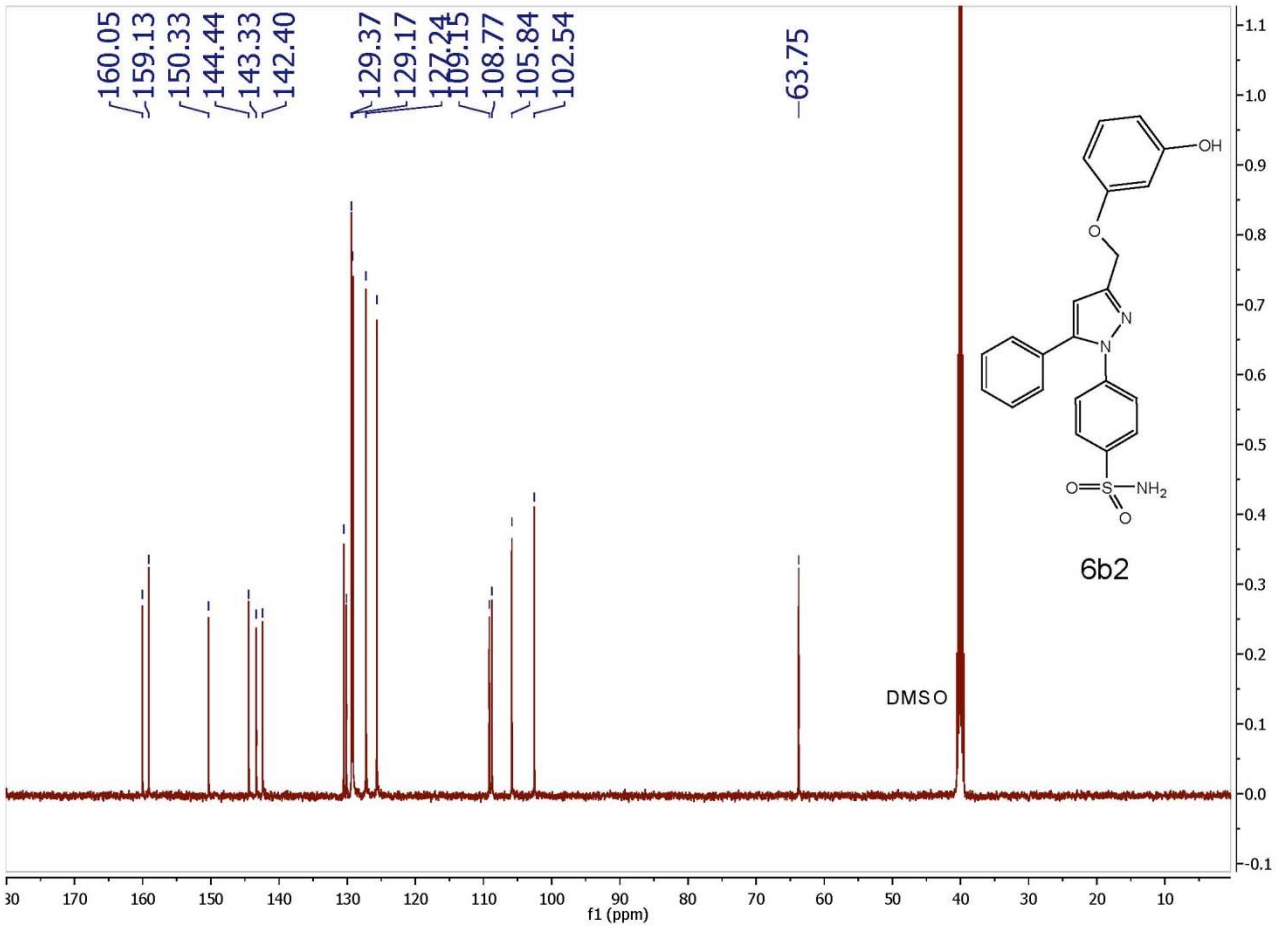

2491

2492 ^{13}C-NMR spectra of **6b2**

2493

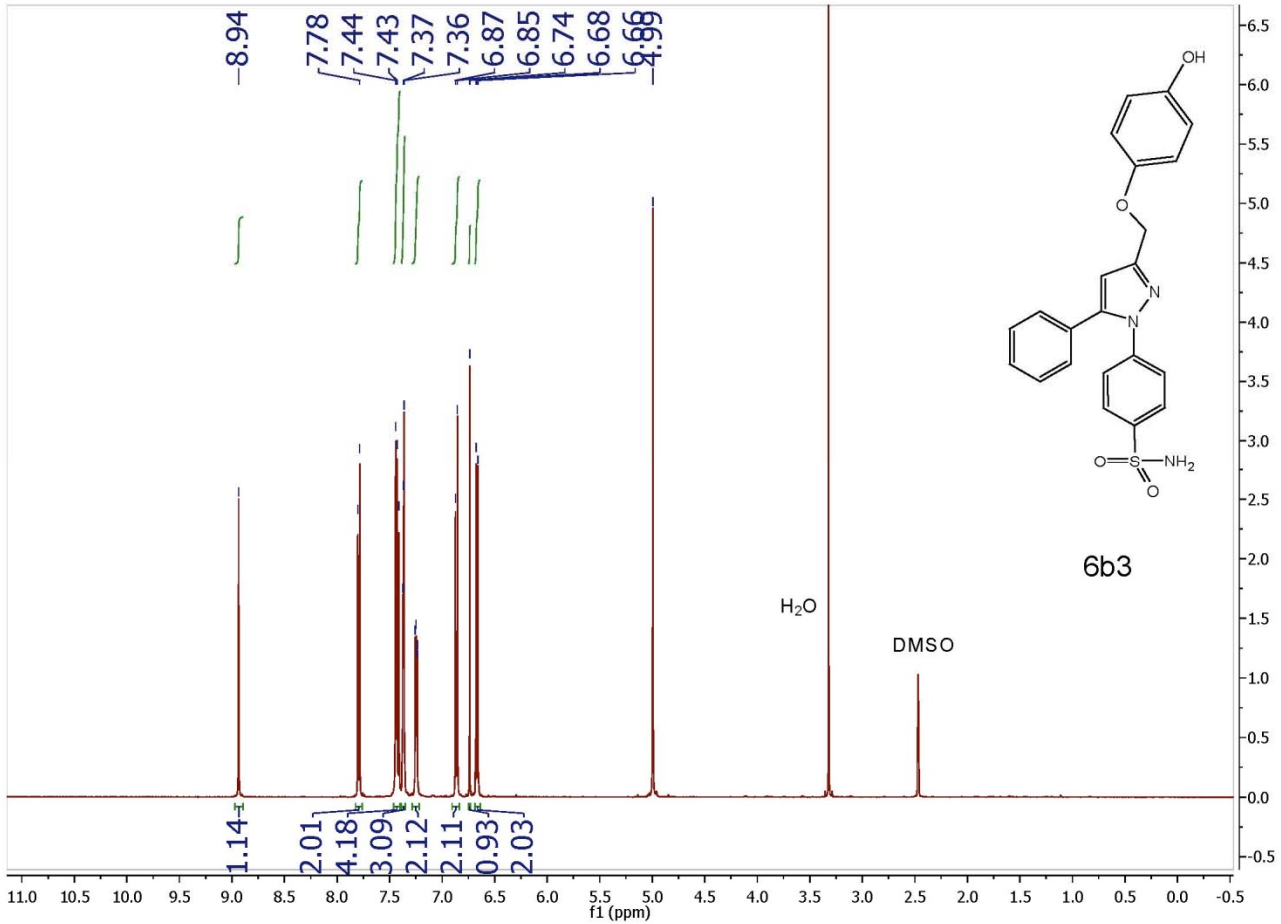

[1]H-NMR spectra of **6b3**

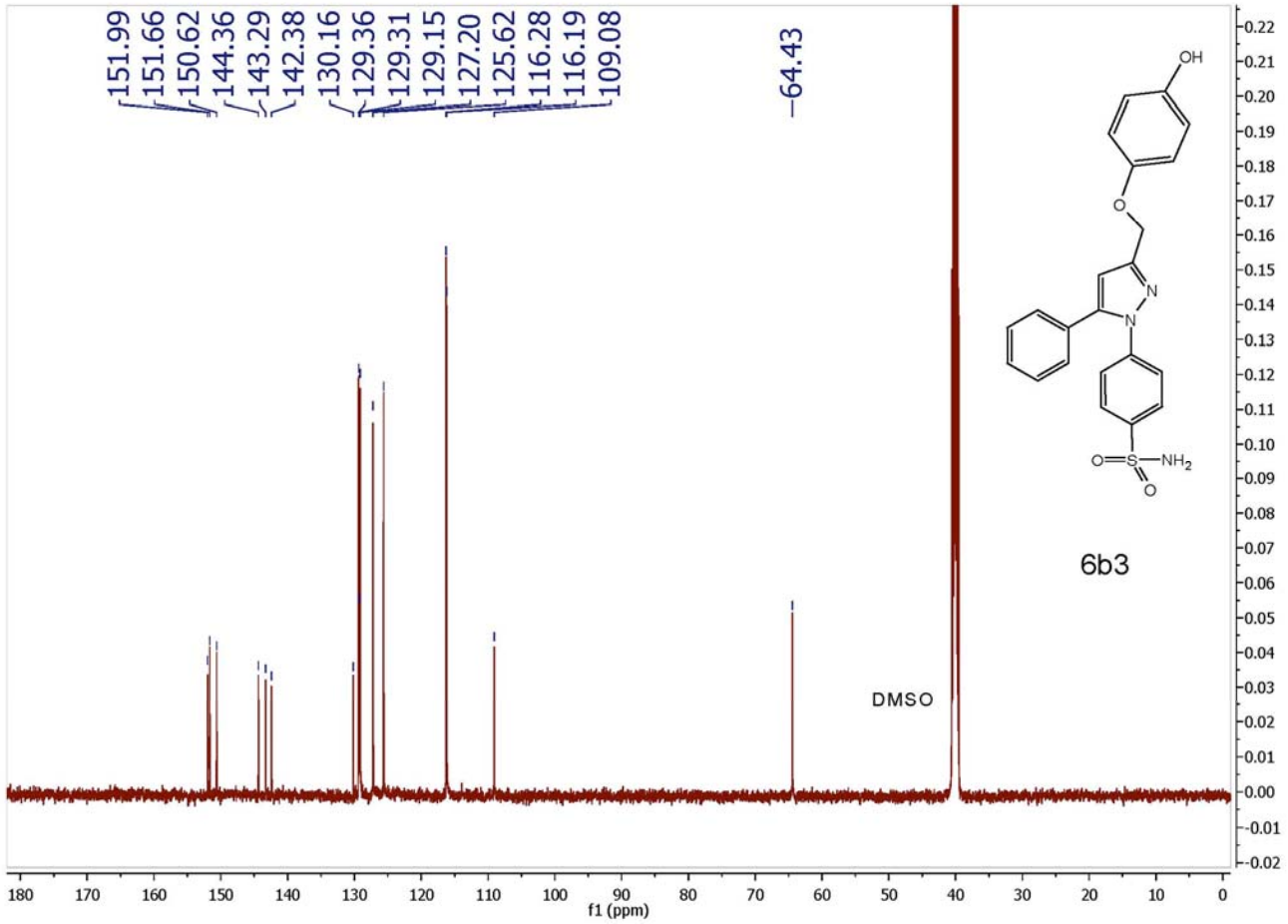

2496

2497 ^{13}C-NMR spectra of **6b3**

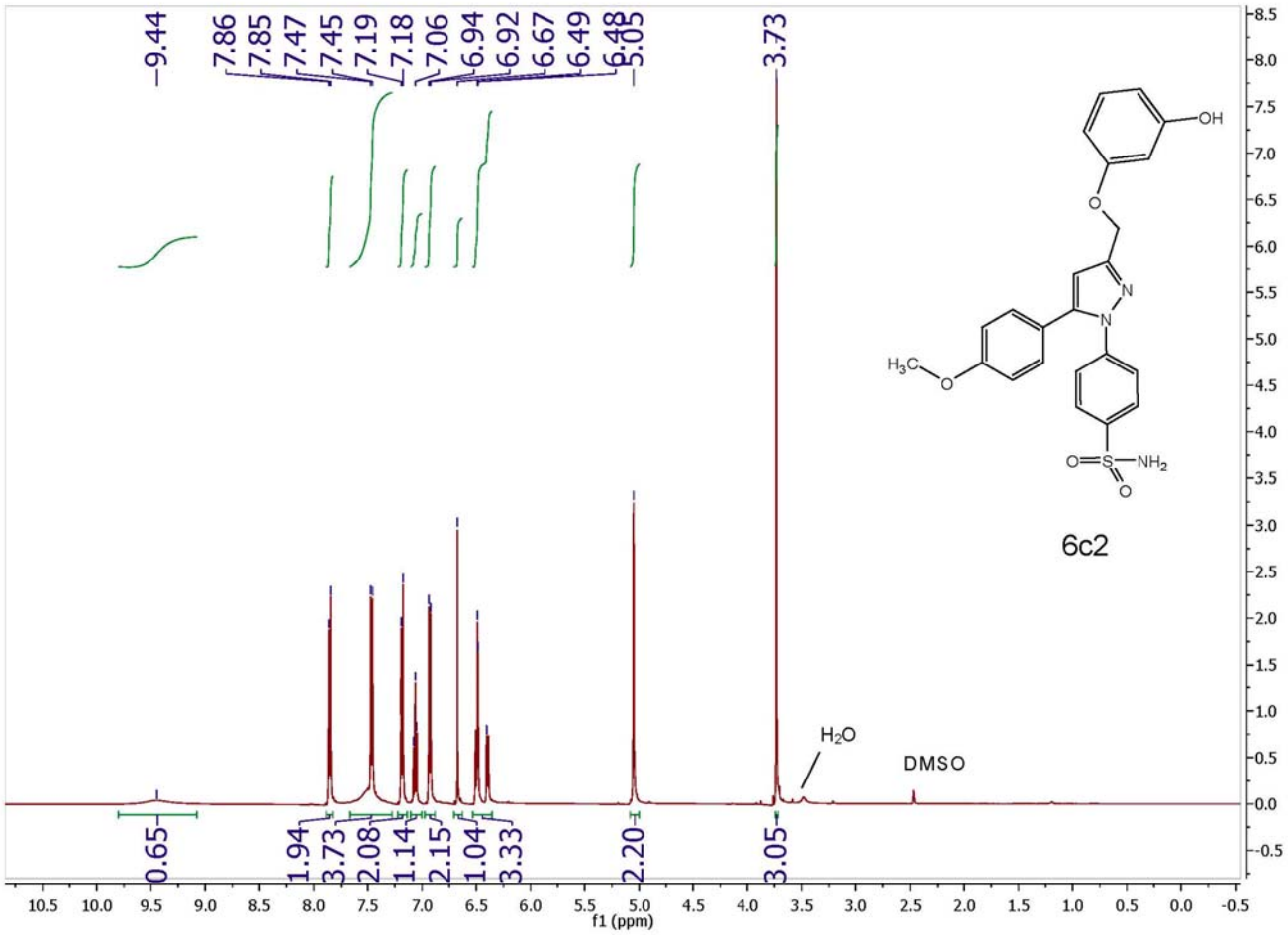

[1]H-NMR spectra of **6c2**

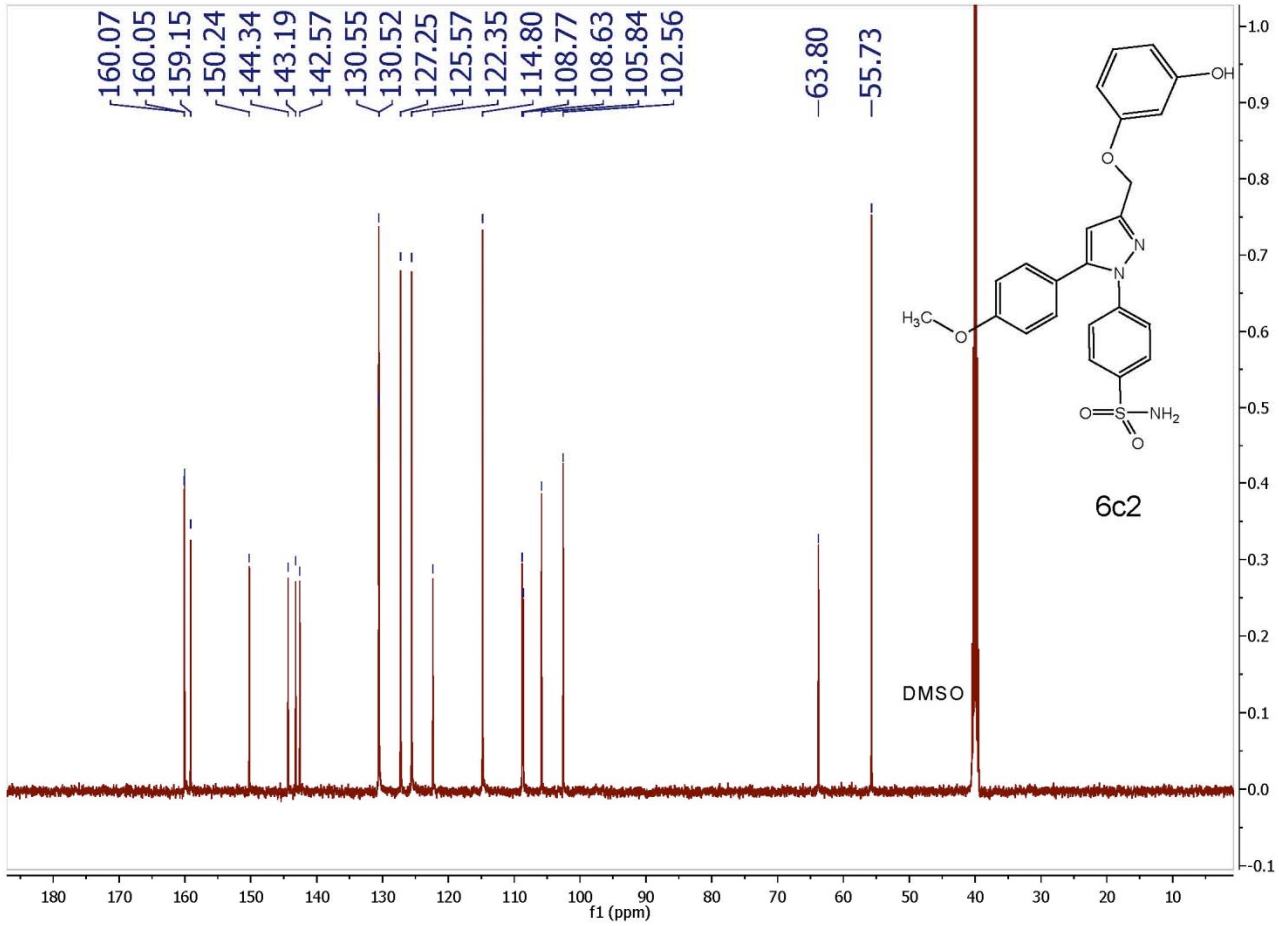

2500

2501 ^{13}C-NMR spectra of **6c2**

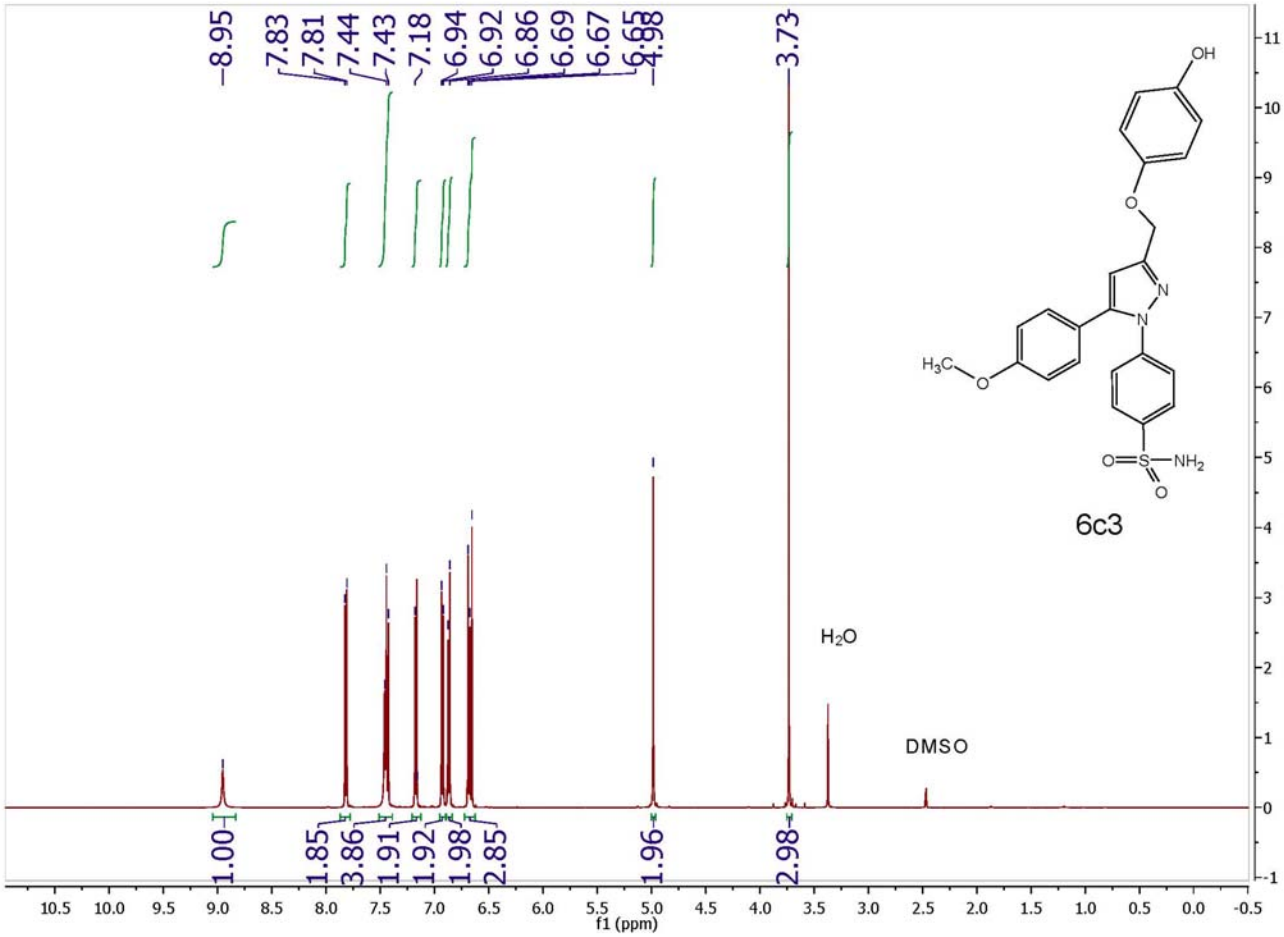

^{1}H-NMR spectra of **6c3**

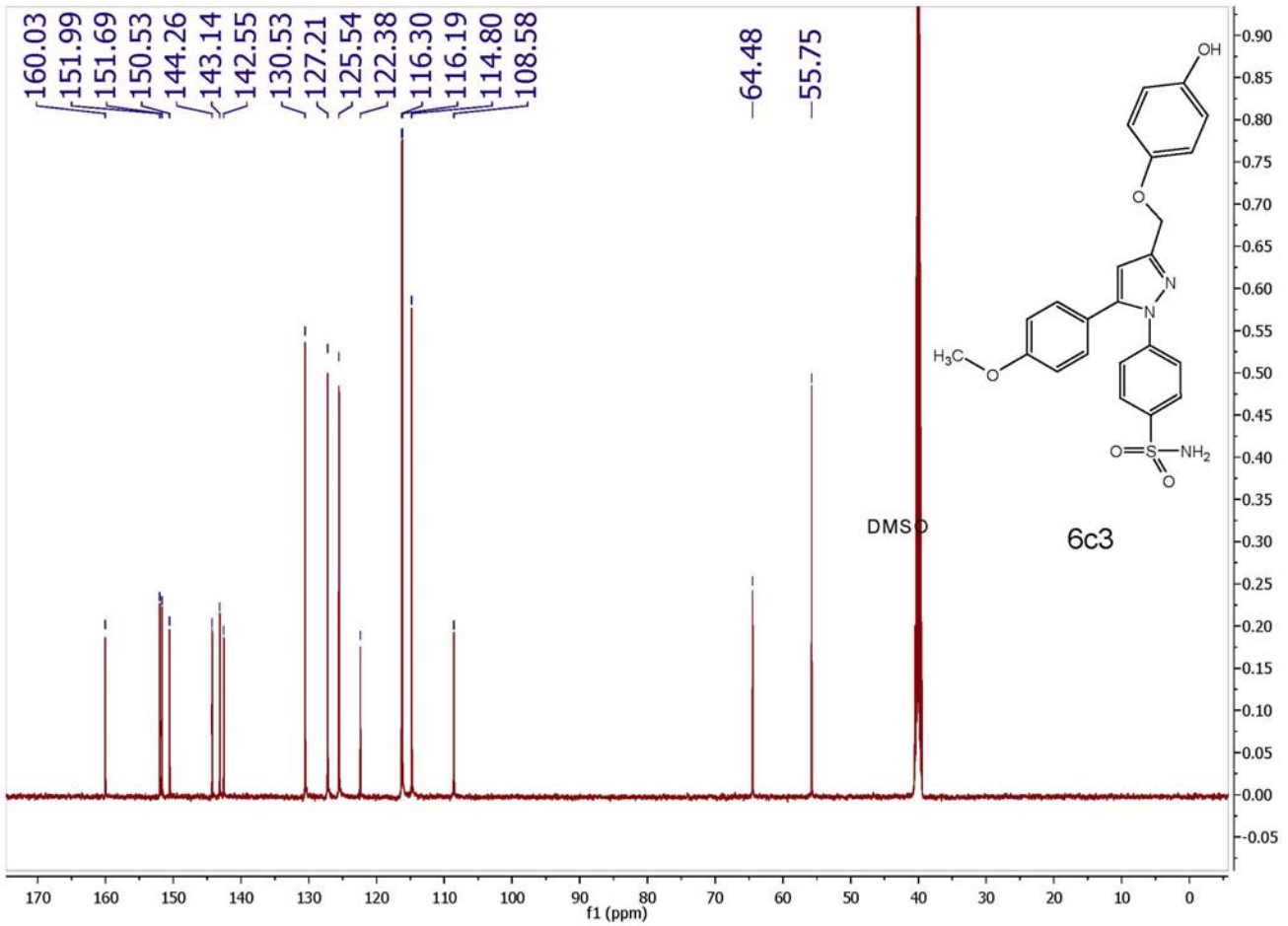

^{13}C-NMR spectra of **6c3**

REFERENCES

1. Xu, C., C.-T. Li, and A.-N. Kong, *Induction of phase I, II and III drug metabolism/transport by xenobiotics.* Archives of Pharmacal Research, 2005. **28**(3): p. 249-268.
2. Testa, B., A. Pedretti, and G. Vistoli, *Reactions and enzymes in the metabolism of drugs and other xenobiotics.* Drug Discovery Today, 2012. **17**(11–12): p. 549-560.
3. Baillie, T.A., et al., *Drug Metabolites in Safety Testing.* Toxicology and Applied Pharmacology, 2002. **182**(3): p. 188-196.
4. Nelson, D., *The Cytochrome P450 Homepage.* Human Genomics, 2009. **4**(1): p. 59 - 65.
5. Guengerich, F.P., *Cytochrome P450 and Chemical Toxicology.* Chemical Research in Toxicology, 2007. **21**(1): p. 70-83.
6. Lewis, D.F., *Human cytochromes P450 associated with the phase 1 metabolism of drugs and other xenobiotics: a compilation of substrates and inhibitors of the CYP1, CYP2 and CYP3 families.* Curr Med Chem, 2003. **10**(19): p. 1955-72.
7. Huttunen, K.M., et al., *Cytochrome P450-activated prodrugs: targeted drug delivery.* Curr Med Chem, 2008. **15**(23): p. 2346-65.
8. Patterson, L.H., et al., *Antitumour prodrug development using cytochrome P450 (CYP) mediated activation.* Anticancer Drug Des, 1999. **14**(6): p. 473-86.
9. Zhang, Y.-Y. and L. Yang, *Interactions between human cytochrome P450 enzymes and steroids: physiological and pharmacological implications.* Expert Opinion on Drug Metabolism & Toxicology, 2009. **5**(6): p. 621-629.
10. Rifkind, A.B., *CYP1A in TCDD Toxicity and in Physiology–with Particular Reference to CYP Dependent Arachidonic Acid Metabolism and other Endogenous Substrates.* Drug Metabolism Reviews, 2006. **38**(1-2): p. 291-335.
11. Prosser, D.E. and G. Jones, *Enzymes involved in the activation and inactivation of vitamin D.* Trends in Biochemical Sciences, 2004. **29**(12): p. 664-673.
12. Guengerich, F.P., *Human cytochrome P450 enzymes*, in *Cytochrome P450*. 1995, Springer. p. 473-535.
13. Lewis, D.F.V., *57 varieties: the human cytochromes P450.* Pharmacogenomics, 2004. **5**(3): p. 305-318.
14. Ingelman-Sundberg, M., *Human drug metabolising cytochrome P450 enzymes: properties and polymorphisms.* Naunyn-Schmiedeberg's Archives of Pharmacology, 2004. **369**(1): p. 89-104.
15. Uttamsingh, V., et al., *RELATIVE CONTRIBUTIONS OF THE FIVE MAJOR HUMAN CYTOCHROMES P450, 1A2, 2C9, 2C19, 2D6, AND 3A4, TO THE HEPATIC METABOLISM OF THE PROTEASOME INHIBITOR BORTEZOMIB.* Drug Metabolism and Disposition, 2005. **33**(11): p. 1723-1728.
16. Rendic, S., *Summary of information on human CYP enzymes: human P450 metabolism data.* Drug Metabolism Reviews, 2002. **34**(1-2): p. 83-448.

17. Lin, J.H. and A.Y.H. Lu, *Role of Pharmacokinetics and Metabolism in Drug Discovery and Development.* Pharmacol Rev, 1997. **49**(4): p. 403-449.
18. Osborne, R., et al., *Morphine and metabolite behavior after different routes of morphine administration: Demonstration of the importance of the active metabolite morphine-6-glucuronide.* Clinical Pharmacology & Therapeutics, 1990. **47**(1): p. 12-19.
19. Zamek-Gliszczynski, M.J., et al., *Integration of hepatic drug transporters and phase II metabolizing enzymes: Mechanisms of hepatic excretion of sulfate, glucuronide, and glutathione metabolites.* European Journal of Pharmaceutical Sciences, 2006. **27**(5): p. 447-486.
20. Mackenzie, P.I., et al., *Nomenclature update for the mammalian UDP glycosyltransferase (UGT) gene superfamily.* Pharmacogenet Genomics, 2005. **15**(10): p. 677-85.
21. Nakamura, A., et al., *Expression of UGT1A and UGT2B mRNA in Human Normal Tissues and Various Cell Lines.* Drug Metabolism and Disposition, 2008. **36**(8): p. 1461-1464.
22. Knights, K.M., A. Rowland, and J.O. Miners, *Renal drug metabolism in humans: the potential for drug–endobiotic interactions involving cytochrome P450 (CYP) and UDP-glucuronosyltransferase (UGT).* British Journal of Clinical Pharmacology, 2013. **76**(4): p. 587-602.
23. Guillemette, C., *Pharmacogenomics of human UDP-glucuronosyltransferase enzymes.* Pharmacogenomics J, 2003. **3**(3): p. 136-158.
24. Richard, K., et al., *Sulfation of Thyroid Hormone and Dopamine during Human Development: Ontogeny of Phenol Sulfotransferases and Arylsulfatase in Liver, Lung, and Brain.* The Journal of Clinical Endocrinology & Metabolism, 2001. **86**(6): p. 2734-2742.
25. Blanchard, R.L., et al., *A proposed nomenclature system for the cytosolic sulfotransferase (SULT) superfamily.* Pharmacogenet Genomics, 2004. **14**(3): p. 199-211.
26. Riches, Z., et al., *Quantitative Evaluation of the Expression and Activity of Five Major Sulfotransferases (SULTs) in Human Tissues: The SULT "Pie".* Drug Metabolism and Disposition, 2009. **37**(11): p. 2255-2261.
27. Pietsch, C.A., T.S. Scanlan, and R.J. Anderson, *Thyronamines Are Substrates for Human Liver Sulfotransferases.* Endocrinology, 2007. **148**(4): p. 1921-1927.
28. Gamage, N.U., et al., *The Structure of Human SULT1A1 Crystallized with Estradiol: AN INSIGHT INTO ACTIVE SITE PLASTICITY AND SUBSTRATE INHIBITION WITH MULTI-RING SUBSTRATES.* Journal of Biological Chemistry, 2005. **280**(50): p. 41482-41486.
29. Taskinen, J., et al., *CONJUGATION OF CATECHOLS BY RECOMBINANT HUMAN SULFOTRANSFERASES, UDP-GLUCURONOSYLTRANSFERASES, AND SOLUBLE CATECHOL O-METHYLTRANSFERASE: STRUCTURE-CONJUGATION RELATIONSHIPS AND PREDICTIVE MODELS.* Drug Metabolism and Disposition, 2003. **31**(9): p. 1187-1197.
30. Louwers, Y.V., et al., *Variants in SULT2A1 Affect the DHEA Sulphate to DHEA Ratio in Patients With Polycystic Ovary Syndrome But Not the Hyperandrogenic*

Phenotype. The Journal of Clinical Endocrinology & Metabolism, 2013. **98**(9): p. 3848-3855.
31. Buonarati, M.H., et al., *Role of sulfation and acetylation in the activation of 2-hydroxyamino-1-methyl-6-phenylimidazo[4,5-b]pyridine to intermediates which bind DNA.* Mutation Research Letters, 1990. **245**(3): p. 185-190.
32. Vasiliou, V., K. Vasiliou, and D. Nebert, *Human ATP-binding cassette (ABC) transporter family.* Human Genomics, 2008. **3**(3): p. 281 - 290.
33. Jones, P.M. and A.M. George, *The ABC transporter structure and mechanism: perspectives on recent research.* Cellular and Molecular Life Sciences CMLS, 2004. **61**(6): p. 682-699.
34. Fromm, M.F., *P-glycoprotein: a defense mechanism limiting oral bioavailability and CNS accumulation of drugs.* International journal of clinical pharmacology and therapeutics, 2000. **38**(2): p. 69-74.
35. Valk, P.V.d., et al., *Original article: Distribution of multi-drug resistance-associated P-glycoprotein in normal and neoplastic human tissues: Analysis with 3 monoclonal antibodies recognizing different epitopes of theP-glycoprotein molecule.* Annals of Oncology, 1990. **1**(1): p. 56-64.
36. Marzolini, C., et al., *Polymorphisms in Human MDR1 (P-glycoprotein): Recent Advances and Clinical Relevance.* Clinical Pharmacology & Therapeutics, 2004. **75**(1): p. 13-33.
37. Clarke, R., F. Leonessa, and B. Trock, *Multidrug Resistance/P-Glycoprotein and Breast Cancer: Review and Meta-Analysis.* Seminars in Oncology, 2005. **32, Supplement 7**(0): p. 9-15.
38. Kumar, R., M. Kaur, and O. Silakari, *Physiological Modulation Approaches to Improve Cancer Chemotherapy : A Review.* Anti-Cancer Agents in Medicinal Chemistry- Anti-Cancer Agents), 2014. **14**(5): p. 713-749.
39. Lin, J.H., *Drug–drug interaction mediated by inhibition and induction of P-glycoprotein.* Advanced Drug Delivery Reviews, 2003. **55**(1): p. 53-81.
40. Huls, M., et al., *The breast cancer resistance protein transporter ABCG2 is expressed in the human kidney proximal tubule apical membrane.* Kidney Int, 2007. **73**(2): p. 220-225.
41. Krishnamurthy, P. and J.D. Schuetz, *ROLE OF ABCG2/BCRP IN BIOLOGY AND MEDICINE.* Annu Rev Pharmacol Toxicol, 2006. **46**(1): p. 381-410.
42. Nicolazzo, J.A. and K. Katneni, *Drug transport across the blood-brain barrier and the impact of breast cancer resistance protein (ABCG2).* Curr Top Med Chem, 2009. **9**(2): p. 130-47.
43. Iqbal, M., et al., *Placental drug transporters and their role in fetal protection.* Placenta. **33**(3): p. 137-142.
44. van Herwaarden, A.E., et al., *Multidrug Transporter ABCG2/Breast Cancer Resistance Protein Secretes Riboflavin (Vitamin B2) into Milk.* Molecular and Cellular Biology, 2007. **27**(4): p. 1247-1253.
45. Staud, F. and P. Pavek, *Breast cancer resistance protein (BCRP/ABCG2).* The International Journal of Biochemistry & Cell Biology, 2005. **37**(4): p. 720-725.
46. Kruh, G.D. and M.G. Belinsky, *The MRP family of drug efflux pumps.* Oncogene, 0000. **22**(47): p. 7537-7552.

47. Oostendorp, R.L., J.H. Beijnen, and J.H.M. Schellens, *The biological and clinical role of drug transporters at the intestinal barrier.* Cancer Treatment Reviews, 2009. **35**(2): p. 137-147.
48. Ito, K., et al., *Apical/Basolateral Surface Expression of Drug Transporters and its Role in Vectorial Drug Transport.* Pharmaceutical Research, 2005. **22**(10): p. 1559-1577.
49. Keppler, D., I. Leier, and G. Jedlitschky, *Transport of glutathione conjugates and glucuronides by the multidrug resistance proteins MRP1 and MRP2.* Biological chemistry, 1997. **378**(8): p. 787-791.
50. König, J., et al., *Conjugate export pumps of the multidrug resistance protein (MRP) family: localization, substrate specificity, and MRP2-mediated drug resistance.* Biochimica et Biophysica Acta (BBA) - Biomembranes, 1999. **1461**(2): p. 377-394.
51. Pond, S. and T. Tozer, *First-Pass Elimination Basic Concepts and Clinical Consequences.* Clin Pharmacokinet, 1984. **9**(1): p. 1-25.
52. Lalka, D., R.K. Griffith, and C.L. Cronenberger, *The Hepatic First-Pass Metabolism of Problematic Drugs.* The Journal of Clinical Pharmacology, 1993. **33**(7): p. 657-669.
53. Lin, J.H., M. Chiba, and T.A. Baillie, *Is the role of the small intestine in first-pass metabolism overemphasized?* Pharmacol Rev, 1999. **51**(2): p. 135-58.
54. Lennernäs, H., *Regional intestinal drug permeation: Biopharmaceutics and drug development.* European Journal of Pharmaceutical Sciences, 2014. **57**(0): p. 333-341.
55. Krishna, D. and U. Klotz, *Extrahepatic Metabolism of Drugs in Humans.* Clin Pharmacokinet, 1994. **26**(2): p. 144-160.
56. Hu, M., *Commentary: Bioavailability of Flavonoids and Polyphenols: Call to Arms.* Molecular pharmaceutics, 2007. **4**(6): p. 803-806.
57. Roberts, M.S., et al., *Enterohepatic circulation: physiological, pharmacokinetic and clinical implications.* Clin Pharmacokinet, 2002. **41**(10): p. 751-90.
58. Erlinger, S., *Review article: new insights into the mechanisms of hepatic transport and bile secretion.* J Gastroenterol Hepatol, 1996. **11**(6): p. 575-9.
59. Bokkenheuser, V.D., C.H. Shackleton, and J. Winter, *Hydrolysis of dietary flavonoid glycosides by strains of intestinal Bacteroides from humans.* Biochem J, 1987. **248**(3): p. 953-6.
60. Yong, M. and H. Ming, *Metabolism and Transport of Anticancer and Anti-Inflammatory Phytochemicals across the Gastrointestinal Tract*, in *Inflammation, Oxidative Stress, and Cancer*. 2013, CRC Press. p. 135-170.
61. Craig, W.J., *Health-promoting properties of common herbs.* The American journal of clinical nutrition, 1999. **70**(3): p. 491s-499s.
62. Bravo, L., *Polyphenols: Chemistry, Dietary Sources, Metabolism, and Nutritional Significance*. Vol. 56. 1998. 317-333.
63. Jeong, E.J., et al., *Coupling of Conjugating Enzymes and Efflux Transporters: Impact on Bioavailability and Drug Interactions.* Current Drug Metabolism, 2005. **6**(5): p. 455-468.
64. Ricciotti, E. and G.A. FitzGerald, *Prostaglandins and Inflammation.* Arteriosclerosis, thrombosis, and vascular biology, 2011. **31**(5): p. 986-1000.

65. Keelan, J.A., et al., *Cytokines, Prostaglandins and Parturition—A Review.* Placenta, 2003. **24, Supplement A**(0): p. S33-S46.
66. Goodwin, G.M., *Prostaglandins: Biochemistry, Functions, Types, and Roles*. 2010: Nova Science Publisher.
67. Williams, C.S., M. Mann, and R.N. DuBois, *The role of cyclooxygenases in inflammation, cancer, and development.* Oncogene, 1999. **18**(55): p. 7908-7916.
68. Holtzman, M.J., *Arachidonic acid metabolism.* Am Rev Respir Dis, 1991. **143**: p. 188-203.
69. Dubois, R.N., et al., *Cyclooxygenase in biology and disease.* The FASEB Journal, 1998. **12**(12): p. 1063-1073.
70. Smith, W.L., D.L. DeWitt, and R.M. Garavito, *CYCLOOXYGENASES: Structural, Cellular, and Molecular Biology.* Annual Review of Biochemistry, 2000. **69**(1): p. 145-182.
71. Rouzer, C.A. and L.J. Marnett, *Cyclooxygenases: structural and functional insights.* J Lipid Res, 2009. **50**(Suppl): p. S29-S34.
72. Helliwell, R.J.A., L.F. Adams, and M.D. Mitchell, *Prostaglandin synthases: recent developments and a novel hypothesis.* Prostaglandins, Leukotrienes and Essential Fatty Acids. **70**(2): p. 101-113.
73. FitzGerald, G.A., A.K. Pedersen, and C. Patrono, *Analysis of prostacyclin and thromboxane biosynthesis in cardiovascular disease.* Circulation, 1983. **67**(6): p. 1174-7.
74. Keeting, P.E., et al., *Rat lens prostaglandin generation proceeds by the non-enzymatic degradation of PGH2 endoperoxide.* Exp Eye Res, 1987. **44**(2): p. 261-8.
75. Vane, J.R., Y.S. Bakhle, and R.M. Botting, *CYCLOOXYGENASES 1 AND 2.* Annu Rev Pharmacol Toxicol, 1998. **38**(1): p. 97-120.
76. Willoughby, D.A., A.R. Moore, and P.R. Colville-Nash, *COX-1, COX-2, and COX-3 and the future treatment of chronic inflammatory disease.* Lancet, 2000. **355**(9204): p. 646-8.
77. Vane, S.J., *Differential inhibition of cyclooxygenase isoforms: an explanation of the action of NSAIDs.* J Clin Rheumatol, 1998. **4**(5 Suppl): p. s3-10.
78. Simmons, D.L., *Variants of cyclooxygenase-1 and their roles in medicine.* Thrombosis Research, 2003. **110**(5–6): p. 265-268.
79. Tanabe, T. and N. Tohnai, *Cyclooxygenase isozymes and their gene structures and expression.* Prostaglandins & Other Lipid Mediators, 2002. **68–69**(0): p. 95-114.
80. O'Neill, G.P. and A.W. Ford-Hutchinson, *Expression of mRNA for cyclooxygenase-1 and cyclooxygenase-2 in human tissues.* FEBS Letters, 1993. **330**(2): p. 157-160.
81. Simmons, D.L., R.M. Botting, and T. Hla, *Cyclooxygenase Isozymes: The Biology of Prostaglandin Synthesis and Inhibition.* Pharmacol Rev, 2004. **56**(3): p. 387-437.
82. Wallace, J.L., *Prostaglandins, NSAIDs, and Gastric Mucosal Protection: Why Doesn't the Stomach Digest Itself?* Vol. 88. 2008. 1547-1565.
83. Peters, R.J.G., et al., *Effects of Aspirin Dose When Used Alone or in Combination With Clopidogrel in Patients With Acute Coronary Syndromes: Observations*

From the Clopidogrel in Unstable angina to prevent Recurrent Events (CURE) Study. Circulation, 2003. **108**(14): p. 1682-1687.
84. O'Banion, M.K., et al., *A serum- and glucocorticoid-regulated 4-kilobase mRNA encodes a cyclooxygenase-related protein.* Journal of Biological Chemistry, 1991. **266**(34): p. 23261-7.
85. Crofford, L.J., *COX-1 and COX-2 tissue expression: implications and predictions.* J Rheumatol Suppl, 1997. **49**: p. 15-9.
86. KANG, R.Y., et al., *EXPRESSION OF CYCLOOXYGENASE-2 IN HUMAN AND AN ANIMAL MODEL OF RHEUMATOID ARTHRITIS.* Rheumatology, 1996. **35**(8): p. 711-718.
87. Sampey, A.V., et al., *Regulation of synoviocyte phospholipase A2 and cyclooxygenase 2 by macrophage migration inhibitory factor.* Arthritis Rheum, 2001. **44**(6): p. 1273-80.
88. Brown, J.R. and R.N. DuBois, *Cyclooxygenase as a Target in Lung Cancer.* Clinical Cancer Research, 2004. **10**(12): p. 4266s-4269s.
89. Hwang, D., et al., *Expression of Cyclooxygenase-1 and Cyclooxygenase-2 in Human Breast Cancer.* Journal of the National Cancer Institute, 1998. **90**(6): p. 455-460.
90. Wang, D. and R.N. DuBois, *The role of COX-2 in intestinal inflammation and colorectal cancer.* Oncogene, 2009. **29**(6): p. 781-788.
91. Aparicio Gallego, G., et al., *Cyclooxygenase-2 (COX-2): a molecular target in prostate cancer.* Clinical and Translational Oncology, 2007. **9**(11): p. 694-702.
92. Wang, Z., *The role of COX-2 in oral cancer development, and chemoprevention/ treatment of oral cancer by selective COX-2 inhibitors.* Curr Pharm Des, 2005. **11**(14): p. 1771-7.
93. Sano, H., et al., *Expression of Cyclooxygenase-1 and -2 in Human Colorectal Cancer.* Cancer Research, 1995. **55**(17): p. 3785-3789.
94. Chen, W.S., et al., *Tumor invasiveness and liver metastasis of colon cancer cells correlated with cyclooxygenase-2 (COX-2) expression and inhibited by a COX-2-selective inhibitor, etodolac.* Int J Cancer, 2001. **91**(6): p. 894-9.
95. Tsujii, M., S. Kawano, and R.N. DuBois, *Cyclooxygenase-2 expression in human colon cancer cells increases metastatic potential.* Proc Natl Acad Sci U S A, 1997. **94**(7): p. 3336-40.
96. Tsujii, M., et al., *Cyclooxygenase regulates angiogenesis induced by colon cancer cells.* Cell, 1998. **93**(5): p. 705-16.
97. Langenbach, R., et al., *Cyclooxygenase knockout mice: Models for elucidating isoform-specific functions.* Biochemical Pharmacology, 1999. **58**(8): p. 1237-1246.
98. Fries, S. and T. Grosser, *The cardiovascular pharmacology of COX-2 inhibition.* Hematology Am Soc Hematol Educ Program, 2005: p. 445-51.
99. Norn, S., et al., *From willow bark to acetylsalicylic acid.* Dan Medicinhist Arbog, 2009. **37**: p. 79-98.
100. Warner, T.D., et al., *Nonsteroid drug selectivities for cyclo-oxygenase-1 rather than cyclo-oxygenase-2 are associated with human gastrointestinal toxicity: a full in vitro analysis.* Proc Natl Acad Sci U S A, 1999. **96**(13): p. 7563-8.

101. Bjarnason, I., et al., *Side effects of nonsteroidal anti-inflammatory drugs on the small and large intestine in humans.* Gastroenterology, 1993. **104**(6): p. 1832-1847.
102. Halen, P.K., et al., *Prodrug Designing of NSAIDs.* Mini Reviews in Medicinal Chemistry, 2009. **9**(1): p. 124-139.
103. Gans, K.R., et al., *Anti-inflammatory and safety profile of DuP 697, a novel orally effective prostaglandin synthesis inhibitor.* Journal of Pharmacology and Experimental Therapeutics, 1990. **254**(1): p. 180-7.
104. Gierse, J.K., et al., *Expression and selective inhibition of the constitutive and inducible forms of human cyclo-oxygenase.* Biochem J, 1995. **305 (Pt 2)**: p. 479-84.
105. Kurumbail, R.G., et al., *Structural basis for selective inhibition of cyclooxygenase-2 by anti-inflammatory agents.* Nature, 1996. **384**(6610): p. 644-648.
106. Llorens, O., et al., *Structural basis of the dynamic mechanism of ligand binding to cyclooxygenase.* Bioorg Med Chem Lett, 1999. **9**(19): p. 2779-84.
107. Gierse, J.K., et al., *A Single Amino Acid Difference between Cyclooxygenase-1 (COX-1) and −2 (COX-2) Reverses the Selectivity of COX-2 Specific Inhibitors.* Journal of Biological Chemistry, 1996. **271**(26): p. 15810-15814.
108. Grosser, T., S. Fries, and G.A. FitzGerald, *Biological basis for the cardiovascular consequences of COX-2 inhibition: therapeutic challenges and opportunities.* J Clin Invest, 2006. **116**(1): p. 4-15.
109. Langman, M.J., et al., *ADverse upper gastrointestinal effects of rofecoxib compared with nsaids.* JAMA, 1999. **282**(20): p. 1929-1933.
110. Hunt, R.H., et al., *The gastrointestinal safety of the COX-2 selective inhibitor etoricoxib assessed by both endoscopy and analysis of upper gastrointestinal events.* Am J Gastroenterol, 2003. **98**(8): p. 1725-1733.
111. Silverstein, F.E., et al., *Gastrointestinal toxicity with celecoxib vs nonsteroidal anti-inflammatory drugs for osteoarthritis and rheumatoid arthritis: The class study: a randomized controlled trial.* JAMA, 2000. **284**(10): p. 1247-1255.
112. Subbaramaiah, K. and A.J. Dannenberg, *Cyclooxygenase 2: a molecular target for cancer prevention and treatment.* Trends in Pharmacological Sciences, 2003. **24**(2): p. 96-102.
113. Arber, N., et al., *Celecoxib for the Prevention of Colorectal Adenomatous Polyps.* New England Journal of Medicine, 2006. **355**(9): p. 885-895.
114. Baron, J.A., et al., *A Randomized Trial of Rofecoxib for the Chemoprevention of Colorectal Adenomas.* Gastroenterology, 2006. **131**(6): p. 1674-1682.
115. Reines, S.A., et al., *Rofecoxib: no effect on Alzheimer's disease in a 1-year, randomized, blinded, controlled study.* Neurology, 2004. **62**(1): p. 66-71.
116. Aisen, P.S., et al., *Effects of rofecoxib or naproxen vs placebo on alzheimer disease progression: A randomized controlled trial.* JAMA, 2003. **289**(21): p. 2819-2826.
117. Aisen, P.S., *Evaluation of Selective COX-2 Inhibitors for the Treatment of Alzheimer's Disease.* Journal of Pain and Symptom Management, 2002. **23**(4, Supplement 1): p. S35-S40.

118. Bertagnolli, M.M., et al., *Celecoxib for the Prevention of Sporadic Colorectal Adenomas.* New England Journal of Medicine, 2006. **355**(9): p. 873-884.
119. Bresalier, R.S., et al., *Cardiovascular Events Associated with Rofecoxib in a Colorectal Adenoma Chemoprevention Trial.* New England Journal of Medicine, 2005. **352**(11): p. 1092-1102.
120. Antman, E.M., et al., *Use of Nonsteroidal Antiinflammatory Drugs: An Update for Clinicians: A Scientific Statement From the American Heart Association.* Circulation, 2007. **115**(12): p. 1634-1642.
121. Group, W., et al., *Aspirin as a Therapeutic Agent in Cardiovascular Disease: A Statement for Healthcare Professionals From the American Heart Association.* Circulation, 1997. **96**(8): p. 2751-2753.
122. North, G.L.T., *Celecoxib as Adjunctive Therapy for Treatment of Colorectal Cancer.* Annals of Pharmacotherapy, 2001. **35**(12): p. 1638-1643.
123. Penning, T.D., et al., *Synthesis and Biological Evaluation of the 1,5-Diarylpyrazole Class of Cyclooxygenase-2 Inhibitors: Identification of 4-[5-(4-Methylphenyl)-3- (trifluoromethyl)-1H-pyrazol-1-yl]benzenesulfonamide (SC-58635, Celecoxib).* Journal of Medicinal Chemistry, 1997. **40**(9): p. 1347-1365.
124. Gaulier, S.M., R. McKay, and N.A. Swain, *A novel three-step synthesis of Celecoxib via palladium-catalyzed direct arylation.* Tetrahedron Letters, 2011. **52**(45): p. 6000-6002.
125. Seedher, N. and S. Bhatia, *Solubility enhancement of Cox-2 inhibitors using various solvent systems.* AAPS PharmSciTech, 2003. **4**(3): p. E33.
126. Shono, Y., et al., *Prediction of food effects on the absorption of celecoxib based on biorelevant dissolution testing coupled with physiologically based pharmacokinetic modeling.* European Journal of Pharmaceutics and Biopharmaceutics, 2009. **73**(1): p. 107-114.
127. Amidon, G., et al., *A Theoretical Basis for a Biopharmaceutic Drug Classification: The Correlation of in Vitro Drug Product Dissolution and in Vivo Bioavailability.* Pharmaceutical Research, 1995. **12**(3): p. 413-420.
128. Hwang, S.H., et al., *Synthesis and Structure−Activity Relationship Studies of Urea-Containing Pyrazoles as Dual Inhibitors of Cyclooxygenase-2 and Soluble Epoxide Hydrolase.* Journal of Medicinal Chemistry, 2011. **54**(8): p. 3037-3050.
129. Duggan, K.C., et al., *(R)-Profens are substrate-selective inhibitors of endocannabinoid oxygenation by COX-2.* Nat Chem Biol, 2011. **7**(11): p. 803-9.
130. Pal, M., et al., *Synthesis and Cyclooxygenase-2 Inhibiting Property of 1,5-Diarylpyrazoles with Substituted Benzenesulfonamide Moiety as Pharmacophore: Preparation of Sodium Salt for Injectable Formulation†.* Journal of Medicinal Chemistry, 2003. **46**(19): p. 3975-3984.
131. Khanapure, S.P., et al., *Synthesis and Structure−Activity Relationship of Novel, Highly Potent Metharyl and Methcycloalkyl Cyclooxygenase-2 (COX-2) Selective Inhibitors.* Journal of Medicinal Chemistry, 2003. **46**(25): p. 5484-5504.
132. Ranatunge, R.R., et al., *Synthesis and Selective Cyclooxygenase-2 Inhibitory Activity of a Series of Novel, Nitric Oxide Donor-Containing Pyrazoles†.* Journal of Medicinal Chemistry, 2004. **47**(9): p. 2180-2193.

133. Lu, Z.-h., et al., *Evaluation of 2 celecoxib derivatives: analgesic effect and selectivity to cyclooxygenase-2/1.* Acta Pharmacol Sin, 2005. **26**(12): p. 1505-1511.
134. Kato, M., et al., *Cyclooxygenase-1 and cyclooxygenase-2 selectivity of non-steroidal anti-inflammatory drugs: investigation using human peripheral monocytes.* Journal of Pharmacy and Pharmacology, 2001. **53**(12): p. 1679-1685.
135. Pommery, N., et al., *New COX-2/5-LOX Inhibitors: Apoptosis-Inducing Agents Potentially Useful in Prostate Cancer Chemotherapy.* Journal of Medicinal Chemistry, 2004. **47**(25): p. 6195-6206.
136. Almansa, C., et al., *Synthesis and Structure−Activity Relationship of a New Series of COX-2 Selective Inhibitors: 1,5-Diarylimidazoles.* Journal of Medicinal Chemistry, 2003. **46**(16): p. 3463-3475.
137. Yoshino, T., et al., *Pharmacological profile of celecoxib, a specific cyclooxygenase-2 inhibitor.* Arzneimittelforschung, 2005. **55**(7): p. 394-402.
138. Paulson, S.K., et al., *Pharmacokinetics of Celecoxib after Oral Administration in Dogs and Humans: Effect of Food and Site of Absorption.* Journal of Pharmacology and Experimental Therapeutics, 2001. **297**(2): p. 638-645.
139. Davies, N., et al., *Clinical Pharmacokinetics and Pharmacodynamics of Celecoxib.* Clinical Pharmacokinetics, 2000. **38**(3): p. 225-242.
140. Paulson, S.K., et al., *Metabolism and Excretion of [14C]Celecoxib in Healthy Male Volunteers.* Drug Metabolism and Disposition, 2000. **28**(3): p. 308-314.
141. Paulson, S.K., et al., *Pharmacokinetics, Tissue Distribution, Metabolism, and Excretion of Celecoxib in Rats.* Drug Metabolism and Disposition, 2000. **28**(5): p. 514-521.
142. Sandberg, M., et al., *Oxidation of celecoxib by polymorphic cytochrome P450 2C9 and alcohol dehydrogenase.* British Journal of Clinical Pharmacology, 2002. **54**(4): p. 423-429.
143. Tang, C., et al., *Major Role of Human Liver Microsomal Cytochrome P450 2C9 (CYP2C9) in the Oxidative Metabolism of Celecoxib, a Novel Cyclooxygenase-II Inhibitor.* Journal of Pharmacology and Experimental Therapeutics, 2000. **293**(2): p. 453-459.
144. Bailey, M.J. and R.G. Dickinson, *Acyl glucuronide reactivity in perspective: biological consequences.* Chemico-Biological Interactions, 2003. **145**(2): p. 117-137.
145. Dickinson, R.G., W.D. Hooper, and M.J. Eadie, *pH-dependent rearrangement of the biosynthetic ester glucuronide of valproic acid to beta-glucuronidase-resistant forms.* Drug Metabolism and Disposition, 1984. **12**(2): p. 247-252.
146. Takashima, T., et al., *Evaluation of Breast Cancer Resistance Protein Function in Hepatobiliary and Renal Excretion Using PET with 11C-SC-62807.* Journal of Nuclear Medicine, 2013. **54**(2): p. 267-276.
147. Takashima-Hirano, M., et al., *Efficient sequential synthesis of PET Probes of the COX-2 inhibitor [11C]celecoxib and its major metabolite [11C]SC-62807 and in vivo PET evaluation.* Bioorganic & Medicinal Chemistry, 2011. **19**(9): p. 2997-3004.

148. Halpin, R.A., et al., *The Disposition and Metabolism of Rofecoxib, a Potent and Selective Cyclooxygenase-2 Inhibitor, in Human Subjects.* Drug Metabolism and Disposition, 2002. **30**(6): p. 684-693.
149. Davies, N.M., X.W. Teng, and N.M. Skjodt, *Pharmacokinetics of rofecoxib: a specific cyclo-oxygenase-2 inhibitor.* Clin Pharmacokinet, 2003. **42**(6): p. 545-56.
150. Zhang, J.Y., et al., *Involvement of human UGT2B7 and 2B15 in rofecoxib metabolism.* Drug Metab Dispos, 2003. **31**(5): p. 652-8.
151. Shao, J., et al., *Regulation of Constitutive Cyclooxygenase-2 Expression in Colon Carcinoma Cells.* Journal of Biological Chemistry, 2000. **275**(43): p. 33951-33956.
152. Velázquez, C., et al., *Synthesis and biological evaluation of 3,4-diphenyl-1,2,5-oxadiazole-2-oxides and 3,4-diphenyl-1,2,5-oxadiazoles as potential hybrid COX-2 inhibitor/nitric oxide donor agents.* Bioorganic & Medicinal Chemistry, 2005. **13**(8): p. 2749-2757.
153. Hidalgo, I.J., T.J. Raub, and R.T. Borchardt, *Characterization of the human colon carcinoma cell line (Caco-2) as a model system for intestinal epithelial permeability.* Gastroenterology, 1989(96): p. 736-49.
154. Jia, X., et al., *Disposition of Flavonoids via Enteric Recycling: Enzyme-Transporter Coupling Affects Metabolism of Biochanin A and Formononetin and Excretion of Their Phase II Conjugates.* Journal of Pharmacology and Experimental Therapeutics, 2004. **310**(3): p. 1103-1113.
155. Hu, M., et al., *Use of Caco-2 Cell Monolayers to Study Drug Absorption and Metabolism*, in *Optimization in Drug Discovery*, Z. Yan and G. Caldwell, Editors. 2004, Humana Press. p. 19-35.
156. Tang, Y.Q. and N. Weng, *Salting-out assisted liquid-liquid extraction for bioanalysis.* Bioanalysis, 2013. **5**(12): p. 1583-98.
157. Chen, J., H. Lin, and M. Hu, *Metabolism of Flavonoids via Enteric Recycling: Role of Intestinal Disposition.* Journal of Pharmacology and Experimental Therapeutics, 2003. **304**(3): p. 1228-1235.
158. Davis, M.E. and M.E. Brewster, *Cyclodextrin-based pharmaceutics: past, present and future.* Nat Rev Drug Discov, 2004. **3**(12): p. 1023-35.
159. Challa, R., et al., *Cyclodextrins in drug delivery: An updated review.* AAPS PharmSciTech, 2005. **6**(2): p. E329-E357.
160. Marnett, L.J. and R.N. DuBois, *COX-2: a target for colon cancer prevention.* Annu Rev Pharmacol Toxicol, 2002. **42**: p. 55-80.
161. Selve, N. and T. Wöhrmann, *Intestinal inflammation in TNBS sensitized rats as a model of chronic inflammatory bowel disease.* Mediators of Inflammation, 1992. **1**(2): p. 121-126.
162. Jeong, E., et al., *In Situ Single-Pass Perfused Rat Intestinal Model for Absorption and Metabolism*, in *Optimization in Drug Discovery*, Z. Yan and G. Caldwell, Editors. 2004, Humana Press. p. 65-76.
163. Paulson, S.K., et al., *Plasma protein binding of celecoxib in mice, rat, rabbit, dog and human.* Biopharmaceutics & Drug Disposition, 1999. **20**(6): p. 293-299.